Resonant collisional transport

Xavier Garbet

Resonant collisional transport

X. Garbet[1,2]

[1]CEA, IRFM, Saint-Paul-lez-Durance, F-13108, France

[2]School of Physical and Mathematical Sciences, Nanyang Technological University, 637371 Singapore

February 6, 2023

Abstract

A variational principle is derived, based on a minimum of entropy production rate. It allows recovering most results of collisional transport boosted by resonances. This note starts with a general introduction to collisional transport enhancement by resonant processes, dubbed as "banana-plateau regime" in neoclassical theory. It then explains how a general variational principle can be constructed, which describes accurately collisional transport processes. This methodology is then used in an axisymmetric tokamak for a single ion species. Usual results for the ion poloidal velocity and heat conductivity are recovered. Electron physics is then implemented. Particle flux and parallel current are computed, with evidence of particle (Ware) pinch and "bootstrap" current, on top of corrections on the Spitzer resistivity. The collisional electron heat diffusivity is also predicted. Finally, 3D (non-axisymmetric) effects are included and illustrated with the effect of magnetic field ripple in tokamaks.

Sections labelled with a star "*" can be skipped on first reading. The symbol $\simeq$ is used here with the meaning of an estimate, i.e. numerical factors are kept - conversely the symbol $\sim$ labels a scaling - hence numerical factors are removed.

1 Introduction

This note addresses the calculation of transport across magnetic surfaces due to collisions in a fusion device. Several monographs on this topic are available for tokamaks [1, 2, 3], stellarators [4, 5], and rippled tokamaks [6]. The book [3] provides a didactic and detailed account of the subject. So why a lecture on this subject? The objectives here are two-fold. First, provide a derivation of neoclassical fluxes based on a minimum entropy production rate. This compact formulation yields an alternative point of view on the physics of collisional transport. Second, extend the approach to 3D magnetic configurations, e.g. stellarators, or tokamaks with ripple. Why is this topic important? It is well known that collisions in a magnetised plasma are responsible for a "classical" transport. A collision between two charged particles results in a deviation of their velocities that was predicted long ago (Rutherford formula). This change of velocity is responsible for a modification of the cyclotron motion of the colliding particles, and therefore a displacement of their guiding-centres since this process is local in physical space, i.e. occurs at the position where the particles collide. After each collision, impinging particles are subject to a random displacement across the magnetic field, of the order of the Larmor radius ρ_c. Hence an individual guiding-centre follows a random walk where its position deviates by a distance $\sim \rho_c$ across the magnetic field every typical collision time τ_{coll}. Theory of Brownian motion tells us that diffusion occurs, i.e. the average quadratic displacement

behaves as

$$\left\langle (\mathbf{x}_\perp(t) - \mathbf{x}_\perp(0))^2 \right\rangle = D_{cl} t$$

where

$$D_{cl} = \lim_{\Delta t \to 0} \left\langle \frac{|\Delta \mathbf{x}_\perp|^2}{2\Delta t} \right\rangle$$

is the Fokker-Planck scattering diffusion coefficient, and the bracket a statistical average, for instance an average over several realisations. The diffusion coefficient D_{cl}, is of the order of $\nu \rho_c^2$, where $\nu = 1/\tau_{coll}$ is a collision frequency. This process, called "classical" diffusion, is well documented, and can be put on a firm ground by solving the Fokker-Planck equation [3]. Classical diffusion occurs in any magnetised plasma. However, it is usually sub-dominant compared with turbulent diffusion. However this is not the end of the story by far. Let us start with tokamaks, or any axisymmetric configuration (e.g. RFP, quasi-axisymmetric stellarator). An isolated particle is well confined because the deconfining effect of the magnetic drift velocity, which is nearly vertical in a tokamak, is "compensated" thanks to the motion of the particle successively at the top and bottom of a magnetic surface. However, when collisions occur, the compensation is no longer perfect, so that charged particles diffuse across magnetic surfaces. In the collisional regime, this process is called Pfirsch-Schlüter diffusion. Compensation of the magnetic drift motion becomes hard to achieve when the particle guiding-centre velocity along the magnetic field, called "parallel velocity"[1] $v_\parallel$, becomes nearly zero $v_\parallel = 0$. Indeed in this case, the time needed to explore a magnetic surface up and down becomes very large. In that limit, even long collision time has a strong deconfining effect. This is in fact a resonant effect located at $v_\parallel = 0$ in the phase space. This process is called "banana-plateau" diffusion. The reasons for this exotic terminology will be seen later on. The enhancement of collisional transport via the magnetic drift is called "neoclassical transport"- the word neoclassical refers to classical transport as the basic reference. One important point to keep in mind is that all these processes coexist, i.e. the total diffusion coefficient reads

$$D = D_{cl} + D_{ps} + D_{bp}$$

where D_{cl}, D_{ps}, and D_{bp} are respectively classical, Pfirsch-Schlüter, and banana-plateau diffusion coefficients. The situation becomes somewhat more intricate when axisymmetry is lost. In a tokamak, this situation is generic due to several reasons. The discrete number of coils lead to periodic variations of the magnetic field in the toroidal direction, called "ripple". Sometimes, additional helical coils are used to control MHD instabilities. Also, small adjustment errors often occur during the assembly of the various coils, which lead to so-called error fields, i.e. departures from the designed magnetic field. Moreover, another class of magnetic configurations is by design non axisymmetric, namely stellarators. Some classes of particles which are locally trapped in minima of the magnetic field are not confined because their magnetic drift is not compensated. Collisions play in some sense a beneficial role by detrapping these particles and thus re-confining them. Nevertheless this effect disappears for vanishing collision frequency, which manifests itself via a diffusion coefficient that behaves as $1/\nu$, a catastrophic behaviour for hot fusion plasmas. Fortunately the situation comes back to acceptable due to the development of a radial electric field and the associated $E \times B$ drift velocity. These complex features can be captured with a variational principle that will be derived in the following sections.

[1] Strictly speaking the notation $u_\parallel$ should be used to make the difference between the guiding-centre and the particle parallel velocities. However it appears that these two coincides in the guiding-centre at order 1 in the small expansion parameter ρ_*

2 Heuristic derivation of neoclassical diffusion

2.1 Ordering parameters

Trajectories of charged particles in a strong magnetic field are characterised by 3 typical frequencies: the highest one is the cyclotron frequency $\Omega_c = e_a B_0/m_a$ (B_0 is a reference cyclotron frequency, e_a the particle charge and m_a its mass), while a second lower one is the transit frequency $\Omega_t = v_\parallel/L_\parallel$, where $v_\parallel$ is the parallel velocity. In this section, we replace $v_\parallel$ by the particle velocity modulus v, i.e. $v_\parallel \sim v$, keeping in mind that this does not allow a proper discrimination between trapped (low $v_\parallel/v$) and passing ($v_\parallel \simeq v$) particles. Distinction between trapped and passing particles will introduced later on. Finally a third frequency is identified, which is associated with the magnetic drift and is noted $\Omega_D = v_D/L_\perp$, where $v_D \simeq v\rho_c/R_0$ is a magnetic drift velocity, $\rho_c = v/\Omega_c$ a gyroradius, and $L_\perp$ a transverse length. A useful estimate of $L_\parallel$ is the connection length between the low and high field side along a field line, i.e. $L_\parallel = qR_0$ (omitting a pre-factor π), where q is the safety factor and R_0 the major radius of a magnetic surface. This estimate can be recovered from the equation of motion on the poloidal angle θ (ignoring the magnetic drift) $d\theta/dt \simeq v_\parallel/L_\parallel$. As to the choice of the perpendicular macroscopic length $L_\perp$, one possible choice is the minor radius r of a magnetic surface, which is representative of gradient lengths[2].

The ratio of these frequencies involves the parameter $\delta = \rho_p/r$, where $\rho_p = \frac{qR_0}{r}\rho_c$. More precisely

$$\frac{\Omega_t}{\Omega_c} \sim \delta = \frac{\rho_p}{r} \qquad\qquad \frac{\Omega_D}{\Omega_t} \sim \frac{\rho_p}{R_0} = \frac{r}{R_0}\delta$$

Recall that a magnetised plasma must verify by definition the constraint $\rho_* = \rho_c/r \ll 1$. The condition $\delta \ll 1$ is slightly more difficult to fulfil $q > 1$ and $r/R_0 < 1$ in tokamaks. Nevertheless this condition is usually satisfied, except in some sharp transport barriers, or very near the magnetic axis. So the ratio δ of the poloidal gyroradius to plasma size will be considered as a small parameter.

Whenever collisions are accounted for, a fourth frequency comes into play, namely the collision frequency ν. In fusion plasmas, the parameter $\Delta = \nu/\Omega_c$ is always smaller than one. It remains to position the collision frequency with respect to the transit frequency. The ratio of collision to transit frequency is

$$\frac{\nu}{\Omega_t} = \frac{a}{\rho_p}\frac{\nu}{\Omega_c} = \frac{\Delta}{\delta}$$

This is a ratio of two small parameters. Hence no conclusion can be drawn on the ordering of transit vs collision times. Regimes will therefore have be identified depending on the value of this parameter.

2.2 Primer on the magnetic equilibrium

2.2.1 General properties of magnetic coordinates

A Fokker-Planck drift-kinetic equation must be solved in order to compute collisional transport in a magnetic configuration. The distribution function depends on 5 variables : 3 coordinates that label the position of a guiding-centre, its parallel velocity, and the magnetic moment (some authors prefer the perpendicular velocity). A clever choice of coordinates greatly simplify the calculations. In particular, choosing a set of magnetic coordinate present many advantages, in particular simpler forms of differential operators. The reader is sent to the lecture note "Magnetic coordinates and equilibrium magnetic

[2]Usually a magnetic surface cross section is not circular - the "minor radius" can nevertheless be chosen as a typical size of its cross section, like an average radius.

field" for details. It is reminded that the magnetic field in a toroidal configuration that satisfies the magnetostatic force balance equation is of the following form

$$\mathbf{B} = \nabla\chi \times \nabla\theta + \nabla\zeta \times \nabla\psi$$

where (θ, ζ) are poloidal and toroidal angles, ψ is related to the flux of poloidal field normalised to 2π[3], and χ is the flux of the toroidal flux normalised to 2π. The toroidal magnetic flux χ is a function of the poloidal magnetic flux ψ such that $d\chi/d\psi = q(\psi)$, where $q(\psi)$ is the safety factor. An equivalent compact formulation of the field, valid only in a tokamak, is

$$\mathbf{B} = I(\psi)\nabla\zeta + \nabla\zeta \times \nabla\psi$$

where $I(\psi)$ is a magnetic flux function, close to the current that passes through the toroidal coils. The Jacobian of the system of coordinates (ψ, θ, ζ) is

$$\sqrt{g} = [(\nabla\zeta \times \nabla\psi) \cdot \nabla\theta]^{-1} = \frac{1}{\mathbf{B} \cdot \nabla\theta} = \frac{qR^2}{I}$$

where R is the major radius. The gradient along the magnetic field can then be computed

$$\mathbf{B} \cdot \nabla F = \frac{I}{R^2}\left(\frac{\partial F}{\partial \zeta} + \frac{1}{q}\frac{\partial F}{\partial \theta}\right)$$

A useful relationship is

$$\frac{\mathbf{B}}{B^2} \times \nabla\psi = I\frac{\mathbf{B}}{B^2} - R^2\nabla\zeta$$

2.2.2 Circular concentric magnetic configuration

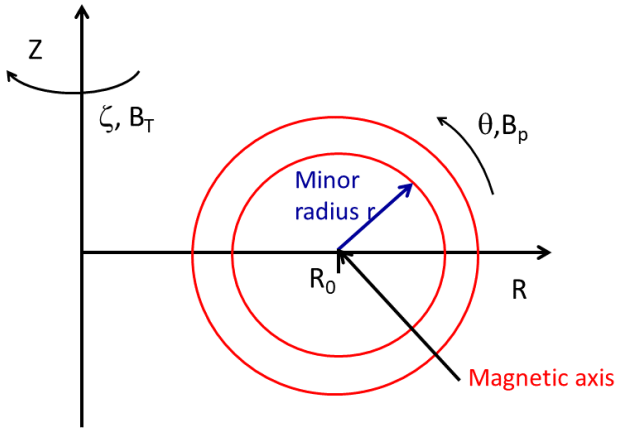

Figure 1: Geometry of circular concentric magnetic surfaces.

Results will be often illustrated with a simplified magnetic configuration where the magnetic surfaces $\psi = cte$ are circular concentric, see Fig. 1. This is not a very accurate description of most tokamaks since their magnetic surfaces are usually shaped, i.e. non circular, and also radially shifted because of a Shafranov shift. The main advantage of this class of equilibria is to provide analytical estimates, and therefore some insight in the underlying physics. The poloidal magnetic flux ψ can then be replaced by the minor

[3]Sign depends on the convention on the toroidal angle

radius of a magnetic surface, with the relationship $\frac{d\psi}{dr} = \frac{r}{q(r)R_0}$, where R_0 is the major radius of the magnetic axis, while the current function I is just $I = B_0 R_0$. The magnetic field then reads

$$\mathbf{B} = B_0 \frac{R_0}{R} \left(\hat{\mathbf{e}}_\zeta + \frac{r}{q(r)R_0} \hat{\mathbf{e}}_\theta \right)$$

where $(\hat{\mathbf{e}}_\theta, \hat{\mathbf{e}}_\zeta)$ are the unit poloidal and toroidal vectors. The Jacobian of the coordinate system (r, θ, ζ) is just $\sqrt{g} = rR^2/R_0$, while the parallel gradient reads

$$\mathbf{B} \cdot \nabla F = \frac{B_0 R_0}{R^2} \left(\frac{\partial F}{\partial \zeta} + \frac{1}{q} \frac{\partial F}{\partial \theta} \right)$$

A further approximation consists in assuming small values of inverse aspect ratio $\epsilon = r/R_0$. The parameter ϵ is then used as an expansion parameter, though this is done for convenience: it is not a fundamental expansion parameter of collisional transport theory - these are derived in the next section.

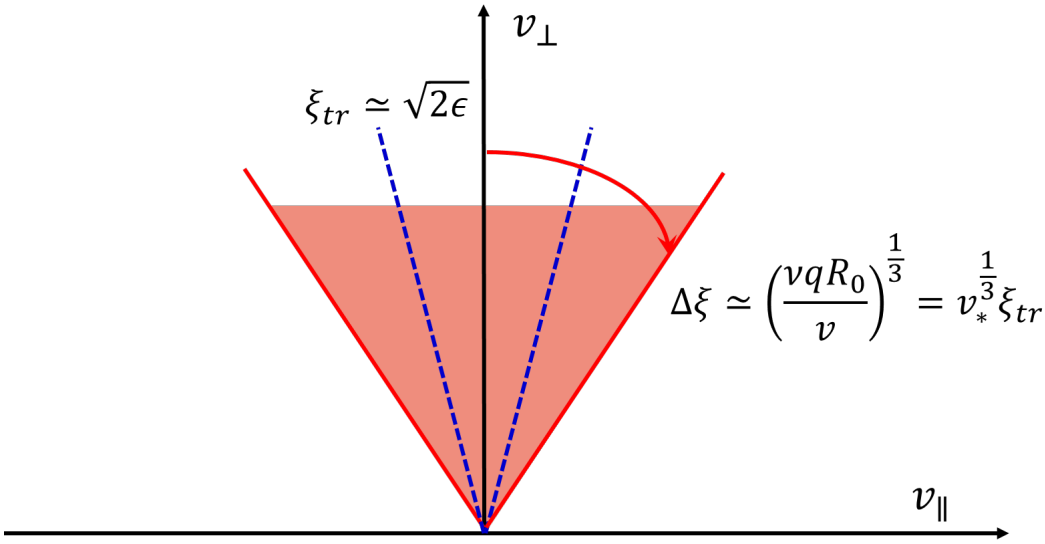

Figure 2: Contribution in the phase space of passing particles near the cone located around the axis $v_\parallel = 0$ and of angle $\Delta\xi$. Plateau regime holds as long as the extent $\Delta\xi$ of the collisional cone is larger than the region where trapped particles are located $\xi \ll \xi_{tr}$. This condition can be recast $\nu_* > 1$.

2.3 Neoclassical transport in a tokamak - heuristic derivation

It is desirable to derive first simple expressions of neoclassical diffusion coefficients in various collisionality regime. As said, the key element here is the magnetic drift velocity v_D, essentially vertical in a tokamak, and assumed upward here to illustrate the mechanisms at work. The magnetic drift pulls a particle out of a magnetic surface in the upper half-plan, whereas it pushes it inside in the lower half-plan. Without collisions, a particle explores equally the upper and lower half planes thanks to its motion along a field line, so that the outward and inward displacements due to the vertical drift compensate. This is no longer true when collisions occur, i.e. outward and inward displacements do not necessarily balance any more. Let us call τ_c the time needed by a particle to move from the upper to lower half-plane, and vice versa. The motion of a guiding centre becomes random under the effect of collisional velocity scattering. In other words, it is similar to a Brownian motion as described by Eq.(1). The diffusion coefficient is $D_\perp \sim \ell_c^2/\tau_c$, where ℓ_c is the mean free path, and is of the order of $\ell_c \sim v_D \tau_c$, so that

$$D_\perp \sim v_D^2 \tau_c$$

Hence the time τ_c plays the role of a jump time in a Brownian motion, ℓ_c being a jump length. Let us first consider the strong collisional regime, called Pfirsch-Schlüter regime. It is defined as the case where the mean free path along a field line $\lambda = v_\parallel/\nu$ is smaller than the connection length $L_\parallel \sim qR_0$. For passing particles, the parallel velocity can be assimilated to the particle velocity modulus v. Hence the Pfirsch-Schlüter regime is reached when $\nu > v/qR_0$. In this high collisional regime, the motion of a particle along the field line is diffusive

$$\left\langle (x_\parallel(t) - x_\parallel(0))^2 \right\rangle \simeq D_\parallel t$$

where $D_\parallel$ the collisional diffusion coefficient, if the order of $D_\parallel \sim \frac{\lambda^2}{\tau_{coll}} \sim \frac{v^2}{\nu}$. Applying this expression to $x_\parallel(t) - x_\parallel(0) = qR_0$ yields an estimate of τ_c

$$\tau_c \sim \nu \frac{q^2 R_0^2}{v^2}$$

Let us now remember that the vertical drift scales as $v\rho_c/R_0$ where $\rho_c = v/\Omega_c$ is the gyro-radius (assimilating the perpendicular velocity $v_\perp$ to the velocity modulus v). Combining these equations yield the Pfirsch-Schlüter diffusion coefficient

$$D_{ps} \sim \nu q^2 \rho_c^2$$

Hence the Pfirsch-Schlüter diffusion coefficient is q^2 larger than the classical diffusion coefficient. Let us now analyse the opposite situation where $\nu < \frac{v}{qR_0}$, i.e. the particle

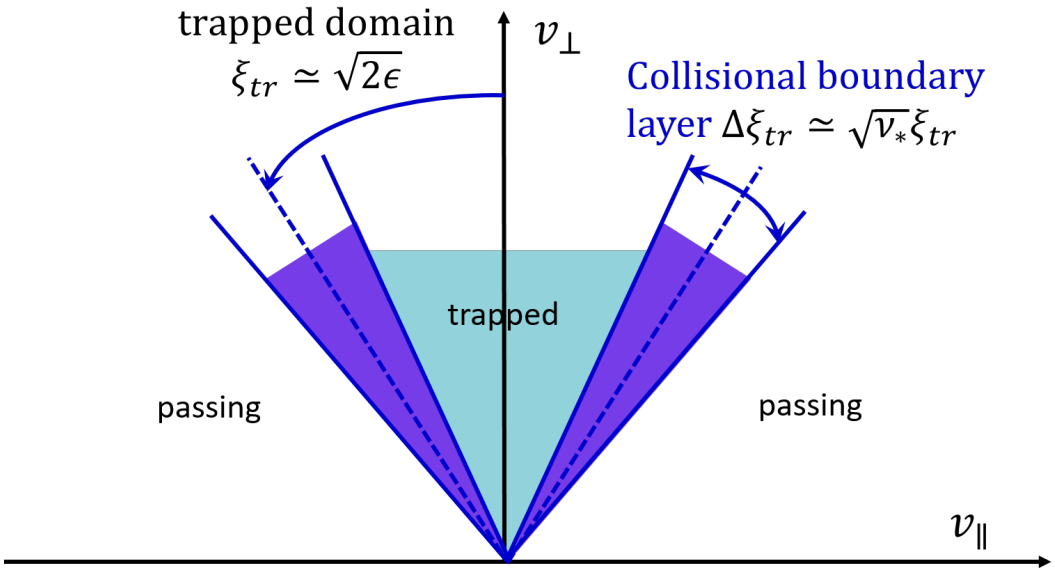

Figure 3: Contribution of trapped particles to collisional transport in the banana regime. Most of the contribution comes from a collisional boundary layer located near the banana-passing border $\xi = \xi_{tr}$ and of width $\Delta\xi_{tr} = \sqrt{\nu_*}\xi_{tr}$. Banana regime holds when $\nu_* < 1$, where $\nu_* = \frac{\nu q R_0}{v\epsilon^{3/2}}$.

makes several turns around the tokamak before enduring a binary collision. This is the point where resonant effects start prevailing. As mentioned, resonant particles bear a nearly zero parallel velocity - in absence of collision these particles drift vertically until they leave the plasma. This situation changes radically when collision occurs. A model collision operator is described in Appendix B, which remains quite complex. However, estimates can be produced by noting that the process at work is a scattering diffusion in the pitch-angle[4] $\xi = \frac{v_\parallel}{v}$ variable. Pitch-angle scattering re-confines resonant particles by changing their parallel velocity from 0 to a finite value. Seen in the phase space, a

[4]Obviously, one can no longer assimilate the parallel velocity $v_\parallel$ to the modulus v when dealing with resonant particles.

region develops in the phase space $(v_\parallel, v_\perp, \varsigma)$ where resonant particles are deeply affected by collisions (see Fig.2). This region is a cone of angle $\Delta\xi$, such that the effective collision frequency $\frac{\nu}{\Delta\xi^2}$ balances the transit frequency on the cone surface $\frac{v_\parallel}{qR_0} = \frac{v}{qR_0}\Delta\xi$ - this balance provides a value of the cone extent $\Delta\xi$

$$\Delta\xi = \left(\frac{\nu qR_0}{v}\right)^{1/3}$$

An effective collision time can then be calculated

$$\tau_{eff} = \frac{1}{\nu_{eff}} = \frac{\Delta\xi^2}{\nu}$$

The fraction of particles affected by this process is just $\Delta\xi$, so that the diffusion coefficient in plateau regime is

$$D_p \sim \Delta\xi v_D^2 \tau_{eff} \sim \frac{v}{qR_0} q^2\rho_c^2 = \frac{qR_0}{v} v_D^2 \tag{1}$$

The expression resembles the Pfirsch-Schlüter diffusion coefficient, with the collision frequency replaced by a transit frequency, so that both expressions match when $\nu = v/qR_0$. Remember however that the two processes are very different - we will come back to this point. The rationale above holds as long as $\Delta\xi$ is larger than the trapped domain. Let us remind that below a pitch-angle $\xi_{tr} \simeq \sqrt{(B_{max} - B_{min})/B_0}$, particles bounce back and forth due to the mirror force along a field line - these are called *toroidally trapped particle*s. In a large aspect ratio tokamak, $(B_{max} - B_{min})/B_0 \simeq 2\epsilon = 2r/R_0$, where r is the minor radius of a magnetic surface. When the collision frequency decreases, the collision cone around the axis $v_\parallel = 0$ and of extension $\Delta\xi \sim (\nu qR_0/v)^{1/3}$ changes into a collisional layer (layer between two cones) near the trapped-passing border $\xi = \xi_{tr} \sim \epsilon^{1/2}$, see Fig.3. The width $\Delta\xi_{tr}$ of this layer is such that the effective collision frequency balances the bounce frequency of a trapped particle $\nu/\Delta\xi_{tr}^2 \sim \omega_b$, where $\omega_b \sim v/(qR_0)\epsilon^{1/2}$ is the bounce frequency. Hence the width of the boundary layer is $\Delta\xi_{tr} \sim \epsilon^{1/2}\nu_*^{1/2}$ where $\nu_*^{1/2}$ is a banana collisionality parameter defined as

$$\nu_* = \frac{\nu qR_0}{v\epsilon^{3/2}} \tag{2}$$

Therefore, the banana regime is reached when the condition $\nu_* < 1$ is satisfied, i.e. the condition under which $\Delta\xi_{tr} \leq \epsilon^{1/2}$. The effect of the vertical drift is essentially to confer a finite width to particle trajectories. The corresponding width is $\delta_b \sim v_D/\omega_b \sim q\rho_c/\epsilon^{1/2}$. The cross section in a poloidal plane of the drift surface of toroidally trapped particles looks like a banana of width δ_b. This is the reason why they are often dubbed "banana" particles. The bounce motion of particles remove the resonance singularity. Collisions acts essentially to transform trapped in passing particles and vice-versa. The fraction of trapped particles is $f_t \sim \epsilon^{1/2}$ while the effective detrapping collision frequency is $\nu_{eff} \sim \nu/\xi_{tr}^2 \sim \nu/\epsilon$. Since the particle bounces several times before a collision occurs, a trapped particle experiences a random walk with jump length equal to the banana width δ_b and a jump time $1/\nu_{eff}$. Only the fraction f_t of trapped particles is affected. This argument yields the banana diffusion coefficient

$$D_b \sim f_t \nu_{eff} \delta_b^2 \sim \frac{\nu}{\epsilon^{3/2}} q^2\rho_c^2$$

The banana regime prevails over the plateau regime when the transit frequency of trapped particles $\xi_{tr}v/qR_0$ gets lower than the effective detrapping collision frequency ν_{eff} i.e. $\nu_* < 1$. With this convention, the transition to the Pfirsch-Schlüter regime occurs when $\nu_* = \epsilon^{-3/2}$. As said, this has a meaning only in the large aspect ratio limit $\epsilon \ll 1$. Here we arrive to a rather subtle point. A difference must be made in the phase space between resonant particles, in the vicinity of the $v_\parallel = 0$ line, and passing particles, subject to a Pfirsch-Schlüter random walk. Hence both physics coexist. Let us call D_{BP}

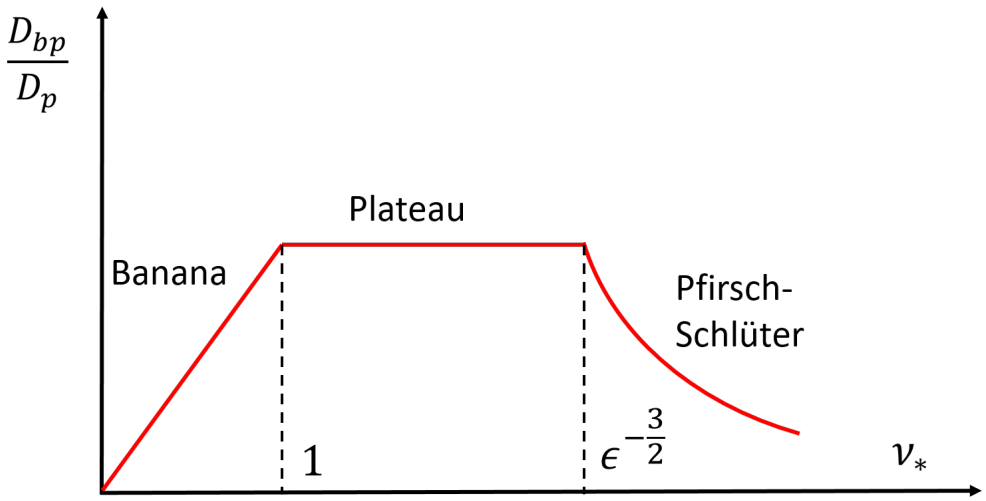

Figure 4: Banana-plateau diffusion coefficient vs collisionality parameter ν_*. Note the decrease as $1/\nu_*$ in the Pfirsch-Schlüter regime $\nu_*\epsilon^{3/2} > 1$.

the diffusion coefficient of resonant particles. The banana and plateau values have been already computed. There exists also a limit in the Pfirsch-Schlüter regime, that can be shown to decrease as the inverse of the collision frequency. Its calculation is beyond the scope of the present section - we just request continuity and decay as $1/\nu$. Therefore the banana-plateau diffusion coefficient normalised to the plateau reference Eq.(1) reads

banana	$\frac{D_{bp}}{D_p} = \nu_*$	when $\nu_* \ll 1$
plateau	$\frac{D_{bp}}{D_p} = 1$	when $1 \ll \nu_* \ll \epsilon^{-3/2}$
Pfirsch-Schlüter	$\frac{D_{bp}}{D_p} = \epsilon^{-3/2}\nu_*^{-1}$	when $\epsilon^{-3/2} \ll \nu_*$

The banana-plateau diffusion coefficient is shown vs ν_* on Fig.4 . Pfirsch-Schlüter diffusion coefficient is always equal to $D_{ps} \sim \nu q^2 \rho_c^2$ - however it becomes subdominant compared with D_{bp} in the banana or plateau regime. Hence the sum of D_{bp} and D_{ps} looks like Fig.5. This figure, shown in many textbooks, give the impression that D_{ps} replaces D_{bp} at high collisionality whereas in fact they coexist. Let us note also that the range of validity of the plateau regime $1 \ll \nu_* \ll \epsilon^{-3/2}$ is narrow, and only makes sense for very small values of the inverse large aspect ratio $\epsilon \ll 1$. For realistic values of ϵ (usually 1/3 at the edge of most tokamaks), the plateau regimes is merely a flattening of the curve D_{bp}/D_p vs ν_*.

2.4 Neoclassical transport in 3D geometry - heuristic derivation

The derivation above holds as long as long as the magnetic configuration exhibits a symmetry. This is the case of a tokamak, which exhibits a toroidal symmetry and was treated above, or a helically symmetric configuration (including quasi-axisymmetric configurations). Situation gets more complicated when symmetry is broken. This occurs in a tokamak when accounting for the finite number of coils, which is responsible for a field oscillation in the toroidal direction called ripple, or when helical external coils are added (resonant magnetic perturbations). Also the adjustment of coils is never perfect. These imperfections in the magnetic field topology are called "error fields", and are also sources of symmetry breaking. Another known configuration that may combine several helical symmetries is the stellarator. We focus here on the case of magnetic ripple. A new class of trapped particles appear, that move back and forth in the local minima of the magnetic field. These are called locally trapped. At this stage two types of effects are possible : the effect of the vertical drift on locally trapped particles, and the effect of ripple on

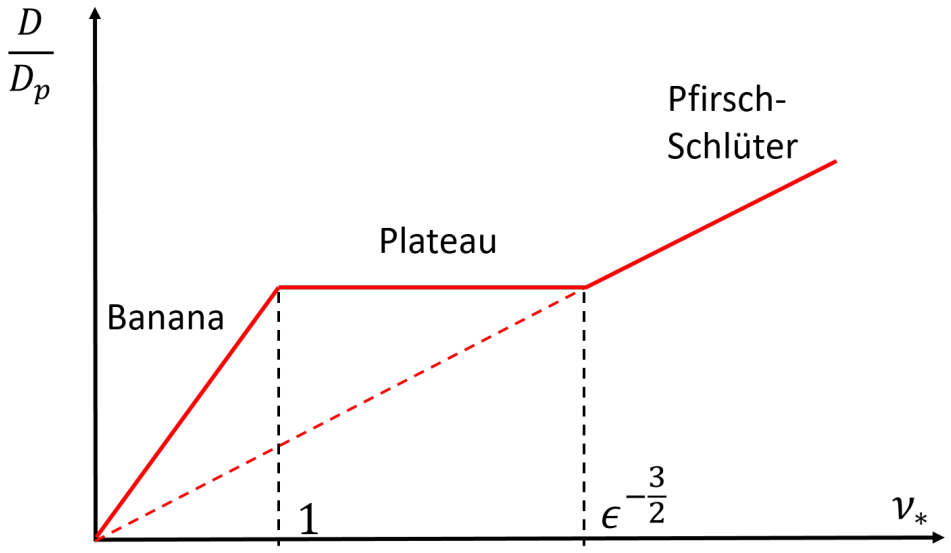

Figure 5: Total collisional diffusion coefficient vs collisionality parameter ν_*. Note the linear increase in the Pfirsch-Schlüter regime $\nu_*\epsilon^{3/2} > 1$ due to the inclusion of the Pfirsch-Schlüter diffusion coefficient.

toroidally trapped particles. The latter is mediated by a random displacement of banana tips. These two cases are now addressed heuristically.

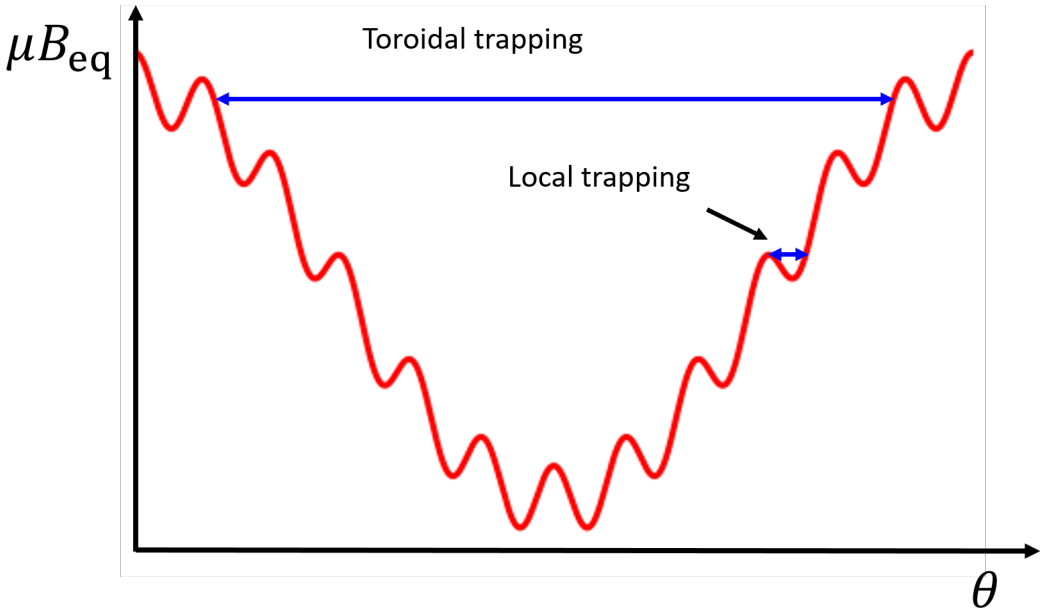

Figure 6: Perpendicular energy $\mu B_{eq}(\theta)$ "seen" by a particle guiding-centre along a field line. Particle bounces back when the equation $E = \mu B_{eq}(\theta)$, E the kinetic energy, admits solutions in θ. Trapping can be local (due tu ripple) or toroidal, due to the $1/R$ decay of the magnetic field.

2.4.1 Effect of a magnetic field ripple on toroidally trapped particles*

Let us call $\delta(r)$ the amplitude of the ripple field, i.e. the amplitude of $\delta B/B$, where δB measures the amplitude of the field corrugation. A realistic ripple amplitude also depends on the poloidal angle θ. However, in order to avoid unnecessary complications, we will limit the discussion to a dependence on minor radius. Because of the mirror force due

to variations of the magnetic field along the field lines, a particle can be locally trapped in a local minimum of the magnetic field due to ripple, or bounce toroidally as it would without ripple. This can be understood with a model of the B field

$$B_{eq} = B_0 \left(1 - \epsilon \cos(\theta) + \delta(r) \cos(N_c \zeta)\right) \tag{3}$$

where N_c is the number of toroidal coils, and $\epsilon = r/R_0 \ll l$ is the inverse aspect ratio[5]. Along a field line $\zeta = \bar{\zeta} + q(r)\theta$, where $\bar{\zeta}$ is a field line label. Plugging the expression of ζ in the field Eq.(3) yields an energy $\mu B_{eq}(\theta)$ as shown on Fig.6. Extending the calculations done above for toroidally trapped particles, the fraction of trapped particles is $\sim \delta^{1/2}$ while the effective detrapping collision frequency is $\nu_\delta \sim \nu/\delta$. In absence of any $E \times B$ drift or magnetic drift due to ripple, the vertical magnetic drift of locally trapped particles that results from the $1/R$ variation of the toroidal field is not compensated since the motion of the particle in the toroidal direction is bounded. Hence the particle cannot explore the magnetic surface - only collisions can reconfine these particles thanks to collisional scattering in the velocity space. The diffusion coefficient reads

$$D_{sb,1/\nu} \sim \delta^{1/2} \frac{1}{\nu_\delta} v_D^2 \sim \delta^{3/2} \frac{v_D^2}{\nu}$$

where the label "sb" stands for superbanana - we will soon see why. This expression is unfavourable as the diffusion coefficient increases at low collisionality. Therefore, collisional transport becomes large when approaching the conditions for fusion. This is the so-called "$1/\nu$ regime". The situation improves somewhat when the $E \times B$ and magnetic drifts (the bit due to ripple) are accounted. The $E \times B$ drift is due to a negative radial electric drift that builds up to ensure charge ambipolarity. Indeed the expression above gives a diffusion coefficient that is larger for ions than for electrons. The $E \times B$ drift velocity is responsible for a particle motion in the poloidal direction with an angular frequency $\Omega_{E\theta} = v_{E\theta}/r$ where $v_{E\theta} = -E_r/B_0$ is the poloidal component of the $E \times B$ drift velocity. Moreover, a magnetic drift appears due to the gradient of ripple amplitude $d\delta/dr$. This magnetic drift generates a poloidal precession of locally trapped particles. For deeply trapped particles, this precession frequency is typically $\Omega_{B\theta} \simeq 1/r \; \mu/e_a \; d\delta/dr$. Overall a locally trapped particle precesses poloidally with a frequency $\Omega_{d\theta} = \Omega_{E\theta} + \Omega_{B\theta}$. This poloidal motion broadens the orbit width of locally trapped particles, which may become quite fat - hence the name "superbanana particles". Let us note that in tokamaks, the precession displaces particles from large to low ripple areas, a feature that has been left aside when ignoring poloidal variations of the ripple amplitude[6]. This variation also provides a mechanism for reconfinement. Let us focus on the consequence of orbit width broadening. The typical radial size or displacement of a superbanana is $\Delta r_\theta \sim v_D/\Omega_{d\theta}$. When lowering the collision frequency, a particle can turn around in the poloidal plane several times before enduring a collision. The motion is random with a step Δr_θ, collision time $1/\nu_\delta$ while the fraction of affected particles is $\delta^{1/2}$. Diffusion coefficient reads

$$D_{sb,\nu} \sim \delta^{1/2} \nu_\delta \Delta r_\theta^2 \sim \frac{1}{\delta^{1/2}} \nu \frac{v_D^2}{\Omega_{d\theta}^2} \tag{4}$$

The behaviour with collision frequency is much more favourable since linear. The two expressions can be fitted by the formula

$$D_{sb} \sim \delta^{1/2} \frac{\nu_\delta}{\Omega_{d\theta}^2 + \nu_\delta^2} v_D^2 \tag{5}$$

The collisional diffusion vs collisionality is illustrated in Fig.(7). However the reader should be aware that this formula is much too simplified, for two reasons:

[5]The component in $\cos\theta$ of the magnetic field comes from a Taylor expansion of the magnetic field for circular concentric magnetic surfaces $B = B_0 R_0/R$ with $R = R_0 + r\cos\theta$.

[6]In a torus, ripple is larger on the low field side where the distance between coils is larger.

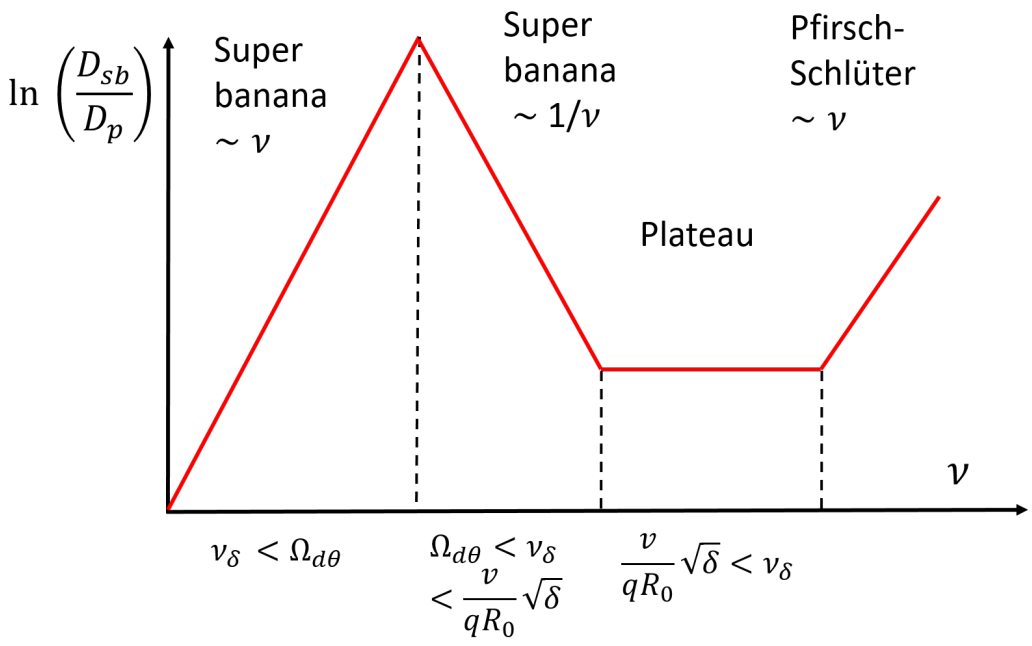

Figure 7: Schematics of neoclassical transport for super-banana particles (log scale).

- For intermediate collisionality $\nu_\delta \simeq \Omega_{d\theta}$, and when $\delta > \epsilon$ (unrealistic for tokamaks, but common in stellarators), a boundary layer develops near the border between locally trapped particles and passing particles [7]. In other words, the collisional cone around the line $v_\parallel = 0$ of width $\delta^{1/2}$ is replaced by a boundary layer around the trapped/passing limit $\xi_{tr} = \delta^{1/2}$, and of width $\Delta\xi$. This width is such that the effective collision frequency $\nu/\Delta\xi^2$ balances the frequency $\Omega_{d\theta}$, i.e. $\Delta\xi \sim (\nu/\Omega_{d\theta}^2)$. The fraction of particles in the boundary layer is $\Delta\xi$ so that the diffusion coefficient is

$$D_{sb,\sqrt{\nu}} \sim \Delta\xi \frac{\nu}{\Delta\xi^2}\Delta r^2 \sim \nu^{1/2}\frac{v_D^2}{\Omega_{d\theta}^{3/2}}$$

  This regime is dubbed $\sqrt{\nu}$, see Fig.9. Eq.(5) should then be replaced by something like

$$D_{sb} \sim \delta^{1/2}\frac{\hat{\nu}}{1 + C_0\hat{\nu}^{1/2} + C_1\hat{\nu}}v_D^2$$

  where $\hat{\nu} = \frac{\nu_\delta}{\Omega_{d\theta}}$, and C_0, C_1 are suitable coefficients.

- Some particles may satisfy the resonance condition $\Omega_{d\theta} = 0$, which clearly invalidates Eq.(4). Two sub regimes can be identified : i) for large enough collisionality the diffusion coefficient does not depend on the collision frequency - this is called the superbanana plateau regime - ii) at lower collisionality, the singularity is resolved by looking into the trajectory broadening associated with second derivative of potential and ripple amplitude in r. The calculation is similar to the banana regime, and leads again to a diffusion coefficient proportional to ν - this is the superbanana regime [8].

This complex behavior is illustrated in Fig.(8). It is stressed again that these are asymptotic values. In practice, several regimes can mix up, so that diffusion is rarely found to match one of these scalings. Nevertheless these expression give a flavour of collisional transport dependence on various parameters. Also, it must be realised that the complications associated with the ν and $\sqrt{\nu}$ only occurs at very low collisionality in the specific case of ripple in a tokamak.

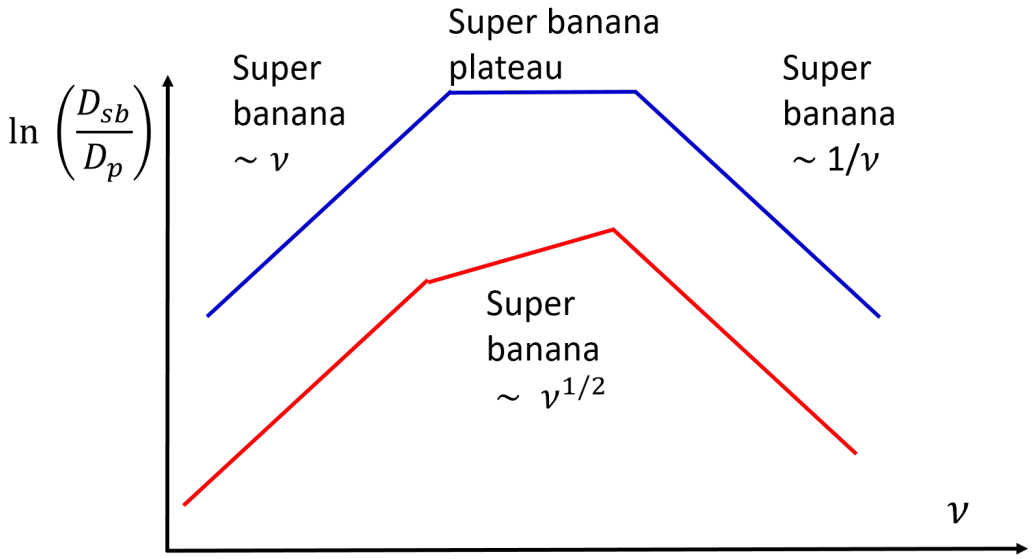

Figure 8: Detail of neoclassical transport for super-banana particles (log scale) at low collisionality for one class of particle energy.

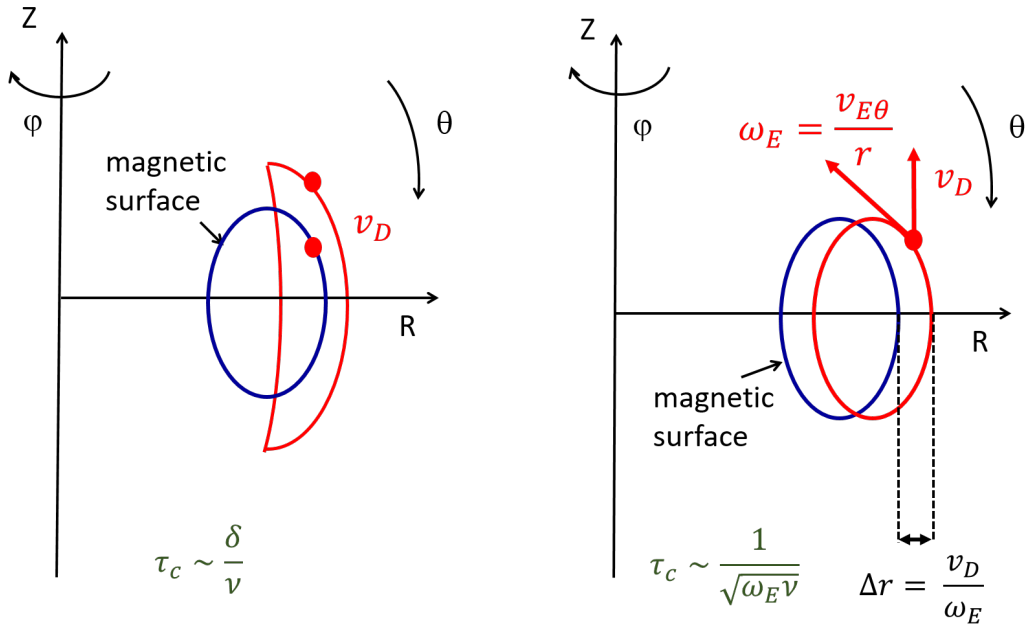

Figure 9: Diffusion of a locally trapped particle. Left panel: in absence of $E \times B$ drift velocity, a locally trapped particle drifts vertically because of its magnetic drift. After an effective collision time, it becomes a toroidally trapped particle (banana). Right panel: in presence of a $E \times B$ drift velocity, a locally trapped particle remains confined, with a drift surface that is shifted by Δr_θ compared with a reference magnetic surface. The effective collision frequency is determined by the condition $\frac{\nu}{\Delta\xi^2} \simeq \Omega_{d\theta}$. This defines a collisional boundary layer near the locally/toroidally trapped border.

2.4.2 Effect of ripple on banana tips

The effect of ripple on toroidally trapped particles is essentially due to the small displacement it induces on the position of the banana tip, Fig.10. The calculation of this displacement is somewhat intricate, but a reasonably accurate estimate is derived in Appendix A, namely

$$\Delta r_\delta = \frac{\pi}{\sqrt{2}} \frac{q^2 \delta}{\epsilon^{3/2}} J_0(N_c q \theta_b) N_c \sin(N_c \bar{\zeta}) \rho_c$$

where $\rho_c = m_a v/e_a B_0$ is the gyroradius. The argument of the Bessel function is larger than 1 since $N_c >> 1$ and $q > 1$, except for vanishing bounce angles θ_b. It can then be approximated by its asymptotic expression $J_0(x) = \sqrt{\frac{2}{\pi x}}\cos(x + \pi/4)$, so that

$$\Delta r_\delta \simeq \sqrt{\frac{\pi N_c}{\theta_b}} \left(\frac{q}{\epsilon}\right)^{3/2} \delta\rho_c \cos\left(Nq\theta_b + \frac{\pi}{4}\right) \sin(N_c\bar{\zeta}) \tag{6}$$

This gives an estimate of the max amplitude of the displacement

$$\Delta r_{\delta,max} \simeq \sqrt{\frac{\pi N_c}{\theta_b}} \left(\frac{q}{\epsilon}\right)^{3/2} \delta\rho_c$$

A more accurate calculation based on the invariance of the longitudinal invariant of motion gives the same relationship with θ_b replaced by $\sin(\theta_b)$. Let us recall that $\Delta r_{\delta,max}$ is the displacement of a banana tip after a bounce time. It is in fact easier to work with an effective velocity v_{Deff} that is the maximum radial velocity dr/dt and is readily calculated from Eq.(6)

$$v_{Deff} \sim \sqrt{N_c q}\frac{\delta}{\epsilon} v_D$$

As mentioned several times now, a diffusion coefficient behaves as $D \simeq f_t v_D^2 \tau_c$, where f_t is the fraction of toroidally trapped particles, and τ_c is a relevant jump time for the random walk process at work. Several frequencies are candidate. An obvious one is the bounce time $1/\Omega_b \sim qR_0/(v\sqrt{\epsilon})$. A second time scale should involve collisions. An educated guess suggests a jump time equal to the collision detrapping time ϵ/ν. However, a more accurate estimate is necessary. A glance at the radial displacement of a banana tip Eq.(6) shows that it changes sign when $\theta_b = \pi/(N_c q)$. This is to be compared with the transition from trapped to passing particles that occurs at $\theta_b = \pi$. In the latter case, the corresponding width in scattering angle $\delta\xi$ was $\sqrt{\epsilon}$. For the effect of ripple on banana tips, the counterpart is rather $\delta\xi \sim \sqrt{\epsilon}/(N_c q)$. The effective collision time is therefore

$$\nu_{eff} \sim \frac{N_c^2 q^2}{\epsilon}\nu$$

The collision frequency is very large compared with the conventional frequency ν. As a consequence banana tips under the effect of ripple are easily in a collisional regime. Finally, it must be remembered that bananas precess around the vertical axis under the effect of both magnetic and $E \times B$ drift velocities. The precession frequency is noted $\Omega_{d\zeta}$. Let us remember that the ripple period in toroidal angle is $2\pi/N_c$, so that the time necessary to cross a period due to the precession scales as $1/(N_c\Omega_{d\zeta})$. The relevant frequency to be compared with the two frequencies Ω_b and ν_{eff} is therefore $\omega_{d\zeta} = N_c\Omega_{d\zeta}$. In usual conditions $\omega_{d\zeta} \ll \Omega_b$, so that 3 situations are met depending on the position of ν_{eff} on the frequency scale.

Let us consider first the case where $\Omega_b \ll \nu_{eff}$. In this case a collision always occurs just before a toroidally trapped particle reaches a bounce point (banana tip). The effective jump time is therefore $1/\Omega_b$. The diffusion coefficient is

$$D_{rp} \sim f_t \frac{v_{Deff}^2}{\Omega_b} \sim N_c q \left(\frac{\delta}{\epsilon}\right)^2 D_p$$

where $D_p = v_D^2 qR_0/v$ is the plateau diffusion coefficient. This regime is called the "ripple-plateau" regime. Since $\delta \ll \epsilon$ in tokamaks, it tends to produce diffusion coefficients that are smaller than the plateau reference, partially compensated by the prefactor $N_c q$.

We now consider the regime $\omega_{d\zeta} \ll \nu_{eff} \ll \Omega_b$. In this case, the relevant jump time is the longest one $1/\nu_{eff}$ the diffusion coefficient reads

$$D_{bd,1/\nu} \sim f_t \frac{v_{Deff}^2}{\nu_{eff}} \sim \frac{1}{\nu_*}\frac{1}{N_c q}\left(\frac{\delta}{\epsilon}\right)^2 D_P$$

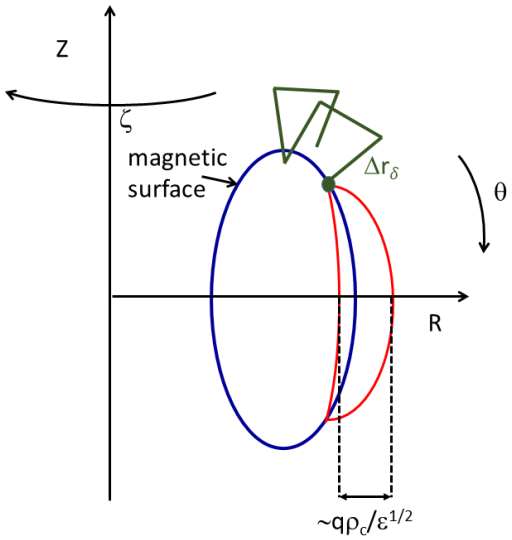

Figure 10: Schematic random motion of a banana tip under the effect of ripple and collisions. The displacement Δr_δ is given by Eq.(6). It changes sign depending on toroidal and poloidal angles.

This expression resembles the $1/\nu$ diffusion coefficient already met for locally trapped particles - a catastrophic behaviour. Once again drifts save the day whenever $\nu_{eff} \ll \omega_{d\zeta}$. The jump time becomes shorter because a particle covers a large number of periods before a collision. This leads to a reduction of the above coefficient by $(\nu_{eff}/\Omega_{d\zeta})^2$. The resulting diffusion coefficient is better written

$$D_{bd} \sim f_t v_{Deff}^2 \frac{\nu_{eff}}{\omega_{d\zeta}^2 + \nu_{eff}^2} \sim \frac{1}{\nu_*} \frac{1}{N_c q} \left(\frac{\delta}{\epsilon}\right)^2 \frac{D_p}{1 + \left(\frac{N_c \Omega_d}{\nu_{eff}}\right)^2}$$

We now see that at low collision frequency, the diffusion coefficient is proportional to ν. So in summary one finds

ripple-plateau	$\frac{D_{rp}}{D_p} = N_c q \left(\frac{\delta}{\epsilon}\right)^2$	when $\Omega_b \ll \nu_{eff}$
banana-drift $1/\nu$	$\frac{D_{bd,1/\nu}}{D_p} = \frac{1}{\nu_*} \frac{1}{N_c q} \left(\frac{\delta}{\epsilon}\right)^2$	when $N_c \Omega_{d\zeta} \ll \nu_{eff} \ll \Omega_b$
banana-drift ν-linear	$\frac{D_{bd}}{D_p} = \left(\frac{\nu_{eff}}{N_c \Omega_{d\zeta}}\right)^2 D_{bd,1/\nu}$	when $\nu_{eff} \ll N_c \Omega_{d\zeta}$

Note that $\nu_{eff}/\Omega_b = \nu_*(N_c q)^2$. It appears that all diffusion coefficients normalised to the plateau reference depends on 3 dimensionless parameters ν_*, $N_c q$ and δ/ϵ, plus the ratio $\omega_{d\zeta}/\nu_{eff}$. As for superbananas, these expressions are dubious at low frequencies, because of complications coming from boundary layers (in the case $\delta < \epsilon$) and resonances $\Omega_{d\zeta} = 0$.

3 General results

We aim now at a detailed calculation of neoclassical fluxes. Our starting point is a tokamak magnetic configuration, an emblematic example of axisymmetric configuration. It can be generalised to other magnetic configurations that exhibit a symmetry, typically helically symmetric stellarators. As mentioned above, there exists already several overviews and textbooks that address this topic. It turns out that exact analytical solutions can be found in many situations. We use here a variational approach that allows the use of general principles stated in the lecture note on "mean field kinetic theory". Though the results are the same, the spirit is somewhat different. Besides it offers unified approach and thus a fruitful comparison with other topics such as turbulent transport and kinetic MHD.

3.1 Drift kinetic equation

Collisional transport is mainly associated with processes at large spatial scales, i.e. larger than a gyroradius. This implies that a gyrokinetic formulation is of no need in that matter, though of course it could be used as well - this is actually mandatory when combining neoclassical and turbulent transport. For now, we use the so-called drift-kinetic approach. There exists in fact several formulations, depending on the choice of variables. The derivation chosen here aims at computing a distribution function for each species, which depends on the guiding-centre position $\mathbf{X} = (\psi, \theta, \zeta)$, magnetic moment μ (an invariant of motion), sign of the parallel velocity $\epsilon_\parallel$ (for passing particles), and total energy (the same as the guiding-centre Hamiltonian) $H = E + e_a\Phi_{eq}$, where Φ_{eq} is the electric potential, and $E = \frac{1}{2}m_a v_\parallel^2 + \mu B_{eq}(\psi, \theta)$. Axisymmetry is reflected by the independence of the Hamiltonian on ζ, and consequently of the distribution function, which does not depend on ζ. Neoclassical theory aims at computing *equilibria in steady-state*, hence is time independent. This does not mean that the total energy H is constant, reason being that in a tokamak an electric field is produced by an inductive field $\mathbf{E}_{ind} = -\frac{\partial \mathbf{A}}{\partial t}$. This field is small compared to the contribution due to the electric potential - so that

$$\frac{dH}{dt} = e_a \mathbf{v}_G \cdot \mathbf{E}_{ind} \simeq e_a v_\parallel E_{ind} \tag{7}$$

where E_{ind} is the parallel component of the inductive field. The inductive effect has little effect on ions, but a crucial one since it is responsible for the current that drives the poloidal field in a tokamak. To simplify the discussion, it will be ignored for now, and re-established when the case of electrons will be discussed.

The drift-kinetic equation then reads

$$v_\parallel \nabla_\parallel F + \mathbf{v}_D \cdot \nabla F = C[F] \tag{8}$$

where F is a function of $\left(H, \mu, \epsilon_\parallel, \psi, \theta\right)$, $\mathbf{v}_D$ and $\mathbf{v}_E$ are the magnetic and $E \times B$ drift velocities, and $\mathcal{C}[F]$. The full collision operator is a complex object - in general it is replaced by a reduced model. An equivalent formulation is

$$-\{H, F\} = C[F] \tag{9}$$

where the bracket designates a Poisson bracket, detailed in the lecture note on trajectories. This is where we start to depart from the traditional approach. In order to use the invariants of motion in the best way possible, it is convenient to replace the poloidal flux ψ, which labels the magnetic surface where the particle is located, by the particle canonical toroidal momentum $P_\zeta = -e_a\psi + m_a \frac{I}{B} v_\parallel$, or equivalently by any other invariant constructed with P_ζ that is dimensional to a flux, for instance[7] $\psi_* = -P_\zeta/e_a$. Since it may be disturbing for the reader, let us comment this point. Let is ignore the collision operator and expand the distribution function as a power series in the small parameter ρ_*

$$F = F_0 + F_1 + o(\rho_*^2)$$

Since $v_D/v_\parallel \sim o(\rho_*)$, it appears from Eq.(8) that $\nabla_\parallel F = 0$, hence F does not depend on θ. An expansion of Eq.(8) then yields an equation over F_1

$$v_\parallel \nabla_\parallel F_1 = -\frac{\partial F_M}{\partial \psi}\, \mathbf{v}_D \cdot \nabla\psi|_{H,\psi}$$

The invariance of P_ζ implies that

$$\mathbf{v}_D \cdot \nabla\psi|_{H,\psi} = v_\parallel \nabla_\parallel \left(\frac{I}{e_a B_{eq}} m_a v_\parallel \right)$$

[7] An alternative choice is $\bar{\psi} = -m_a \left\langle \frac{I}{B_{eq}} v_\parallel \right\rangle_t - P_\zeta/e_a$, where the bracket is a time average.

so that an explicit expression of F_1 is derived

$$F_1 = -m_a v_\parallel \frac{I}{e_a B_{eq}} \left. \frac{\partial F_M}{\partial \psi} \right|_{H,\psi} \tag{10}$$

In the "Hamiltonian" approach, the solution of Eq.(9) without equation is a distribution function that depends on the invariants of motion only, i.e. $F = F_0\left(\psi_*, H, \mu, \epsilon_\parallel\right)$. A Taylor expansion based on the expression of $\psi_* = \psi - \frac{I}{e_a B_{eq}} m_a v_\parallel$ immediately reproduces the result Eq.(10), hence proving the equivalence between the two approaches.

3.2 Structure of flows

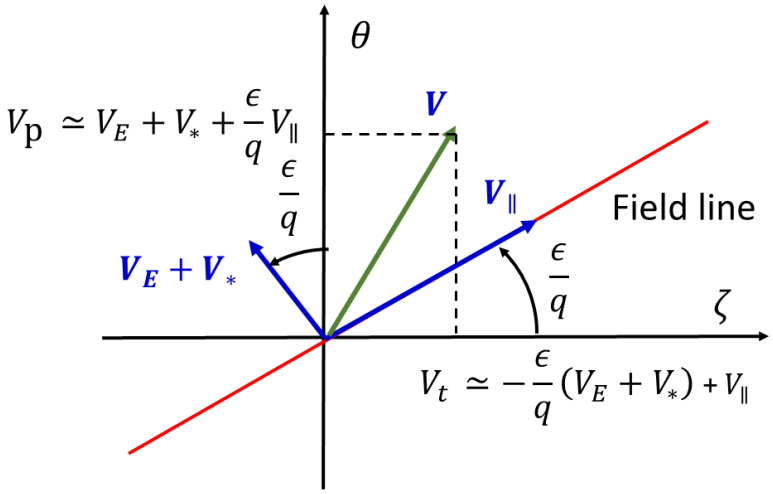

Figure 11: Structure of flows in a tokamak. The plasma fluid velocity is the sum of a parallel flow, plus perpendicular diamagnetic and $E \times B$ flows. Hence the toroidal velocity is close to the parallel velocity minus the projection of perpendicular flows.

Neoclassical theory aims at calculating the solution of equation Eq.(9). As said, the solution of $\{H, F\} = 0$ is a function of invariants of motion $(H, \mu, \psi_*, \epsilon_\parallel)$, or equivalently of the 3 action variables $\mathbf{J}$. On the other hand, the solution of $C(F) = 0$ is a local Maxwellian, which is usually not a function of invariants of motion. Hence the difficulty is to reconcile these two asymptotic solutions of the kinetic equation. This can be done numerically. A different strategy is adopted here by guessing an approximate solution, then compute a perturbed distribution function and associated transport. The trial distribution function is

$$F_0(\mathbf{J}) = F_{M0}(\mathbf{J}) \left\{ 1 + \frac{m_a}{T_{eq}} \bar{v}_\parallel(\mathbf{J}) W_\parallel(\mathbf{J}) \right\} \tag{11}$$

where $\bar{v}_\parallel(\mathbf{J})$ has the same parity as the parallel velocity, but is a function of the invariants of motion. The reasons for this choice are commented in Appendix C. The function F_{M0} is an unshifted Maxwellian

$$F_{M0}(H, \psi_*) = \mathcal{N}_{eq}(\psi_*) \left(\frac{m_a}{2\pi T_{eq}(\psi_*)} \right)^{3/2} \exp\left\{ -\frac{H}{T_{eq}(\psi_*)} \right\}$$

where

$$\mathcal{N}_{eq}(\psi) = N_{eq}(\psi) \exp\left(\frac{e_a \Phi_{eq}(\psi)}{T_{eq}(\psi)} \right)$$

is an effective density. The function $W_\parallel(\mathbf{J})$ can be calculated exactly in standard neoclassical theory, at least for some model operators - here it will be build in a different way. The notation $\mathbf{J}$ stands for $(H, \mu, \psi_*, \epsilon_\parallel)$. Before moving to detailed calculations, it is interesting to analyse the consequences of the trial distribution function Eq.(11). Flows are averages of the distribution function over moments. Hence the computation of the parallel flows from Eq.(11) requires to perform integrals over the velocity space. The volume integration in the guiding-centre in the phase space is

$$d\gamma = d^3\mathbf{x}d^3\mathbf{p} = d\mathcal{V}m_a^3 dv_\parallel \frac{2\pi}{m_a} B_\parallel^* d\mu$$

where $d\mathcal{V} = d\psi \frac{d\theta}{\mathbf{B}_{eq}\cdot\nabla\theta} d\zeta$ is a volume element in the physical space and $B_\parallel^* = B_{eq} + \frac{m_a v_\parallel}{e_a}\mathbf{e}_\parallel \cdot \nabla \times \mathbf{e}_\parallel$ is the Jacobian of the guiding-centre transform. It turns out that $B_\parallel^* = B + o(\rho_*\beta)$ - since β is small in fusion plasmas, i.e. scales as ρ_*, we set $B_\parallel^* = B_{eq}$ up to second order in the small parameter ρ_*. The parallel velocity and magnetic moment are not suitable variables whenever collisions come into play - the reason is that the test particle collision particle operator is separable in velocity and pitch-angle angle. A first step is to make use of the kinetic energy E and pitch-angle variable $\lambda = \mu B_0/E$ - here, B_0 is a reference magnetic field. The parallel velocity then reads

$$v_\parallel(\psi, \theta, E, \lambda) = \pm\sqrt{\frac{2T_{eq}(\psi)}{m_a}}\left(\frac{E}{T_{eq}}\right)^{1/2}\sqrt{1 - \lambda b(\psi, \theta)}$$

where $b(\psi, \theta) = B(\psi, \theta)/B_0$. The weighted element of phase space reads

$$d\gamma F_{M0} = d\mathcal{V}\frac{1}{\sqrt{\pi}}\sum_{\epsilon_\parallel=\pm1}\frac{dE}{T_{eq}}\left(\frac{E}{T_{eq}}\right)^{1/2}\exp\left(-\frac{E}{T_{eq}}\right)\frac{b(\psi, \theta)d\lambda}{2\sqrt{1 - \lambda b(\psi, \theta)}} \tag{12}$$

We are now in a position to compute the "parallel velocity" $\bar{v}_\parallel$, function of invariants of motion. Using Eq.(10), let us note that

$$F_{M0}(\psi_*, H) = F_{M0}(\psi, E)\left\{1 - \frac{m_a}{T_{eq}(\psi)}v_\parallel(\psi, \theta, E, \lambda)V_{*\zeta}(\psi, \theta, E)\right\} \tag{13}$$

where

$$V_{*\zeta}(\psi, \theta, E) = I(\psi)\frac{T_{eq}(\psi)}{e_a B_{eq}(\psi, \theta)}\frac{\partial\Xi}{\partial\psi}(\psi, E) \tag{14}$$

and

$$\frac{\partial\Xi}{\partial\psi} = \left.\frac{\partial \ln F_M}{\partial\psi}\right|_{\psi,H} = \frac{dP_{eq}}{P_{eq}d\psi} + \frac{e_a}{T_{eq}}\frac{d\Phi_{eq}}{d\psi} + \left(\frac{E}{T_{eq}} - \frac{5}{2}\right)\frac{dT_{eq}}{T_{eq}d\psi} \tag{15}$$

The field $V_{*\zeta}$ is dimensional to a velocity, and turns out to coincide with the toroidal component of the diamagnetic velocity. Combining Eq.(11) with Eq.(13), one finds

$$F_0 = F_{M0}\left[1 + \frac{m_a}{T_{eq}}\left(\bar{v}_\parallel W_\parallel - v_\parallel V_{*\zeta}\right)\right] \tag{16}$$

Let us recall that $\bar{v}_\parallel$ is a function of the invariants of motion, hence $(H, \lambda, \psi_*, \epsilon_\parallel)$. Since this term is of order of ρ_* second order corrections can be ignored, so that ψ_* can be replaced by ψ (equivalent to an approximation of thin orbits) and $\bar{v}_\parallel$ can thus be as well written as a function of $(E, \lambda, \psi, \epsilon_\parallel)$. As said, it can be computed exactly when using a model collision operator [5]. Its general structure is

$$\bar{v}_\parallel(\psi, E, \lambda, \epsilon_\parallel) = \epsilon_\parallel\sqrt{\frac{2T_{eq}}{m_a}}\left(\frac{E}{T_{eq}}\right)^{1/2}v_\lambda(\psi, \lambda) \tag{17}$$

Moreover the function $W_\parallel$ can be written as

$$W_\parallel(\psi, E) = W_{\parallel 0}(\psi) + W_{\parallel 1}(\psi)\left(\frac{E}{T_{eq}} - \frac{5}{2}\right)$$

This corresponds to an expansion in the 2 first Sonine polynomial $S_0(E/T_{eq}) = 1$ and $S_1(E/T_{eq}) = (5/2 - E/T_{eq})$ - see Appendix C for a short introduction to expansions in Sonine and Legendre polynomials. Given Eqs.(14,15), the distribution function finally reads

$$F_0 = F_{M0}\left[1 + \frac{\mathcal{U}_{eq}}{T_{eq}}\right] \tag{18}$$

where

$$\mathcal{U}_{eq}(\psi, \theta, \lambda, E, \epsilon_\parallel) = \mathcal{U}_0(\psi, \theta, \lambda, \epsilon_\parallel) + \mathcal{U}_1(\psi, \theta, \lambda, \epsilon_\parallel)\left(\frac{E}{T_{eq}} - \frac{5}{2}\right)$$

is part of the thermodynamical potential that is odd in parallel velocity. Its components are of the form

$$\mathcal{U}_n = m_a \bar{v}_\parallel W_{\parallel n} - m_a v_\parallel V_{*\zeta n}$$

where

$$V_{*\zeta 0} = \frac{I T_{eq}}{e_a B_{eq}}\left(\frac{dP_{eq}}{P_{eq} d\psi} + \frac{e_a}{T_{eq}}\frac{d\Phi_{eq}}{d\psi}\right) \tag{19}$$

$$V_{*\zeta 1} = \frac{I}{e_a B_{eq}}\frac{dT_{eq}}{d\psi} \tag{20}$$

We are now in position to compute from Eq.(16) the mean parallel velocity

$$V_{\parallel eq}(\psi, \theta) = \frac{1}{N_{eq}}\int d^3\mathbf{p} v_\parallel F_0$$

and the parallel heat flux

$$q_{\parallel eq}(\psi, \theta) = \frac{P_{eq}}{N_{eq}}\int d^3\mathbf{p}\left(\frac{E}{T_{eq}} - \frac{5}{2}\right) v_\parallel F_0$$

After some calculations detailed in Appendix D, the following expressions of the mean parallel velocity and heat fluxes are found

$$V_{\parallel eq}(\psi, \theta) = -\left(\frac{1}{N_{eq} e_a}\frac{dP_{eq}}{d\psi} + \frac{d\Phi_{eq}}{d\psi}\right)\frac{I(\psi)}{B_{eq}(\psi, \theta)} + f_c W_{\parallel 0}(\psi)\frac{B_{eq}(\psi, \theta)}{B_0} \tag{21}$$

and

$$\frac{2}{5}\frac{q_{\parallel eq}(\psi, \theta)}{P_{eq}(\Psi)} = -\frac{I(\psi)}{B_{eq}(\psi, \theta)}\frac{1}{e_a}\frac{dT_{eq}}{d\psi} + f_c W_{\parallel 1}(\psi)\frac{B_{eq}(\psi, \theta)}{B_0} \tag{22}$$

Several important conclusions can be drawn from these two expressions:

- Parallel velocity and heat flux are not surface flux functions, i.e. do not depend on ψ only

- this is consistent with considerations that come from fluid dynamics. Indeed using $\mathbf{V} = \mathbf{V}_E + \mathbf{V}_* + V_{\parallel eq}\mathbf{e}_\parallel$, where $\mathbf{V}_* = \frac{\mathbf{B}_{eq}\times\nabla P_{eq}}{N_{eq} e_a B_{eq}^2}$ is the diamagnetic velocity, and $\mathbf{V}_E = \frac{\mathbf{B}_{eq}\times\nabla\Phi_{eq}}{B_{eq}^2}$ the $E \times B$ drift velocity, plus the condition $\nabla \cdot \mathbf{V} = 0$, it appears that the fluid velocity is of the form

$$\mathbf{V} = K(\psi)\mathbf{B}_{eq} - \left(\frac{1}{N_{eq} e_a}\frac{dP_{eq}}{d\psi} + \frac{d\Phi_{eq}}{d\psi}\right) R^2 \nabla\zeta \tag{23}$$

In the same way, the heat flux is found of the form

$$\mathbf{q} = L(\psi)\mathbf{B}_{eq} - \frac{5}{2}\frac{P_{eq}}{e_a}\frac{dT_{eq}}{d\psi}R^2\nabla\zeta \tag{24}$$

Projecting these relations along the unit vector $\mathbf{e}_{\|}$ yields the same expression as Eqs.(21, 22), with $K = f_c W_{\|0}/B_0$, and $L = \frac{5}{2}P_{eq}f_c W_{\|1}/B_0$. In other words, the velocity $V_{*\zeta}$ can be identified with the toroidal projection of the diamagnetic and $E \times B$ drift velocities, while $W_{\|}$ is the non diamagnetic part of the plasma toroidal flow.

- this poloidally asymmetric parts of the parallel velocity and heat flux are called Pfirsch-Schlüter flows. They result from the compressibility of the perpendicular velocity (or heat flux), which must be balanced by a parallel flow. This mechanism is illustrated in Fig.12.

- Hence the velocity $V_{*\zeta}$ is clearly related to the toroidal projection of the diamagnetic velocity. It will loosely be called diamagnetic velocity in the following. The sign minus can be understood with the help of Fig. 11.

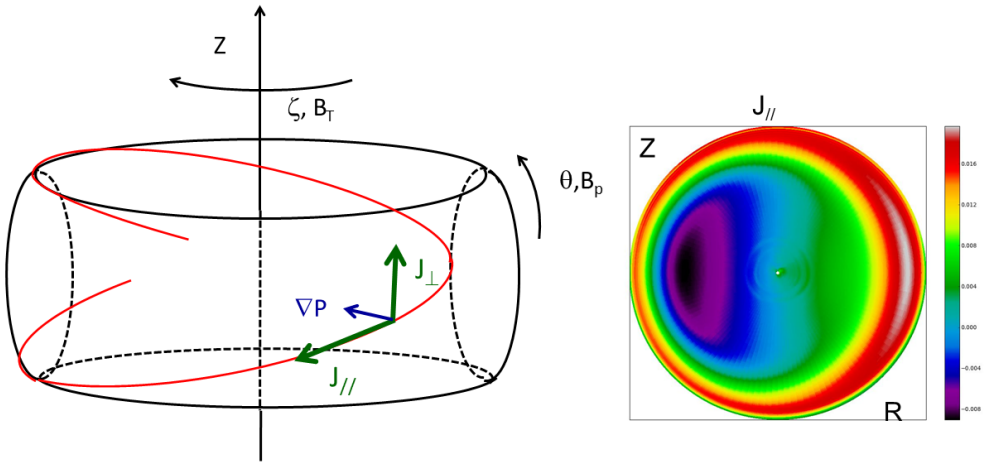

Figure 12: Illustration of the Pfirsch-Schlüter on current density. The diamagnetic perpendicular current density that satisfies a magnetostatic equilibrium is $\mathbf{J}_{dia} = \frac{\mathbf{B}_{eq}}{B_{eq}^2} \times \nabla P_{eq}$. Its divergence is non zero and must be balanced by a parallel current density such that $\nabla \cdot \left(J_{\|}\mathbf{e}_{\|} + \mathbf{J}_{dia}\right) = 0$. This process is illustrated on the left panel. Note that the part of the diamagnetic current that bears a non zero divergence is near vertical, and is in fact related to the magnetic drift of particles. The right panel shows the contour line of a parallel Pfirsch-Schlüter flows (here for a heavy impurity) as computed by the GYSELA code.

3.3 Variational principle

3.3.1 Entropy functional

A variational principle is used here to compute neoclassical transport coefficients. Obviously, much of forthcoming derivations involve a collision operator. The latter is essentially

a Boltzmann collision operator derived for Coulombian interaction, i.e. the Fokker-Planck equation reads

$$\frac{\partial F_a}{\partial t} - \{H_a, F_a\} = \sum_b C_{ab}(F_a, F_b) \tag{25}$$

where $C_{ab}(F,F_b)$ is the collisional operator between particles of species a and b

$$C_{ab}\left(F_a, F_b\right) = \frac{1}{2}\gamma_{ab}\frac{\partial}{\partial \mathbf{p}} \cdot \int d^3\mathbf{p}' \mathfrak{L} \cdot \left(F_b(\mathbf{x}, \mathbf{p}', t)\frac{\partial F_a(\mathbf{x}, \mathbf{p}, t)}{\partial \mathbf{p}} - F_a(\mathbf{x}, \mathbf{p}, t)\frac{\partial F_b(\mathbf{x}, \mathbf{p}', t)}{\partial \mathbf{p}'} \right) \tag{26}$$

where

$$\gamma_{ab} = 4\pi \frac{e_a^2 e_b^2}{\left(4\pi\epsilon_0\right)^2} \ln \Lambda$$

with $\ln \Lambda$ the Coulombian logarithm, and

$$\mathfrak{L} = \frac{u^2\mathbf{I} - \mathbf{u}\mathbf{u}}{u^3}$$

with

$$\mathbf{u} = \frac{\partial H_a(\mathbf{x}, \mathbf{p}, t)}{\partial \mathbf{p}} - \frac{\partial H_b(\mathbf{x}, \mathbf{p}', t)}{\partial \mathbf{p}'}$$

the relative velocity. When resonant Hamiltonian perturbations are accounted for, additional sources of entropy production come from the resonant motion of particles. This case was treated in the note "Mean field kinetic theory". Details can be found in the references [9, 10, 11]. The distribution function of a species "a" is written

$$F_a = \exp\left(-\frac{H_a - U_a}{T_0}\right)$$

where H_a is the total Hamiltonian and U_a a thermodynamic potential. The unperturbed part of the distribution function reads similarly

$$F_{eq,a} = \exp\left[-\frac{1}{T_0}\left(H_{eq,a} - U_{eq,a}\right)\right] \tag{27}$$

where $H_{eq,a}$ and $U_{eq,a}$ are the mean parts of the Hamiltonian and thermodynamic potential. An entropy functional is then derived that reads

$$\mathcal{S} = \sum_a \mathcal{S}_{t,a} + \sum_a \mathcal{S}_{res,a} + \sum_{ab} \mathcal{S}_{coll,ab}$$

where

$$\mathcal{S}_{t,a}\left(U_{eq,a}, U_{eq,a}^\dagger\right) = \frac{2}{T_0^2}\int d\gamma F_{eq,a} U_{eq}^\dagger \frac{\partial U_{eq,a}}{\partial t} \tag{28}$$

$$\mathcal{S}_{res,a}\left(U_{eq,a}, U_{eq,a}^\dagger\right) = -\frac{2}{T_0^2}\int d\gamma \frac{\partial U_{eq,a}^\dagger}{\partial \mathbf{J}} \cdot \mathbf{\Gamma}_a \tag{29}$$

and

$$\begin{aligned}\mathcal{S}_{coll,ab}(U_{eq,a}^\dagger, U_{eq,b}^\dagger) = {} & \frac{\gamma_{ab}}{4T_0^2}\int d^3\mathbf{x} d^3\mathbf{p} d^3\mathbf{p}' F_{H_a,eq} F_{H_b,eq} \\ & \left[\frac{\partial U_{eq,a}^\dagger}{\partial \mathbf{p}} - \frac{\partial U_{eq,b}^\dagger}{\partial \mathbf{p}'}\right] \cdot \mathfrak{L} \cdot \left[\frac{\partial U_{eq,a}^\dagger}{\partial \mathbf{p}} - \frac{\partial U_{eq,b}^\dagger}{\partial \mathbf{p}'}\right]\end{aligned} \tag{30}$$

where

$$\nabla_{\mathbf{J}} \cdot \mathbf{\Gamma}_a = -\left\langle \{H_a, U_a\} \right\rangle$$

and the bracket is an average over the angle variables and time. Incidentally, this expression demonstrates the self-adjointness property of the collision operator. The extremum of the functional $\mathcal{S}$ for all variations of $U^\dagger_{eq,a}$ near $U_{eq,a}$ yields a transport equation

$$\frac{\partial U_{eq,a}}{\partial t} + \nabla_{\mathbf{J}} \cdot \mathbf{\Gamma}_a = \sum_b \mathcal{C}_{ab}(U_{eq,a}, U_{eq,b})$$

This entropy principle is close to the one devised by Rosenbluth et al. [12].

3.3.2 Structure of the resonant entropy production rate

It will be seen in the following that under reasonable assumptions, $U_{\parallel,a1} = 0$, while $U_{\parallel,a0}$ can be identified as the equilibrium parallel velocity $V_{\parallel,a}$. For a given species, fluxes and thermodynamical forces can be properly defined from the resonant production rate using the following expression

$$\begin{aligned}\dot{S}_{res,a} &= -2\int d^3\mathbf{x} N_{eq,a}\left(\frac{\Gamma_{Na}}{N_{eq,a}}\left(\frac{d\ln N^\dagger_{eq,a}}{d\psi} + \frac{e_a}{T_{eq,a}}\frac{d\Phi^\dagger_{eq}}{d\psi}\right)\right. \\ &+ \left.\frac{\mathcal{M}_{\parallel,a}}{N_{eq,a}m_a v_{Ta}}\frac{V^\dagger_{\parallel eq,a}}{v_{Ta}} + \frac{\Gamma_{Ta}}{N_{eq,a}T_{eq,a}}\frac{d\ln T^\dagger_{eq,a}}{dr}\right)\end{aligned}$$

where Γ_{Na} and Γ_{Ta} are the particle and heat fluxes, and $\mathcal{M}_{\parallel,a}$ is the rate of dissipated parallel momentum due to collisional transport. Resonant fluxes are therefore functional derivatives of the resonant entropy production rate.

3.3.3 Entropy production rate due to profile evolution

The entropy production rate due to profile evolution reads for a single species

$$\mathcal{S}_t\left(U_{eq}, U^\dagger_{eq}\right) = \frac{2}{T_0^2}\int d\gamma F_{eq,a} U^\dagger_{eq,a}\frac{\partial U_{eq,a}}{\partial t}$$

Using the expression Eq.(33), an explicit expression is

$$\begin{aligned}\mathcal{S}_t\left(U_{eq}, U^\dagger_{eq}\right) &= 2\int d\gamma F_{eq,a}\left[\ln N^\dagger_{eq,a} + \frac{e_a\Phi^\dagger_{eq}}{T_{eq,a}} + \right. \\ &\left. E\left(\frac{1}{T^\dagger_{eq,a}} - \frac{1}{T_0}\right) - \frac{3}{2}\ln T^\dagger_{eq} + \frac{m_a v_\parallel V^\dagger_{\parallel eq,a}}{T_{eq,a}}\right] \\ &\left[\frac{\partial \ln N_{eq,a}}{\partial t} + \left(\frac{E}{T_{eq}} - \frac{3}{2}\right)\frac{1}{T_{eq,a}}\frac{\partial T_{eq,a}}{\partial t} + \frac{m_a v_\parallel}{T_{eq,a}}\frac{\partial V_{\parallel eq,a}}{\partial t}\right]\end{aligned}$$

This expression can be made somewhat more enlightening by assuming that $U^\dagger_{eq,a}$ is close to $U_{eq,a}$, so that

$$\begin{aligned}\mathcal{S}_t\left(U_{eq}, U^\dagger_{eq}\right) &= 2\int d\gamma F_{eq,a}\left[\frac{\delta N_{eq,a}}{N_{eq,a}} + \frac{e_a\delta\Phi_{eq}}{T_{eq,a}} + \right. \\ &\left.\left(\frac{E}{T_{eq,a}} - \frac{3}{2}\right)\frac{\delta T_{eq,a}}{T_{eq,a}} + \frac{m_a v_\parallel \delta V_{\parallel eq,a}}{T_{eq,a}}\right] \\ &\left[\frac{1}{N_{eq,a}}\frac{\partial N_{eq,a}}{\partial t} + \left(\frac{E}{T_{eq,a}} - \frac{3}{2}\right)\frac{1}{T_{eq,a}}\frac{\partial T_{eq,a}}{\partial t} + \right. \\ &\left.\frac{m_a v_\parallel}{T_{eq,a}}\frac{\partial V_{\parallel eq,a}}{\partial t}\right]\end{aligned} \tag{31}$$

where $\delta N_{eq,a} = N^\dagger_{eq,a} - N_{eq,a}$, $\delta T_{eq,a} = T^\dagger_{eq,a} - T_{eq,a}$, and $\delta V_{\parallel eq,a} = V^\dagger_{\parallel eq,a} - V_{\parallel eq,a}$.

4 Single ion species

4.1 Resonant entropy production rate

As mentioned above, the low collisionality regime is deeply impacted by resonant particles at vanishing parallel velocity $v_\parallel = 0$.

4.1.1 General formulation

The resonant entropy production rate can be calculated exactly for some model collision operators. We use here a different approach. We consider Hamiltonian systems such the unperturbed motion of particles is integrable and quasi-periodic, and therefore characterised by 3 invariants of motion, and 3 angle variables. The resonant entropy production rate can be calculated for any Hamiltonian perturbation that involve a single helical perturbation. We use here a trick that consists in separating the magnetic field B into a part B_0 that does not depend on θ (it may depend on ψ though), and a remaining part $\tilde{B}$ that is considered as a perturbation. This makes sense only if $\tilde{B}$ is smaller than B_0 - this is equivalent to consider tokamaks with a small inverse aspect ratio $\epsilon \ll 1$, a stringent but acceptable limitation as long as the objective is to illustrate the neoclassical machinery. Species labels are dropped in this section (except for charge and mass) since the resonant entropy production rate results from the dynamics of the considered species only. The Hamiltonian can be split in "equilibrium" and perturbed parts

$$H = H_{eq} + \widetilde{H}$$

where $H_{eq} = 1/2 m_i v_\parallel^2 + \mu B_0 + e_i \Phi_{eq}(J_3)$[8] and $\widetilde{H} = \mu \tilde{B}$, where e_i is the ion charge, and m_i its mass. This means that at lowest order in ϵ, no particle trapping occurs. The magnetic configuration is assimilable to a periodic screw pinch. Trapping emerges when adding the perturbed part of the Hamiltonian

$$\widetilde{H} = -\mu B_0 \epsilon \cos\theta$$

For $\epsilon \ll 1$, the expression of the third action reads

$$J_3 = e_i \psi - m_i R_0 u_\parallel$$

where $I = B_0 R_0$ has been used, and $u_\parallel$ is the parallel velocity of passing particles in a screw pinch, an invariant of motion[9]. At equilibrium, particles stay on magnetic surfaces, so that the second action reads

$$J_2 = e_i \chi(\psi)$$

Using $d\ell \simeq q R d\theta$, $d\chi/d\psi = q$, it appears that $J_2 \simeq e_a \chi(\psi)$. This gives an explicit expression of $u_\parallel$ as function of (J_2, J_3)

$$u_\parallel(J_2, J_3) = \frac{1}{m_i R_0}\left(J_3 - G(J_2)\right)$$

where $G(J_2) = e_i \psi(J_2/e_i)$, and $dG/dJ_2 = 1/q(J_2/e_i)$, q is the safety factor expressed as function of the toroidal flux χ. It can be verified that $\Omega_2 = u_\parallel/(qR_0)$ and $\Omega_3 \simeq u_\parallel/R_0$, where the $E \times B$ poloidal drift frequency $e_i \frac{d\Phi}{dJ_3}$ is neglected compared with the toroidal transit frequency $u_\parallel/R_0$ (the ratio is of order ρ_*). The resonant condition $u_\parallel = 0$ reads

$$J_3 = G(J_2)$$

[8] The dependence Φ_{eq} on J_3 is demonstrated in the note on trajectories

[9] Again, this is not true in a torus.

and draws a surface in the action space $\mathbf{J} = (J_1, J_2, J_3)$. Remains to compute the entropy production rate due to the perturbed Hamiltonian. Fortunately, this calculation is standard (see note an "Mean field kinetic theory") and produces the following result

$$\mathcal{S}_{res}\left[U_{eq}, \partial_{\mathbf{J}} U_{eq}^{\dagger}\right] = \frac{1}{T_0^2}\int d\gamma F_{eq}(\mathbf{J})\delta(\mathbf{n}\cdot\mathbf{\Omega})h^2(\mathbf{J})\Lambda(\mathbf{J})\left(\mathbf{n}\cdot\frac{\partial U_{eq}^{\dagger}}{\partial \mathbf{J}}\right)^2 \tag{32}$$

where

$$\Lambda(\mathbf{J}) = \begin{cases} \frac{\pi}{2} & \eta \geq 1 \\ 2\mathcal{I}\eta & \eta \leq 1 \end{cases}$$

and $\mathcal{I} \simeq 1.38$. The parameter η is defined as the ratio $\eta = \tau_b/\tau_d$ of a bounce time $\tau_b = 1/\omega_b$ to the detrapping time τ_d. The later is defined as $\tau_d = \omega_b^2/D_\Omega$, where $D_\Omega = \frac{1}{2}\left\langle \Delta\Omega^2 \right\rangle/\Delta t$ is the Fokker-Planck diffusion coefficient of the resonant pulsation $\Omega = \mathbf{n}\cdot\mathbf{\Omega} - \omega$ due to collisions. Hence

$$\eta = \frac{D_\Omega}{\omega_b^3} = \frac{1}{2}\frac{\left\langle \Delta\Omega^2 \right\rangle}{\Delta t}\frac{1}{\omega_b^3}$$

The expression for $\eta \gg 1$ breaks down for large values of η. It ultimately decreases as $1/\eta$. The entropy production rate corresponds to a perturbed Hamiltonian of the form

$$\widetilde{H} = -h\cos(\mathbf{n}\cdot\boldsymbol{\alpha} - \omega t)$$

For the case considered, $\omega = 0$, $n_2 = 1$ and $n_1 = n_3 = 0$ and $h = \mu B_0 \epsilon$. The plateau regime corresponds to the collisional regime $\eta \geq 1$. In the opposite case $\eta \leq 1$, the particle experiences many bounce times before it experiences a collision - this is in fact the banana regime. The physics that goes with a resonant increase of entropy is illustrated in Fig. 13.

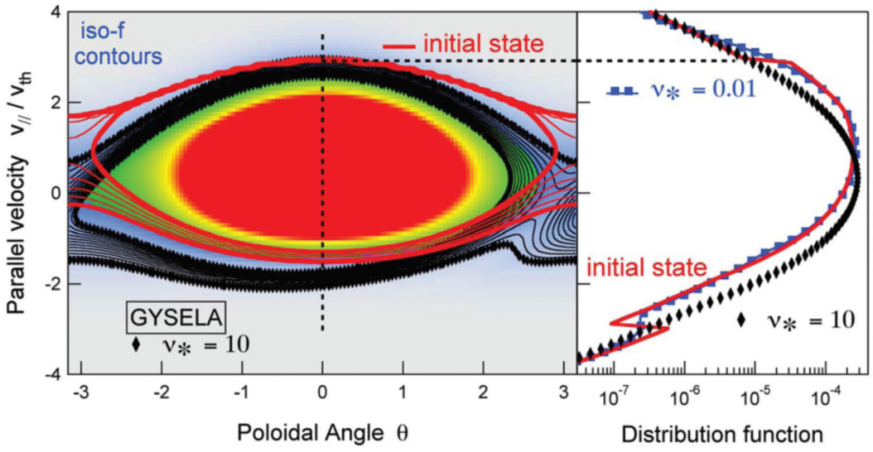

Figure 13: Increase of entropy associated with a boundary layer in the phase space. In presence of a single Hamiltonian perturbation in the phase space, an island develops. The distribution function is constant along the lines of motion. This produces a jump at the island separatrix between the distribution functions outside and inside the island. This discontinuity is resolved by collisions, via the onset of a boundary layer. This figure corresponds to the case of ions in a tokamak (courtesy G. Dif-Pradalier).

4.1.2 Thermodynamical potential

A comparison of the distribution function Eq.(27) with the trial distribution function Eq.(11) provides the thermodynamic potential U_{eq}

$$\frac{U_{eq}}{T_0} = \ln \mathcal{N}_{eq} + H_{eq}\left(\frac{1}{T_{eq}} - \frac{1}{T_0}\right) - \frac{3}{2}\ln T_{eq} + \frac{m_i u_\parallel W_\parallel}{T_{eq}} \tag{33}$$

where the function $\bar{v}_\parallel$ has been assimilated to $u_\parallel$. Keeping in mind that $J_1 = e_i\mu/m_i$, and that $J_3 \simeq -e_i\psi$ at lowest order in ρ_* , partial derivatives of U_{eq} are readily calculated

$$\frac{1}{T_0}\left.\frac{\partial U_{eq}}{\partial J_2}\right|_{J_1,J_3} = \frac{m_i}{T_{eq}}\frac{\partial u_\parallel}{\partial J_2}W_\parallel$$

$$\frac{1}{T_0}\left.\frac{\partial U_{eq}}{\partial J_3}\right|_{J_1,J_2} = -\frac{1}{e_i}\frac{\partial \Xi}{\partial \psi} - \frac{m_i}{e_i T_{eq}}u_\parallel\frac{\partial W_\parallel}{\partial \psi} + \frac{m_i}{T_{eq}}\frac{\partial u_\parallel}{\partial J_3}W_\parallel$$

In the considered case where the unique non zero wave number is $n_2 = 1$, only the partial derivative with respect to J_2 matters

$$\frac{1}{T_0}\left.\frac{\partial U_{eq}}{\partial J_2}\right|_{J_1,J_3} = \frac{1}{T_{eq}}\frac{W_\parallel}{qR_0}$$

4.1.3 Banana-plateau entropy production rate

We are now in a position to compute the entropy resonant production rate. The calculation is restricted to a single ion species to start with - the ion charge number is $Z = 1$ (hydrogenoid ion), so that the plasma is a mix of electrons and ions with equal densities. Let us recall that the perturbed Hamiltonian is $h = \mu B_0\epsilon$ - we define in the following a normalised perpendicular energy $u = \mu B_0/T_{eq}$. For a perturbation $\mathbf{n} = (0, 1, 0)$, The Hamiltonian "curvature" is

$$C = \left.\frac{\partial^2 H_{eq}}{\partial J_2^2}\right|_{J_1,J_3} = \frac{1}{m_i q^2 R_0^2}$$

so that the bounce frequency is

$$\omega_b = \sqrt{Ch} = \frac{\sqrt{\frac{\mu B_0}{m_i}\epsilon}}{qR_0} = \frac{v_{Ti}}{qR_0}\sqrt{u\epsilon}$$

where $v_{Ti} = \sqrt{T_{eq}/m_i}$ is the thermal velocity. Obviously the resonant frequency is $\Omega = \Omega_2 = u_\parallel/qR_0$. The scattering in parallel velocity happens to be

$$\frac{1}{2}\left\langle \Delta v_\parallel^2 \right\rangle = \nu_{d,ii}\frac{v^2}{2} = \nu_{d,ii}v_{Ti}^2 x^2 \tag{34}$$

where[10] $x = \sqrt{E/T_{eq}}$, and ν is the ion-ion collisional frequency. This collision frequency can be split in a thermal value ν_i times a energy dependent form factor $\bar{\nu}(x)$

$$\nu_{d,ii} = \nu_i\bar{\nu}(x) \tag{35}$$

where[11]

$$\nu_i = \frac{4\sqrt{\pi}}{3}\frac{e_i^4}{(4\pi\epsilon_0)^2}\frac{N_{eq}}{m_i^2 v_{Ti}^3}\ln\Lambda$$

[10]The notation x is not particularly smart given that x is often used as a spatial coordinate. But it is the usual notation for calculations that involve collisions. We will stick to it to allow comparison with classical works in the matter.

[11]To compare with Helander-Sigmar's notation $\nu_i = \frac{2}{3}\sqrt{\frac{2}{\pi}}\hat{\nu}_{ii}$ and $\hat{\nu}_{ii} = 1/\tau_{ii}$, $\tau_i = \sqrt{2}\tau_{ii} = \frac{1}{\nu_i}$.

Ω	C	$\langle \Delta\Omega^2 \rangle$	Ω_b	η	$d\gamma F_M \delta(\Omega)$
$\frac{v_\parallel}{qR_0}$	$\frac{1}{m_i q^2 R_0^2}$	$\frac{1}{q^2 R_0^2}\left\langle \Delta v_\parallel^2 \right\rangle$	$\frac{1}{qR_0}\sqrt{\frac{\mu B_0 \epsilon}{m_i}}$	$\eta = \nu_* \frac{\bar{\nu}(\sqrt{u})}{\sqrt{u}}$	$\frac{d^3\mathbf{x}}{\sqrt{2\pi}} dv_\parallel du e^{-u} \delta\left(v_\parallel\right) N_{eq} \frac{qR_0}{v_{Ti}}$

Table 1: Principal parameters when the Hamiltonian perturbation is due to the $1/R$ decay of the magnetic field, and the perturbed Hamiltonian is $\widetilde{H} = -\mu B_0 \epsilon \cos(\theta)$.

is the thermal ion collision frequency. Here $\ln\Lambda$ denotes the Coulomb logarithm. The form factor is given by the following relation

$$\bar{\nu}(x) = \frac{3}{4}\sqrt{2\pi}\frac{\mathrm{erf}(x) - G(x)}{x^3}$$

where

$$\mathrm{erf}(x) = \frac{2}{\sqrt{\pi}}\int_0^x dx' \exp\left(-x'^2\right)$$
$$G(x) = \frac{\mathrm{erf}(x) - x\mathrm{erf}'(x)}{2x^2}$$

Close to the resonance $v_\parallel = 0$, one has $x \simeq (\mu B_0/T_{eq})^{1/2} = \sqrt{u}$. The η parameter thus reads

$$\eta = \nu_{*i}\frac{\bar{\nu}\left(\sqrt{u}\right)}{\sqrt{u}}$$

where is defined in Eq.(2), but for thermal values, i.e. $\nu_{*i} = \frac{\nu_i qR_0}{v_{Ti}\epsilon^{3/2}}$. The weighted element of integration is

$$d\gamma F_M \delta(\Omega) = N_{eq}\frac{qR_0}{v_{Ti}}\frac{d^3\mathbf{x}}{\sqrt{2\pi}} dv_\parallel du e^{-u}\delta\left(v_\parallel\right)$$

All these quantities are summarised in Table 1. The entropy production rate bears a simple form that reads

$$\mathcal{S}_{res}\left[U_{eq}, \partial_{\mathbf{J}} U_{eq}^\dagger\right] = \int \frac{d^3\mathbf{x}}{\sqrt{2\pi}} N_{eq}\frac{v_{Ti}}{qR_0}\epsilon^2 \int_0^{+\infty} du e^{-u}\Lambda(r,u)u^2\left(\frac{W_\parallel}{v_{Ti}}\right)^2 \tag{36}$$

where

$$\Lambda(\mathbf{J}) = \begin{cases} \frac{\pi}{2} & \text{if } \nu_{*i} \geq 1 \\ 2\mathcal{I}\nu_{*i}\frac{\bar{\nu}(\sqrt{u})}{\sqrt{u}} & \text{if } \nu_{*i} \leq 1 \end{cases}$$

4.1.4 Resonant entropy production rate in the low aspect ratio limit

Banana regime

The resonant entropy production rate Eq.(36) can be rewritten in the regime $\nu_* \ll 1$ as

$$\mathcal{S}_{res}\left[U_{eq}, \partial_{\mathbf{J}} U_{eq}^\dagger\right] = \frac{4\mathcal{I}}{\sqrt{2\pi}}\int d^3\mathbf{x} N_{eq}\sqrt{\epsilon}\frac{\nu_i}{v_{Ti}^2}\int_0^{+\infty} dx e^{-x^2} x^4 \bar{\nu}(x) W_\parallel^2$$

where $x^2 = \frac{m_i v^2}{2T_{eq}}$. It is traditional to introduce a bracket $\{\}$ that stands for a weighted average in the velocity space[12]

$$\{G\} = \frac{1}{N_{eq}}\int d^3\mathbf{v}\frac{m_i v_\parallel^2}{T_{eq}} F_{M0} G \tag{37}$$

[12]This bracket is the traditional notation for an average in the velocity space in neoclassical theory. However it should not be confused with the notation $\{\ ,\ \}$ for Poisson brackets. The difference lies in the coma.

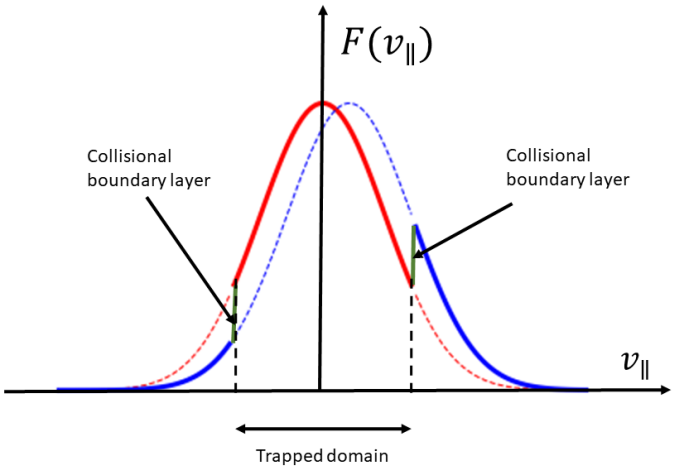

Figure 14: Distribution function near the trapped/passing boundary. Passing particles can move freely along the field lines, so that their distribution is shifted. Trapped electrons cannot move freely, up to their diamagnetic velocity, so that their distribution function is unshifted, when expressed as functions of (H, μ, P_ζ). As a consequence boundary layers develop at the passing/trapped interface, which is resolved by collisions. Resonant neoclassical transport originate from this region.

for any function $G(v, \xi)$. Note that if the G function depends on v only, this average reads as

$$\{G\} = \frac{4\pi}{3} \frac{m_i}{N_{eq} T_{eq}} \int_0^{+\infty} dv v^4 F_{M0} G = \frac{8}{3\sqrt{\pi}} \int_0^{+\infty} dx x^4 e^{-x^2} G(x) \tag{38}$$

The entropy production rate then becomes[13]

$$\mathcal{S}_{res}\left[U_{eq}, \partial_{\mathbf{J}} U_{eq}\right] = \frac{3\mathcal{I}}{2} \int d^3\mathbf{x} N_{eq} \frac{\nu_i}{v_{Ti}^2} \sqrt{\epsilon} \left\{ \nu_{d,ii} \tau_{ii} \left(W_{\parallel 0} - \left(\frac{5}{2} - x^2 \right) W_{\parallel 1} \right)^2 \right\} \tag{39}$$

Introducing the notation $\nu_{ij} = \tau_{ii} \left\{ \nu_{d,ii} S_i S_j \right\}$, a compact expression is

$$\mathcal{S}_{res}\left[U_{eq}, \partial_{\mathbf{J}} U_{eq}\right] = \sqrt{2} \int d^3\mathbf{x} N_{eq} \frac{\nu_i}{v_{Ti}^2} f_t \left[\nu_{00} W_{\parallel 0}^2 - 2\nu_{01} W_{\parallel 0} W_{\parallel 1} + \nu_{11} W_{\parallel 1}^2 \right] \tag{40}$$

where $f_t = \frac{3\mathcal{I}}{2\sqrt{2}} \sqrt{\epsilon} \simeq 1.46\sqrt{\epsilon}$ is the fraction of passing particles, close to the value found in the literature even if the calculation is done differently. This expression can be made quantitative by using the relationships

$$\begin{aligned} \tau_{ii} \left\{ \nu_{d,ii} \right\} &= \left(2 - \sqrt{2} \ln \left(1 + \sqrt{2} \right) \right) \\ \tau_{ii} \left\{ \nu_{d,ii} x^2 \right\} &= \frac{1}{\sqrt{2}} \\ \tau_{ii} \left\{ \nu_{d,ii} x^4 \right\} &= \frac{9}{4} \end{aligned}$$

one finds

$$\begin{aligned} \nu_{00} &= 0.753 \\ \nu_{01} &= \nu_{10} = 0.882 \\ \nu_{11} &= 1.956 \end{aligned}$$

[13] Beware that $W_{\parallel 1}$ is not the coefficient of S_1, but its opposite.

Plateau regime

In the collisional case $\nu_* \simeq 1$, the resonant entropy production rate Eq.(36)

$$\mathcal{S}_{res}\left[U_{eq}, \partial_{\mathbf{J}} U_{eq}\right] = \int d^3\mathbf{x} N_{eq} \frac{v_{Ti}}{qR_0} \epsilon^2 \frac{1}{v_{Ti}^2} \left[W_{\|0}^2 + W_{\|0} W_{\|1} + \frac{13}{4} W_{\|1}^2 \right] \tag{41}$$

Note that these entropy production rates have been computed as functions of $\partial_{\mathbf{J}} U_{eq}$ instead of $\partial_{\mathbf{J}} U_{eq}^\dagger$ for readability. Hence all W_n should be replaced by $W_{\|n}^\dagger$ when time will come to compute an extremum.

Physics behind this increase of entropy is relatively easy to understand, and illustrated in Fig.(14). Passing particles move freely along the field lines, so that their distribution is shifted in the $v_\|$ direction. Trapped electrons cannot move freely, up to their diamagnetic velocity, so that their distribution function is unshifted, when expressed as functions of (H, μ, P_ζ). As a consequence a boundary layer develops at the passing/trapped interface, which is resolved by collisions. Resonant neoclassical transport originates from this region.

4.2 Collisional entropy production rate

We now have to compute the collisional production rate. This is in general a difficult task. We use here a simplified pitch-angle collision operator as given by Eq.(72) (without the diffusion in gyroangle since we deal here with guiding-centres), namely

$$C_i[F] = \nu_{d,ii} \mathcal{L}[F] + \nu_{d,ii} \frac{m v_\| M_\|}{T_{eq}} F_{M0} \tag{42}$$

where

$$\mathcal{L}[F] = \frac{1}{2} \frac{\partial}{\partial \xi} \left[\left(1 - \xi^2\right) \frac{\partial F}{\partial \xi} \right]$$

and $\xi = v_\|/v$ is the pitch-angle. A useful alternative expression of the pitch-angle collision operator is

$$\mathcal{L}[F] = \frac{2}{b} \frac{v_\|}{v^2} \frac{\partial}{\partial \lambda} \left[\lambda v_\| \frac{\partial F}{\partial \lambda} \right]$$

where $b(r,\theta) = B(r,\theta)/B_0 = 1 - \epsilon\cos(\theta)$.

The velocity $U_\|(\mathbf{x})$ must be chosen such that parallel momentum is conserved, i.e. $\int d^3\mathbf{v} v_\| C[F] = 0$. Using $d^3\mathbf{v} = 2\pi v^2 dv d\xi$

$$\left[\int d^3\mathbf{p} \frac{m_i v_\|^2}{T_{eq}} \nu_{d,ii} F_{M0} \right] M_\| = \int d^3\mathbf{v} \nu_{d,ii} v_\| F$$

Let us now go back to the trial distribution function Eq.(18), and give a look at the relation Eq.(19). The collisional entropy production rate comes essentially from passing particles[14]. For these particles $\bar{v}_\|$ and $v_\|$ are close. Let us finally note that a reasonable proxy of $\mathcal{U}_{eq}$ at vanishing values of the inverse aspect ratio ϵ is

$$\mathcal{U}_{eq} = m_a v_\| U_{\|eq} \tag{43}$$

where

$$U_{\|eq} = W_\| - V_{*\zeta} \tag{44}$$

and correspondingly

$$U_{\|n} = W_{\|n} - V_{*\zeta n}$$

[14] they are in greater number than trapped particles and there is no resonant amplification here

where $V_{*\zeta 0}$ and $V_{*\zeta 1}$ are given by Eqs.(19,20). The constraint of momentum conservation Eq.(43) provides a relationship between the velocity moment $M_\parallel$ and the flow $U_{\parallel eq}$

$$M_\parallel = \frac{\left\{\nu_{d,ii} U_{\parallel eq}\right\}}{\left\{\nu_{d,ii}\right\}}$$

Let us now compute the collisional entropy production rate

$$\mathcal{S}_{coll}\left(U_{eq}, U_{eq}\right) = -\int d\gamma \ln F_{eq} \mathcal{C}\left[F_{eq}\right] = -\frac{1}{T_0^2}\int d\gamma F_{eq} U_{eq} \mathcal{C}\left[U_{eq}\right]$$

where

$$C[U_{eq}] = F_{M0}\nu_{d,ii}\mathcal{L}[U_{eq}] + \nu_{d,ii}\frac{m_i v_\parallel M_\parallel}{T_{eq}} F_{M0}$$

The collisional entropy production rate contains two contributions, which corresponds to the two parts of the collision operator, i.e. the pitch-angle scattering operator, and the momentum conservation piece. The first contribution reads

$$\mathcal{S}^{(1)}_{coll}\left(U_{eq}, U_{eq}\right) = \frac{1}{2T_0^2}\int d^3\mathbf{x} 2\pi \int_0^{+\infty} dv v^2 F_{M0}(v)\nu_{d,ii}(v)\int_{-1}^{1} d\xi \left(1-\xi^2\right)\left(\frac{\partial U_{eq}}{\partial \xi}\right)^2$$

Using Eq.(43), it appears that

$$\mathcal{S}^{(1)}_{coll}\left(U_{eq}, U_{eq}\right) = \frac{m_i}{T_{eq}}\int d^3\mathbf{x} N_{eq}\left\{\nu_{d,ii} U^2_{\parallel eq}\right\}$$

A similar calculation shows that the contribution associated with the momentum closure term in the collision operator reads

$$\mathcal{S}^{(1)}_{coll}\left(U_{eq}, U_{eq}\right) = -\frac{m_i}{T_{eq}}\int d^3\mathbf{x} N_{eq}\frac{\left\{\nu_{d,ii} U_{\parallel eq}\right\}^2}{\left\{\nu_{d,ii}\right\}}$$

A total entropy production rate is therefore

$$\mathcal{S}_{coll}(U_{eq}, U_{eq}) = \frac{m_i}{T_{eq}}\int d^3\mathbf{x} N_{eq}\left[\left\{\nu_{d,ii} U^2_{\parallel eq}\right\} - \frac{\left\{\nu_{d,ii} U_\parallel\right\}^2}{\left\{\nu_{d,ii}\right\}}\right]$$

We now use the expansion $U_{\parallel eq} = U_{\parallel 0} S_0 - U_{\parallel 1} S_1$. It appears readily that the Sonine polynomial does not contribute S_0, so that

$$\mathcal{S}_{coll}(U_{eq}, U_{eq}) = \int d^3\mathbf{x} N_{eq}\left(\frac{U_{\parallel 1}(\psi)}{v_{Ti}}\right)^2\left[\left\{\nu_{d,ii} S_1^2\right\} - \frac{\left\{\nu_{d,ii} S_1\right\}^2}{\left\{\nu_{d,ii}\right\}}\right]$$

In other words the collisional entropy production depends on the parallel heat flux U_1 only. Using the definition $\nu_{ij} = \tau_{ii}\left\{\nu_{d,ii} S_i S_j\right\}$, an alternative expression is

$$\mathcal{S}_{coll}(U_{eq}, U_{eq}) = \sqrt{2} c_{coll}\int d^3\mathbf{x} N_{eq}\frac{\nu_i}{v_{Ti}^2}\left(W_{\parallel 1} - V_{*\zeta 1}\right)^2 \tag{45}$$

where $c_{coll} = \nu_{11} - \frac{\nu_{01}^2}{\nu_{00}}$. A straightforward calculation yields $c_{coll} = 0.923$. It appears that this coefficient can be computed exactly from the full collision operator, yielding $c_{coll} = 2$. This value is adopted in the following. As for the resonant entropy production rate, $\dot{S}_{coll}(U_{eq}, U_{eq})$ is computed as a function of U_{eq}, which should be replaced by $U^\dagger_{eq}$ when computing its extremum. One key feature of Eq.(45) is that it involves $U_{\parallel 1} = W_{\parallel 1} - V_{*\zeta 1}$, i.e. the parallel heat flux. Hence collisions try to enforce a relaxation of the parallel heat flux to 0. The corresponding distribution function is a local Maxwellian.

4.3 Extremum of the total entropy production rate

4.3.1 Computing an extremum

The total production rate is the sum of 3 contributions: a first one $\mathcal{S}_t(U_{eq}, U_{eq}^\dagger)$ associated with the time evolution of various profiles Eq.(31), a second one that is due to resonant production $\mathcal{S}_{res}$ as given by Eqs.(40,41), and a third one due to non resonant collisional dissipation $\mathcal{S}_{coll}$ Eq.(45). As mentioned several times, the two last are quadratic functions of $U_{eq}^\dagger$, while the first one is linear in $\delta U_{eq} = U_{eq}^\dagger - U_{eq}$. The extremum with respect to $N_{eq}^\dagger, T_{eq}^\dagger, U_{\|0}^\dagger, U_{\|1}^\dagger$ yields time evolution equations for the density, temperature, parallel momentum and heat flux. An extra equation on the electric potential is obtained by summing all charge density equations over species. However in the single ion species case, it is redundant with the ion density evolution equation. As long as an equilibrium is computed, it is sufficient to find an extremum of $\mathcal{S} = \mathcal{S}_{res} + \mathcal{S}_{coll}$. This is certainly justified for the electric potential that is the fastest field to reach its equilibrium value. This is because a magnetised plasma stays close to charge neutrality, as long as relevant scales are much longer than the Debye length. The evolution equation for the parallel momentum is a disappointment: no relaxation frequency is found. This is a well known result : there is no banana-plateau amplification of the collisional damping rate. This result makes sense since neoclassical amplification comes from a resonant process that takes place at zero parallel velocity $v_\|$. It thus appears that the collision dissipation is always of the Pfirsch-Schlüter type. Therefore the only quantity of interest in terms of relaxation rate is the heat diffusivity. We now proceed with the computation of the extremum of $\mathcal{S}_{res} + \mathcal{S}_{coll}$.

4.3.2 Force balance equation

Comparing Eqs.(40,41) with Eq.(45) it turns out that the collisional entropy production rate is $1/\sqrt{\epsilon}$ than the resonant entropy production rate. Let us assume that ϵ is very small. Then the collisional entropy production rate prevails. Its extremum with respect to W_1 imposes that $W_{\|1} = V_{*\zeta 1}$, or equivalently $U_{\|1} = 0$, i.e. vanishing parallel heat flux. The component $U_{\|0}$ is the ion toroidal velocity[15] V_t, so that

$$W_\| = V_t + V_{*\zeta} \tag{46}$$

A practical expression of the toroidal diamagnetic velocity $V_{*\zeta}$ is

$$V_{*\zeta} = \frac{T_{eq}}{e_i B_p}\left[\frac{dP_{eq}}{P_{eq}dr} + \frac{e_i}{T_{eq}}\frac{d\Phi_{eq}}{dr} + \left(\frac{E}{T_{eq}} - \frac{5}{2}\right)\frac{dT_{eq}}{T_{eq}dr}\right] \tag{47}$$

where B_p is the poloidal magnetic field. The $n = 0$ component of Eq.(46) reads

$$-\frac{d\Phi_{eq}}{dr} - V_t B_p + W_{\|0} B_p = \frac{1}{N_{eq} e_i}\frac{dP_{eq}}{dr}$$

This is nothing else than the radial force balance equation. Hence the quantity $W_0 B_p/B_t$ is in fact poloidal velocity V_p, consistently with the general expression of the flow Eq.(23). The extremum with respect to W_0 imposes that

$$W_{\|0} = \frac{\nu_{01}}{\nu_{00}} W_{\|1} = 1.17 V_{*\zeta 1}$$

in the banana regime, while

$$W_{\|0} = -\frac{1}{2} W_{\|1} = -0.5 V_{*\zeta 1}$$

[15] This can be verified by computing the average parallel velocity from the distribution function.

where $V_{*\zeta 1}$ is given by Eq.(20). Hence the poloidal velocity is of the form

$$V_p = k_{V_p} \frac{1}{e_i B_t} \frac{dT_{eq}}{dr} \tag{48}$$

where $k_{V_p} = 1.17$ in the banana regime, and $k_{V_p} = -0.5$ in the plateau regime. The change of sign is a remarkable feature of this coefficient.

The structure of the solution in banana regime is worth being commented. The distribution function is given by Eq.(16), and reads

$$F_0 = F_{M0} \left[1 + \frac{m_a \bar{v}_\parallel}{T_{eq}} \left(\frac{E}{T_{eq}} - 1.33 \right) \frac{I}{e_a B_{eq}} \frac{dT_{eq}}{d\psi} - \frac{m_a v_\parallel}{T_{eq}} V_{*\zeta} \right]$$

where the function $\bar{v}_\parallel$ can be retraced from the note on mean field kinetic theory. It is also given in all classical references in neoclassical theory[13, 14, 15, 5]

$$\bar{v}_\parallel = \epsilon_\parallel \sqrt{\frac{2E}{m_a}} H\left(\lambda_{\min} - \lambda\right) \int_\lambda^{\lambda_{\min}} \frac{d\lambda'}{\left\langle \sqrt{1 - \lambda' b(\theta)} \right\rangle}$$

where the bracket is a flux surface average, and $\lambda = \lambda_{\min}$ is the passing/trapped boundary. This structure illustrates rather well the notion of boundary layer. In the trapped domain $\lambda_{\min} \leq \lambda \leq \lambda_{\max}$, the function $\bar{v}_\parallel$ is null. This form results from a flattening of the distribution within the trapped domain. In the passing domain $0 \leq \lambda \leq \lambda_{\min}$, the function $\bar{v}_\parallel$ gets closer to the conventional parallel velocity $v_\parallel$ when $\lambda \to 0$. This structure of the distribution function is shown on Fig.15. Note that the derivative of the distribution function is infinite at $\lambda = \lambda_{\min}$. Collisions smooth out this discontinuity, which is responsible for the resonant increase of entropy.

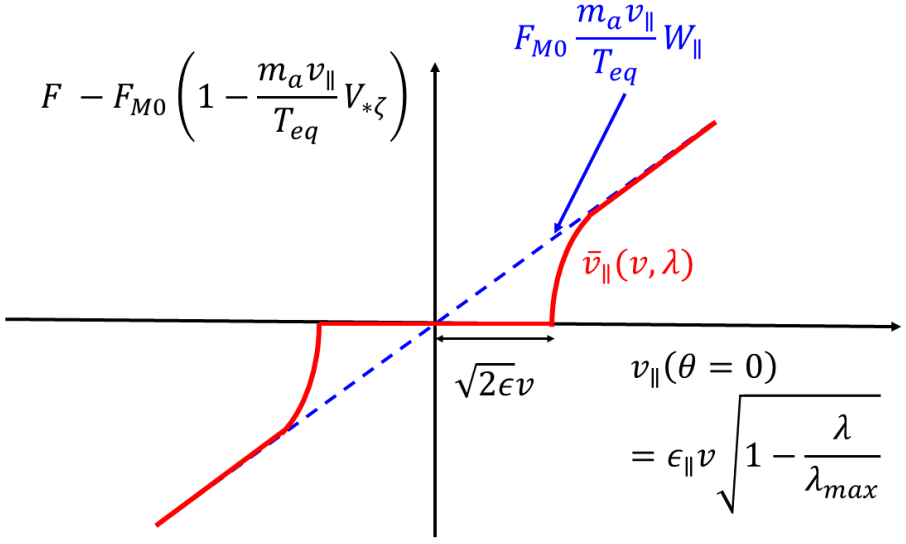

Figure 15: Profile of the distribution function vs parallel velocity at $\theta = 0$ and at given μ.

4.3.3 Heat equation

The residual entropy production rate reads

$$\begin{aligned} \mathcal{S}_{residual}\left[U_{eq}, \partial_{\mathbf{J}} U_{eq}\right] &= \sqrt{2} \int d^3\mathbf{x} N_{eq} \frac{\nu_i}{v_{Ti}^2} \left(\nu_{11} - \frac{\nu_{01}^2}{\nu_{00}} \right) f_t V_{*\zeta 1}^2 \\ &= 1.35 \int d^3\mathbf{x} N_{eq} \nu_i \frac{q^2 \rho_{Ti}^2}{\epsilon^{3/2}} \left[\frac{dT_{eq}}{T_{eq} dr} \right]^2 \end{aligned} \tag{49}$$

in the banana regime and

$$\mathcal{S}_{residual}\left[U_{eq},\partial_{\mathbf{J}}U_{eq}\right]=3\int d^3\mathbf{x}N_{eq}\frac{v_{Ti}}{qR_0}\epsilon^2\frac{1}{v_{Ti}^2}V_{*\zeta 1}^2=3\int d^3\mathbf{x}N_{eq}\frac{v_{Ti}}{qR_0}q^2\rho_{Ti}^2\left[\frac{dT_{eq}}{T_{eq}dr}\right]^2$$

in the plateau regime. The general form is

$$\mathcal{S}_{residual}\left[U_{eq},\partial_{\mathbf{J}}U_{eq}^{\dagger}\right]=\int d^3\mathbf{x}N_{eq}\chi_T\left[\frac{1}{T_{eq}}\frac{dT_{eq}^{\dagger}}{dr}\right]^2$$

where the quadratic dependence in $U_{eq}^{\dagger}$ has been re-established. The entropy production rate associated with the temperature evolution reads

$$\mathcal{S}_t\left(U_{eq},U_{eq}^{\dagger}\right)=3\int d^3\mathbf{x}\frac{\delta T_{eq}}{T_{eq}}\frac{1}{T_{eq}}\frac{\partial T_{eq}}{\partial t}$$

The volume element reads $d^3\mathbf{x}=4\pi^2R_0rdr$ in cylindrical geometry. The extremum of $\mathcal{S}_t+\mathcal{S}_{residual}$ is calculated after an integration by parts to isolate $T_{eq}^{\dagger}$[16]. This gives a heat equation

$$\frac{3}{2}\frac{\partial T_{eq}}{\partial t}-\frac{1}{r}\frac{\partial}{\partial r}\left(rN_{eq}\chi_T\frac{\partial T_{eq}}{\partial r}\right)=0 \tag{50}$$

The transport coefficient χ_T can then be identified with the heat diffusivity. Hence

$$\chi_T=1.35\nu_i\frac{q^2\rho_{Ti}^2}{\epsilon^{3/2}}$$

in the banana regime, while

$$\chi_T=3\frac{v_{Ti}}{qR_0}q^2\rho_{Ti}^2$$

in the plateau regime. Of course in presence of heating, a source should be added on the right hand side of Eq.(50). This equation can be understood as a prototype of all transport equations in a fusion device. In this particular case, it the heat equation determines the temperature profile for a given heat source - see Fig.16[17]. We will see however that the structure of the heat flux can be more complex than a simple Fourier law.

4.3.4 Finite inverse aspect ratio corrections

One drawback of the method described above is its inaccuracy. Indeed the "small parameter" ϵ is not small in practice[18]. It makes therefore more sense to find an extremum of $\mathcal{S}=\mathcal{S}_{res}+\mathcal{S}_{coll}$ calculated up to second order in $\sqrt{\epsilon}$. However the calculation of $\mathcal{S}_{coll}$ as was done above becomes somewhat inaccurate. This is because $\bar{v}_{\|}$ was identified with $v_{\|}$. This approximation introduces errors of order $\sqrt{\epsilon}$ since the integral of $\bar{v}_{\|}$ over the velocity space is proportional to the fraction of passing particles. The exact calculation is lengthy and will not be reproduced here. A fast way to re-establish an expression that makes more sense is to add a weight f_c to all places where the coefficients W_n appears, since the function $W_{\|}$ is the coefficient of $\bar{v}_{\|}$. Note that there is no such weight for the diamagnetic velocity since all particles contribute to the diamagnetic velocity, including trapped particles. The total entropy in the banana regime becomes

$$\mathcal{S}=\sqrt{2}\int d^3\mathbf{x}N_{eq}\frac{\nu_i}{v_{Ti}^2}\left[f_tf_c\left(\nu_{00}W_{\|0}^2-2\nu_{01}W_{\|0}W_{\|1}+\nu_{11}^2W_{\|1}^2\right)+2\left(f_cW_{\|1}-V_{*\zeta 1}\right)^2\right]$$

[16]Beware that a factor 2 then appears which has no counterpart in the extremum of $\mathcal{S}_t$.

[17]As a simple check, the reader can verify that for a constant heat source S_T, and density N_{eq}, the steady solution of the heat equation with boundary condition $T_{eq}(r=a)=0$ is just $T_{eq}=\frac{S_T}{4N_{eq}\chi_T}(a^2-r^2)$.

[18]$\epsilon=r/R_0=1/3$ in the edge of most tokamaks, and gets lower near the axis.

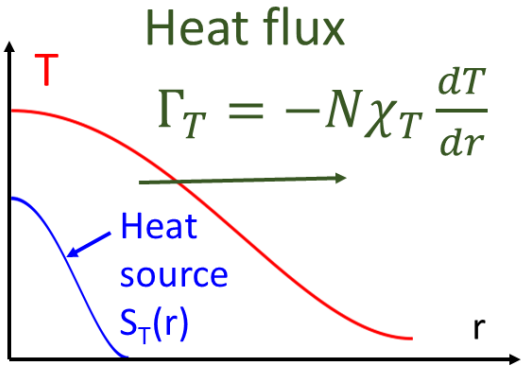

Figure 16: Schematics of a temperature profile that results from a central heating and an outward heat flux.

This expression is close to the one found in [5]. The extremum is therefore (almost) the same. The extremum with respect to W_0 gives the relation $\nu_{00}W_{\|0} = \nu_1 W_{\|1}$ and

$$W_{\|1} = \frac{V_{*\zeta 1}}{f_c + f_t\left(\nu_{11} - \frac{\nu_{01}^2}{\nu_{00}}\right)} = \frac{V_{*\zeta 1}}{f_c + 0.462 f_t}$$

The residual entropy production rate reads

$$\mathcal{S}_{residual}\left[U_{eq}, \partial_{\mathbf{J}} U_{eq}\right] = \int d^3\mathbf{x} N_{eq}\nu_i \frac{q^2\rho_{Ti}^2}{\epsilon^{3/2}} \frac{1.35}{f_c + 0.462 f_t}\left[\frac{dT_{eq}}{T_{eq}dr}\right]^2$$

which obviously provides the requested correction on the heat diffusivity. More detailed expressions can be found in [16, 17]. The poloidal rotation is still $V_p = (\epsilon/q)(\nu_{01}/\nu_{00})W_{\|1}$ so that the coefficient k_{V_p} now reads

$$k_{V_p} = \frac{1.17}{f_c + 0.462 f_t}$$

Clearly the correction due to finite values of $\sqrt{\epsilon}$ is not small.

5 Electron transport

5.1 Electron entropy production rate

5.1.1 Electron collision operator

A model of collision operator for electrons reads

$$C_e[F_e] = C_{ee}[F_e] + C_{ei}[F_e]$$

where $C_{ee}[F_e]$ is the electron-electron collision operator. It is taken identical to the ion-ion collision operator Eq.(42)

$$C_{ee}[F_e] = \nu_{d,ee}\mathcal{L}[F_e] + \nu_{d,ee}\frac{m_e v_\| M_{\|e}}{T_{eq,e}} F_{M0e}$$

where it is recalled that F_{M0e} is the unshifted electron Maxwellian distribution function. The velocity $M_{\|e}$ is constrained to ensure momentum conservation

$$M_{\|e} = \frac{1}{\{\nu_{d,ee}\}} \int d^3\mathbf{v} \nu_{d,ee} v_\| F_e \tag{51}$$

It is reminded that the parenthesis $\{...\}$ is not a parenthesis nor a Poisson bracket, but an average over the velocity space, as defined in Eq.(37), or Eq.(38) in the specific case of an isotropic distribution function. The operator $C_{ei}[F_e]$ accounts for the collisional drag force between electrons and ions. We choose here the following model operator

$$C_{ei}[F_e] = \nu_{d,ei} \mathcal{L}[F_e] + \nu_{d,ei} \frac{m_e v_\| V_{\|eq,i}}{T_{eq,e}} F_{M0e} \tag{52}$$

We see now why this operator makes sense, by specifying the expression of the collision frequencies $\nu_{d,ee}$ and $\nu_{d,ei}$. The electron-electron collision frequency $\nu_{d,ee}$ is given by Eq.(35) where $\nu_i = \frac{1}{\tau_i} = \frac{1}{\sqrt{2}\tau_{ii}}$ should be replaced by $\nu_e = \frac{1}{\tau_e} = \frac{1}{\tau_{ei}}$. Its explicit expression is

$$\nu_e = \frac{4\sqrt{2\pi}}{3} \frac{e^4}{(4\pi\epsilon_0)^2} \frac{N_{eq,e}}{m_e^2 v_{Te}^3} \ln\Lambda$$

Note the $\sqrt{2}$ difference with the ion thermal collision frequency Eq.(36). The electron-ion pitch-angle collision frequency is somewhat simpler

$$\nu_{d,ei} = \frac{3\sqrt{2\pi}}{4} \frac{N_{eq,i} Z^2}{N_{eq,e}} \frac{\nu_e}{x_e^3}$$

where Z is the ion charge number. This formula can also be related to the electron ion collision time τ_{ei} by using the relationship

$$\frac{1}{\tau_{ee}} = \frac{1}{\sqrt{2}} \frac{N_{eq,e}}{N_{eq,i} Z^2} \frac{1}{\tau_{ei}} \tag{53}$$

To get quantitative formulas, the following results will turn out useful

$$\begin{aligned}
\tau_{ee} \{\nu_{d,ee}\} &= \left(2 - \sqrt{2} \ln\left(1 + \sqrt{2}\right)\right) \simeq 0.753 \\
\tau_{ee} \left\{\nu_{d,ee} x^2\right\} &= \frac{1}{\sqrt{2}} \simeq 0.707 \\
\tau_{ee} \left\{\nu_{d,ee} x^4\right\} &= \frac{9}{4}
\end{aligned}$$

Moreover

$$\tau_{ei} \left\{\nu_{d,ei} x^{2n}\right\} = n!$$

The electron-ion collision friction force is defined as

$$R_{\|ei} = \int d^3\mathbf{v} m_e v_\| C_{ei}[F_e]$$

Electron-electron collisions do play any role since momentum is strictly conserved. Let us now use the model operator Eq.(52). A straightforward calculation yields

$$R_{\|ei} = -N_{eq,e} m_e \left(\frac{1}{N_{eq,e}} \int d^3\mathbf{v} v_\| \nu_{d,ei} F_e - \{\nu_{d,ei}\} V_{\|eq,i} \right)$$

Let us now consider the special case of a shifted Maxwellian distribution function

$$F_e = F_{M0e} \left[1 + \frac{m_e v_\|}{T_{eq,e}} \left(V_{\|eq,e} + \frac{2}{5} \frac{q_{\|eq,e}}{N_{eq,e} T_{eq,e}} \left(x_e^2 - \frac{5}{2} \right) \right) \right]$$

The friction force then reduces to

$$R_{\parallel ei} = -N_{eq,e} m_e \nu_{ei} \left[V_{\parallel eq,e} - V_{\parallel eq,i} - \frac{3}{5} \frac{q_{\parallel eq,e}}{N_{eq,e} T_{eq,e}} \right]$$

which is identical to the expression given in Appendix B with a more precise operator. This is mainly the justification for the choice of the model operator Eq.(52). Obviously the action/reaction theorem imposes that $R_{\parallel ie} = -R_{\parallel ei}$. This implies that the ion-electron collision frequency is very small, and will be ignored. In the following we will use an effective scattering electron collision frequency defined as

$$\nu_{d,e} = \nu_{d,ee} + \nu_{d,ei} \tag{54}$$

As a last remark, let us stress that for a vanishing parallel electron heat flux, collision friction enforces $R_{\parallel ei} \simeq 0$, and therefore $V_{\parallel eq,e} \simeq V_{\parallel eq,i}$.

5.1.2 Reformulation of the electron kinetic equation

Electrons are more mobile than the ions along the field lines due to their small mass. Hence they carry most of the current density in a hot plasma. Consequently, the inductive field must be accounted for. When accounting for the energy time variation Eq.(7), the drift-kinetic equation Eq.(55) becomes for electrons

$$v_\parallel \nabla_\parallel F_e + \mathbf{v}_{De} \cdot \nabla F_e + \frac{e E_{ind}}{T_{eq,e}} v_\parallel F_{M0e} = C[F_e]$$

where e is the proton charge. It is convenient to introduce a "Spitzer" distribution function $F_{sp,e}$ such that

$$C[F_{sp,e}] = \frac{e E_{ind}}{T_{eq,e}} v_\parallel F_{M0e}$$

Given the model collision operator above, it reads

$$\nu_{d,e} \mathcal{L}[F_{sp,e}] + \frac{m_e v_\parallel}{T_{eq,e}} F_{M0e} \left(\nu_{d,ee} M_{\parallel e} + \nu_{d,ei} V_{\parallel i} \right) = \frac{m_e v_\parallel}{T_{eq,e}} F_{M0e} \frac{e E_{ind}}{m_e} \tag{55}$$

The drift-kinetic equation then reads

$$v_\parallel \nabla_\parallel F_e + \mathbf{v}_{De} \cdot \nabla F_e = C[F_e - F_{sp,e}]$$

Given the parity in parallel velocity, Spitzer distribution function $F_{sp,e}$ reads

$$F_{sp,e} = F_{M0e} \left(1 + \frac{U_{sp,e}}{T_{eq,e}} \right)$$

where

$$U_{sp,e} = \frac{m_e v_\parallel}{T_{eq,e}} U_{sp\parallel}$$

is a "Spitzer" thermodynamic potential. The parallel Spitzer flow $U_{sp\parallel}$ is then written in the ion rest frame, for convenience

$$U_{sp\parallel} = \tilde{U}_{sp\parallel} + V_{\parallel eq,i}$$

The relative parallel Spitzer flow $\tilde{U}_{sp\parallel}$ can itself be decomposed over Sonine polynomials

$$\tilde{U}_{sp\parallel} = U_{sp0} + U_{sp1} \left[\frac{E}{T_{eq,e}} - \frac{5}{2} \right]$$

5.1.3 Spitzer resistivity

The calculation of the Spitzer thermodynamic potential has been subject of a large number of studies, including by Spitzer himself. It is therefore considered as a given. Nevertheless it is interesting to compute the resistivity with the simplified operator above. It is convenient to write the flow $M_{\|e}$ in the ion rest frame, i.e $M_{\|e} = V_{\|eq,i} + \tilde{M}_{\|e}$. The Vlasov equation Eq.(55) then implies

$$\nu_{d,e}\tilde{U}_{sp\|} = \nu_{d,ee}\tilde{M}_{\|e} + \gamma_{ind}$$

where $\gamma_{ind} = -eE_{ind}/m_e$ is homogeneous to an acceleration. Momentum conservation Eq.(51) imposes that

$$\{\nu_{d,ee}\}\,\tilde{M}_{\|e} = \left\{\nu_{d,ee}\tilde{U}_{sp\|}\right\}$$

so that

$$\left\{\frac{\nu_{d,ee}\nu_{d,ei}}{\nu_{d,e}}\right\}\tilde{M}_{\|e} = \left\{\frac{\nu_{d,ee}}{\nu_{d,e}}\right\}\gamma_{ind}$$

The current density associated with the Spitzer distribution function is equal to

$$J_{\|} = -e\int d^3\mathbf{v}F_{sp,e}v_{\|} + N_{eq,e}eV_{\|eq,i} = -N_{eq,e}e\left\{\tilde{U}_{sp\|}\right\}$$

Using the solution found above, one finds

$$J_{\|} = \left(\frac{\left\{\frac{\nu_{d,ee}}{\nu_{d,e}}\right\}^2}{\left\{\frac{\nu_{d,ee}\nu_{d,ei}}{\nu_{d,e}}\right\}} + \left\{\frac{1}{\nu_{d,e}}\right\}\right)\frac{N_{eq,e}e^2}{m_e}E_{ind}$$

This is an Ohm's law, as expected. It is reminiscent of the Drude's calculation for electrical conductivity, see Fig.17. The resistivity appears to match the exact value when $Z \gg 1$, and fits reasonably well when $Z = 1$.

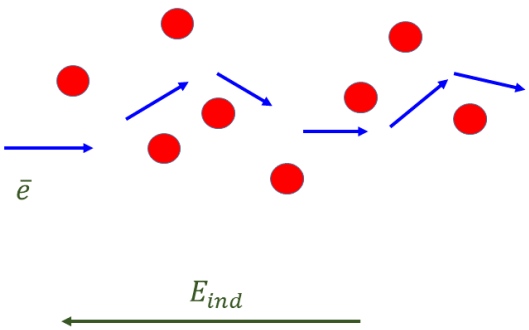

Figure 17: Drude model of conductivity. Electrons are accelerated along a field line by an inductive field, force is $-eE_{ind}$. Electrons are scattered by ions (assumed immobile) via collisions, resulting in a drag force $-m_e\nu_{ei}V_{\|,e}$. Force balance leads to an average electron velocity along the field line $V_{\|eq,e} = -\frac{e}{m_e}E_{ind}$, and hence a current density $J_{\|} = \frac{N_{eq,e}e^2}{m_e\nu_{ei}}E_{ind}$, and hence a conductivity $\sigma = \frac{N_e e^2}{m_e\nu_{ei}}$.

5.1.4 Electron collisional entropy production rate

The calculation of the electron collisional entropy production rate requires a bit of care, compared with ions. Indeed the inductive field appears as a source of entropy production, which must be accounted for. We thus use the original formulation in terms of test thermodynamical potentials. The Fokker-Planck equation is equivalent to get an extremum of the following functional

$$\mathcal{S}_{coll}\left(U_{eq},U_{eq}\right)=-2\int d\gamma F_{M0e}\frac{1}{T_{eq,e}^2}U_{eq,e}^{\dagger}\left(\mathcal{C}\left[U_{eq,e}\right]+\gamma_{ind}\frac{m_e v_{\parallel}}{T_{eq,e}}F_{M0e}\right)$$

with respect of all variations of $U_{eq,e}^{\dagger}$ near $U_{eq,e}$, with $U_{eq,e}=U_{sp,e}$ for the specific Spitzer problem at hand. A straightforward calculation provides the following expression

$$\begin{aligned}\mathcal{S}_{coll}\left(U_{eq},U_{eq}\right) &= -2\int d^3\mathbf{x}\frac{N_{eq,e}}{v_{Te}^2}\left\{\nu_{d,ei}\tilde{U}_{sp\parallel}\tilde{U}_{sp\parallel}^{\dagger}\right\}\\ &+ 2\int d^3\mathbf{x}\frac{N_{eq,e}}{v_{Te}^2}\left[\left\{\nu_{d,ee}\tilde{U}_{sp\parallel}\tilde{U}_{sp\parallel}^{\dagger}\right\}-\frac{\left\{\nu_{d,ee}\tilde{U}_{sp\parallel}\right\}\left\{\nu_{d,ee}\tilde{U}_{sp\parallel}^{\dagger}\right\}}{\left\{\nu_{d,ee}\right\}}\right]\\ &- 2\int d^3\mathbf{x}\frac{N_{eq,e}}{v_{Te}^2}\gamma_{ind}\left\{\tilde{U}_{sp\parallel}^{\dagger}\right\}\end{aligned}$$

Unfortunately, the projection of the variational principle on Sonine polynomials does not provide the result above. An option is to replace it with a functional that reproduces the Spitzer result, for instance

$$\begin{aligned}\mathcal{S}_{coll}(U_{eq},U_{eq}) &= 2\sqrt{2}c_{coll,e}\int d^3\mathbf{x}\frac{N_{eq,e}}{v_{Te}^2}\nu_e U_{\parallel 1,e}U_{\parallel 1,e}^{\dagger}\\ &+ 2\int d^3\mathbf{x}\frac{N_{eq,e}}{v_{Te}^2}\nu_e\left(U_{\parallel 0,e}-U_{spitzer}\right)U_{\parallel 0,e}^{\dagger}\end{aligned}\tag{56}$$

where $U_{\parallel 0,e}=V_{\parallel,e}-V_{\parallel,i}$ and $U_{\parallel 1,e}=\frac{2}{5}\frac{q_{\parallel eq,e}}{N_{eq,e}T_{eq,e}}$. This contribution must be added to the ion entropy production rate

$$\mathcal{S}_{coll}(U_{eq},U_{eq})=2\sqrt{2}c_{coll,i}\int d^3\mathbf{x}N_{eq,i}\frac{\nu_i}{v_{Ti}^2}U_{\parallel 1,i}U_{\parallel 1,i}^{\dagger}$$

Therefore the total collision entropy production rate contains 3 parts. The first one is due to a collisional scattering ion the velocity space (the same as Eq.(45)), the second is its counterpart for electrons and the third one is the electron-ion friction force adjusted to reproduce the Spitzer result. We will see that the latter is in fact not accurate enough to reproduce the neoclassical prediction for the current driven by density and temperature gradients (bootstrap current), but other expedients can be used to do so. As mentioned before, the collisional entropy production prevails in the limit of small inverse aspect ratio. In this case, the solution satisfies $q_{\parallel eq,e}\simeq 0$, $q_{\parallel eq,i}\simeq 0$. This then implies that the parallel electron heat flux can be ignored in the friction force. As mentioned above, electron-ion friction force imposes $V_{\parallel eq,e}\simeq V_{\parallel eq,i}$ in the vicinity of the resonant area in the phase space.

5.1.5 Resonant entropy production rate for electrons

The calculation of the resonant entropy production is then essentially the same for electrons and ions. However some additional difficulties emerge in the calculation for electrons due to the inductive field. In particular the parallel Spitzer flow $U_{sp,e}$ must be accounted for when computing the electron distribution function. Moreover $V_{\parallel eq,e}\simeq V_{\parallel eq,i}$ in the vicinity of the resonant layer. On the other hand, the entropy functional is still built by multiplying the Fokker-Planck equation by $U_{eq,e}^{\dagger}$, i.e. the same as for the ions, with ions

replaced by electrons. This said, we do not need to repeat the calculations done for ions. We focus on the banana regime, which is of interest in weakly collisional plasmas - plateau regime does not raise any major difficulty. Details can be found in Appendix E. Let us remind the structure of the ion resonant entropy production Eq.(39)

$$\mathcal{S}_{res,i}\left[U_{eq},\partial_{\mathbf{J}}U_{eq}\right]=2\int d^3\mathbf{x}\frac{N_{eq,i}}{v_{Ti}^2}f_t\left\{\nu_{d,i}W_{\parallel,i}W_{\parallel,i}^{\dagger}\right\} \tag{57}$$

Hence the resonant entropy production for electrons reads

$$\mathcal{S}_{res,e}\left[U_{eq},\partial_{\mathbf{J}}U_{eq}\right]=2\int d^3\mathbf{x}\frac{N_{eq,e}}{v_{Te}^2}f_t\left\{\nu_{d,e}\left(W_{\parallel,e}+U_{sp\parallel}\right)W_{\parallel,e}^{\dagger}\right\} \tag{58}$$

5.2 Computing fluxes and parallel current

5.2.1 Alternative expression of the resonant entropy production rate

A seen above, collisions in the bulk of a species enforce a parallel heat flux $U_{1,a}=\frac{2}{5}\frac{q_{\parallel a}}{N_{eq,a}T_{eq,a}}$ that vanishes for each species, leaving only the component $U_{0,a}$ that is identified with the toroidal velocity. Hence for each species "a"

$$W_{\parallel,a}=V_{t,a}+V_{*\zeta,a}$$

where

$$V_{*\zeta,a}=\frac{T_{eq,a}}{e_aB_p}\left[\frac{d\ln P_{eq,a}}{dr}+\frac{e_a}{T_{eq,a}}\frac{d\Phi_{eq}}{dr}+\left(\frac{E}{T_{eq,a}}-\frac{5}{2}\right)\frac{d\ln T_{eq,a}}{dr}\right]$$

Using the force balance equation

$$-\frac{d\Phi_{eq}}{dr}-V_{t,a}B_p+V_{p,a}B_t=\frac{T_{eq,a}}{e_a}\frac{d\ln P_{eq,a}}{dr}$$

one gets the following expression for the flow $W_{\parallel,a}$

$$W_{\parallel,a}=\frac{B_t}{B_p}\left[V_{pa}+\frac{1}{e_aB_t}\left(\frac{E}{T_{eq,a}}-\frac{5}{2}\right)\frac{dT_{eq,a}}{dr}\right]$$

and thus a useful expression of the resonant entropy production rate

$$\begin{aligned}\mathcal{S}_{res,a}\left[U_{eq},\partial_{\mathbf{J}}U_{eq}\right] &= 2\int d^3\mathbf{x}N_{eq,a}f_t\frac{q^2\rho_{Ta}^2}{\epsilon^2}\\ &\left\{\nu_{d,a}\left[\frac{e_aB_t}{T_{eq,a}}\left(V_{p,a}+\frac{\epsilon}{q}U_{sp\parallel,a}\right)+\left(\frac{E}{T_{eq,a}}-\frac{5}{2}\right)\frac{d\ln T_{eq,a}}{dr}\right]\right.\\ &\left.\left[\frac{e_aB_t}{T_{eq,a}}V_{p,a}^{\dagger}+\left(\frac{E}{T_{eq,a}}-\frac{5}{2}\right)\frac{d\ln T_{eq,a}^{\dagger}}{dr}\right]\right\}\end{aligned}$$

where in fact the Spitzer shift $U_{sp\parallel,a}$ has to be included only for electrons. Here $\rho_{Ta}^2=\frac{m_av_{Ta}}{e_aB_t}$ is a thermal particle gyroradius.

5.2.2 Explicit expression of the electron resonant entropy production

Because the ion collision frequency is $\sqrt{m_i/m_e}$ larger than the electron collision frequency, the ion resonant entropy production rate is dominant. Hence it must be made extremum before finding an extremum for electrons. As a result, Eq.(48) yields the ion poloidal velocity

$$V_{p,i}=k_{V_p}\frac{1}{ZeB_t}\frac{dT_{eq,i}}{dr}$$

where Z is the ion charge number, and $k_{V_p} = 1.17$ in banana regime. Also the ion heat diffusivity remains the same. Combining the force balance equations for both ions and electrons, one then finds an expression of the electron poloidal velocity

$$\begin{aligned} -\frac{eB_t V_{p,e}}{T_{eq,e}} &= \frac{d\ln N_{eq,e}}{dr} + \frac{T_{eq,i}}{ZT_{eq,e}}\frac{d\ln N_{eq,i}}{dr} + \frac{d\ln T_{eq,e}}{dr} \\ &+ \left(1-k_{V_p}\right)\frac{T_{eq,i}}{ZT_{eq,e}}\frac{d\ln T_{eq,i}}{dr} - eB_p\frac{V_{t,e}-V_{t,i}}{T_{eq,e}} \end{aligned}$$

Note that $V_{\|,a} \simeq V_{t,a}$ in the limit of small inverse aspect ratio $\epsilon \ll 1$. Moreover, a subtle point is that $V_{t,e}$ must be set equal $V_{t,i}$ in the calculation of the resonant response of electrons, but not in the trial thermodynamic potential! Hence an explicit expression of the electron resonant entropy production is then found, namely

$$\begin{aligned} \mathcal{S}_{res,e}\left[U_{eq}, \partial_{\mathbf{J}} U_{eq}\right] &= 2\int d^3\mathbf{x} N_{eq,e} f_t \frac{q^2\rho_{Te}^2}{\epsilon^2} \\ &\left\{\nu_{d,e}\left[\frac{d\ln N_{eq,e}}{dr} + \frac{T_{eq,i}}{ZT_{eq,e}}\frac{d\ln N_{eq,i}}{dr} + \left(\frac{E}{T_{eq,e}} - \frac{3}{2}\right)\frac{d\ln T_{eq,e}}{dr}\right.\right. \\ &\left. -0.17\frac{T_{eq,i}}{ZT_{eq,e}}\frac{d\ln T_{eq,i}}{dr} - \frac{eB_p}{T_{eq,e}}U_{sp\|}\right] \\ &\left[\frac{d\ln N^\dagger_{eq,e}}{dr} + \frac{T_{eq,i}}{ZT_{eq,e}}\frac{d\ln N^\dagger_{eq,i}}{dr} + \left(\frac{E}{T_{eq,e}} - \frac{3}{2}\right)\frac{d\ln T^\dagger_{eq,e}}{dr}\right. \\ &\left.\left. -0.17\frac{T_{eq,i}}{ZT_{eq,e}}\frac{d\ln T^\dagger_{eq,i}}{dr} - \frac{eB_p}{T_{eq,e}}\left(V^\dagger_{t,e} - V^\dagger_{t,i}\right)\right]\right\} \end{aligned} \tag{59}$$

5.2.3 Particle and heat fluxes

Particle and heat fluxes are obtained by computing an extremum of this functional with respect to electron density and temperature gradients. The solution of the Spitzer problem turns out to be

$$\left\{\left(\nu_{d,ei} + \nu_{d,ee}\right)U_{sp\|}\right\} = -1.66\frac{eE_{ind}}{m_e}$$

Let us also remember that $\nu_e = 1/\tau_{ei}$ and $1/\tau_{ee}$ is given by Eq.(53). Fluxes are computed by using the following relationships

$$\begin{aligned} \left\{\nu_{d,ee}\right\} &= \nu_{ei}\left(1 + \frac{0.53}{Z}\right) \\ \left\{\nu_{d,ee}x^2\right\} &= \nu_{ei}\left(1 + \frac{0.5}{Z}\right) \\ \left\{\nu_{d,ee}x^4\right\} &= \nu_{ei}\left(2 + \frac{1.59}{Z}\right) \end{aligned}$$

In the case where $Z \gg 1$, electron-electron collisions can be ignored. In the more realistic case $N_{eq,e} = N_{eq,i}Z$ and Z of a few units, one gets the following particle flux, obtained by computing an extremum with respect to $\frac{dN_{eq,e}}{dr}$

$$\begin{aligned} \Gamma_{Ne} &= -f_t\nu_e\frac{q^2\rho_{Te}^2}{\epsilon^2}N_{eq,e}\left[\left(1 + \frac{0.53}{Z}\right)\left(1 + \frac{T_{eq,i}}{ZT_{eq,e}}\right)\frac{d\ln N_{eq,e}}{dr}\right. \\ &\left. - \left(0.5 + \frac{0.30}{Z}\right)\frac{d\ln T_{eq,e}}{dr} - 0.17\left(1 + \frac{0.53}{Z}\right)\frac{T_{eq,i}}{ZT_{eq,e}}\frac{d\ln T_{eq,i}}{dr}\right] \\ &- 1.66 f_t N_{eq,e}\frac{E_{ind}}{B_p} \end{aligned}$$

The structure of the particle flux is the same as in classical textbooks [14, 18, 5]. The numerical coefficients are estimates and should not be considered too seriously[19]. One striking feature of the particle flux is the presence of terms that are not proportional to the density gradient, bur rather to the density itself see Fig.18. These terms are called pinch velocities. Indeed a negative pinch velocity results in a peaked density profile, even without a source - hence a "pinch effect". One component of the neoclassical pinch velocity is proportional to the temperature gradient, and corresponds to a thermodiffusion. This one is expected since the temperature gradient is a thermodynamic force. the second one is more of a surprise, since proportional to the inductive field. It will be commented in more details in the next section.

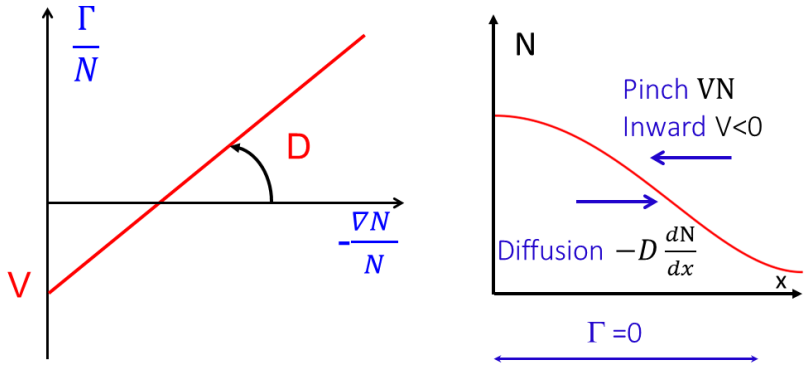

Figure 18: Particle flux vs density gradient. A pinch occurs when the particle flux is not zero at vanishing density gradient. The diffusion coefficient is the slope of the curve flux vs gradient. In absence of particle sources, the particle flux vanishes. In absence of pinch, the resulting density profile would be flat. However when the pinch velocity is not zero, a non flat profile established due to a balance between diffusion and pinch.

The heat flux is given by the extremum with respect to the temperature at constant $A_{1,e} = \frac{\delta P_{e,eq}}{P_{e,eq}} - \frac{e\delta\Phi_{eq}}{T_{e,eq}}$. In other words, we need to compute the moment associated with $(x^2 - \frac{5}{2})$. The solution of the Spitzer problem for the moment x^2 is

$$\left\{\left(\nu_{d,ei} + \nu_{d,ee}\right) x^2 U_{sp\|}\right\} = -2.96 \frac{eE_{ind}}{m_e}$$

One then gets

$$\begin{aligned}\Gamma_{Te} &= -f_t \nu_e \frac{q^2 \rho_{Te}^2}{\epsilon^2} P_{eq,e} \left[-\left(\frac{3}{2} + \frac{0.83}{Z}\right)\left(1 + \frac{T_{eq,i}}{ZT_{eq,e}}\right)\frac{d\ln N_{eq,e}}{dr} \right. \\ &\quad \left. -\left(\frac{7}{4} + \frac{1.58}{Z}\right)\frac{d\ln T_{eq,e}}{dr} + 0.17\left(\frac{3}{2} + \frac{0.83}{Z}\right)\frac{T_{eq,i}}{ZT_{eq,e}}\frac{d\ln T_{eq,i}}{dr}\right] \\ &+ 1.19 f_t P_{eq,e}\frac{E_{ind}}{B_p}\end{aligned}$$

The structure is similar to the particle flux, i.e. a heat pinch velocity proportional to the density gradient (the Onsager symmetrical to thermodiffusion), and a pinch velocity proportional to the inductive field.

[19] Helander and Sigmar find 0.59 instead of 0.80 for the coefficient of the temperature gradient when $Z = 1$.

5.2.4 Parallel current density

Let us recall first that the extremum of the collisional resonant entropy production Eq.(56) yields the Spitzer current. Hence the extremum of Eq.(59) with respect to $V_{t,e}^{\dagger}$) yields a correction to the Spitzer current. Unfortunately this calculation is not accurate due to the approximation done in the calculation of the collisional entropy production rate. A more precise approach proposed in Helander and Sigmar's book is as follows. Let us remark that the difference of the current density with its Spitzer value reads

$$J_{\parallel} - J_{\parallel spitzer} = -e \int d^3\mathbf{p} v_{\parallel} \left(F - F_{sp}\right)$$

where F_{sp} is calculated in the ion rest frame (see section above). Let us now make use of the Spitzer function defined as

$$C\left[F_{M0} v_{\parallel} \tau_{sp}\right] = F_{M0} v_{\parallel}$$

The function τ_{sp} can be interpreted as a collision time (inverse of a collision frequency). Using the collision self-adjointness property, the following identity is found

$$\int d^3\mathbf{p} v_{\parallel} \left(F - F_{sp}\right) = \int d^3\mathbf{p} C\left[F - F_{sp}\right] v_{\parallel} \tau_{sp}$$

The resonant entropy production rate that matters for the current is therefore the same as above, but weighted by the function τ_{sp}. All calculations done, one finds

$$\begin{aligned} V_{\parallel e} - V_{\parallel i} - U_{spitzer} &= -f_t \left\{\tau_{sp} \nu_{d,e} U_{sp\parallel}\right\} \\ &+ f_t \left\{\tau_{sp} \nu_{d,e} \frac{T_{eq,e}}{eB_p} \left[\frac{d\ln N_{eq,e}}{dr} + \frac{T_{eq,i}}{ZT_{eq,e}} \frac{d\ln N_{eq,i}}{dr}\right.\right. \\ &\left.\left. + \left(\frac{E}{T_{eq,e}} - \frac{3}{2}\right) \frac{d\ln T_{eq,e}}{dr} - 0.17 \frac{T_{eq,i}}{ZT_{eq,e}} \frac{d\ln T_{eq,i}}{dr}\right]\right\} \end{aligned}$$

The parallel current density satisfies the equality $J_{\parallel} = -N_{eq,e} e \left(V_{\parallel eq,e} - V_{\parallel eq,i}\right)$. A complete calculation requires the solution of the Spitzer problem to compute $\hat{f}_s$. However in the case $Z \gg 1$, then $\tau_{sp} = 1/\nu_{d,ei}$ and $\nu_{d,e} \simeq \nu_{d,ei}$, and also $U_{sp\parallel} = -\tau_{sp} \frac{eE_{ind}}{m_e}$ so that

$$\begin{aligned} J_{\parallel} - J_{\parallel spitzer} &= -f_t \frac{32}{3\pi\sqrt{2}} \frac{N_{eq,e} e^2}{m_e \nu_{ei}} E_{ind} \\ &- f_t \frac{T_{eq,e}}{B_p} \left[\frac{d\ln N_{eq,e}}{dr} + \frac{T_{eq,i}}{ZT_{eq,e}} \frac{d\ln N_{eq,i}}{dr}\right] \\ &+ f_t \frac{T_{eq,e}}{B_p} \left[\frac{d\ln T_{eq,e}}{dr} - 0.17 \left(1 + \frac{0.53}{Z}\right) \frac{T_{eq,i}}{ZT_{eq,e}} \frac{d\ln T_{eq,i}}{dr}\right] \end{aligned}$$

Let us insist on the fact that the derivation is approximate. This said, the structure is the right one. It appears that the first term of the r.h.s. is a correction to the Spitzer conductivity, while the second represents a current generated by density and temperature gradients. The latter is called bootstrap current. The reduction of the Spitzer conductivity is due to the decrease of free charge carriers due to trapping : only passing electrons can carry current, and their fraction is $f_c = 1 - f_t$.

5.3 Physics of Ware pinch and bootstrap current

5.3.1 Interest of Ware pinch and bootstrap current

Two striking features of the results above are

- an inward flux of electrons proportional to the inductive field, and called Ware pinch,

- a contribution to the parallel current proportional to density and temperature gradients called bootstrap current.

Both play a favourable role in tokamak plasmas since an inward pinch allows a density peaking near the magnetic axis without a particle source (always difficult to produce in the plasma core). Since fusion power is proportional to the square of the density, such a peaking is welcome in terms of fusion power. Bootstrap current can provide a very significant contribution to the total plasma current. One drawback of tokamak is that the poloidal magnetic field is produced thanks to the current density, itself generated by the inductive field. A tokamak thus works as a transformer, where the primary is a set of poloidal coils that produce the poloidal magnetic field, and the secondary is the plasma itself. The variation of currents in the transformer primary induce a current in the plasma. A tokamak plasma is therefore a transient, that lasts as long as some magnetic flux is available in the primary of the transformer to induce an electric field in the plasma, the transformer secondary. Hence bootstrap current brings a welcome "free" contribution to the current density - free in the sense that it comes from the gradients that are anyway necessary to reach fusion conditions - and thus spares some magnetic flux consumption in the transformer primary. Other methods are possible based on RF wave propagation and absorption ("current drive"), but these are expensive schemes. On the side of drawbacks, an excessive density peaking may lead to impurity accumulation. Also the bootstrap current density is off-axis since all gradients must vanish on the magnetic axis. This situation may lead to instabilities, and indeed no plasma have been shown to last for ever with 100 % bootstrap current.

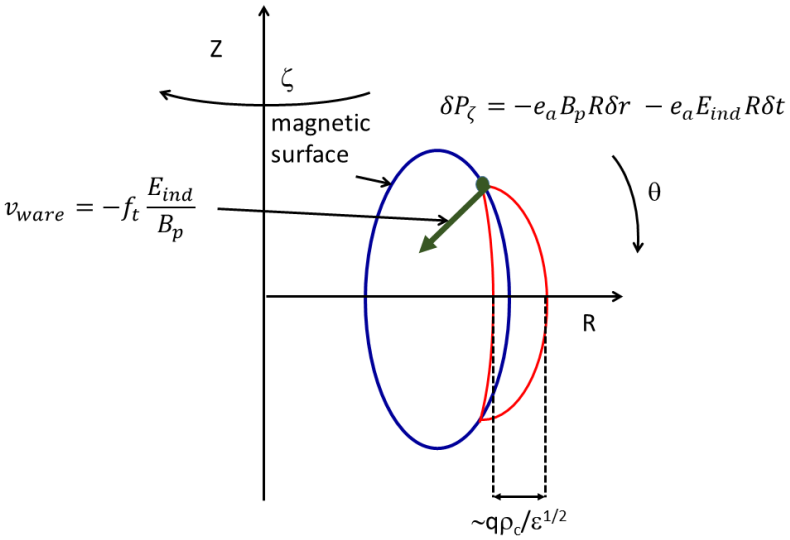

Figure 19: Schematic of the Ware pinch mechanism. The toroidal canonical momentum computed at a banana tip varies because of the induction. This variation must be compensated by a radial shift of the banana tip. The ware pinch is this radial shift per unit time multiplied by the fraction of trapped particles.

5.3.2 Physics of the Ware pinch

The inward Ware pinch is carried by trapped electrons. Let us remember that the canonical toroidal momentum $P_\zeta = -e_a\psi + m_a \frac{I}{B} v_\parallel$ is an invariant of motion. Trapped electrons feel the inductive field mostly at turning points $v_\parallel = 0$. As said in previous section, the inductive field E_{ind} comes from the time variation of the poloidal field. More exactly the Lenz law states that the loop voltage $V_{loop} = -\partial_t \Psi$, with $\Psi = -2\pi\psi$ (the function ψ

was defined as minus the poloidal flux normalised to 2π), and $V_{loop} = 2\pi R E_{ind}$, so that $E_{ind} = \partial_t \psi / R$. An alternative path is to notice that $\psi = -A_t R$, where A_t is the toroidal component of the vector potential, and $E_{ind} = -\partial_t A_t$. Hence the canonical toroidal momentum varies by, see Fig. 19,

$$\delta P_\zeta^{(1)} = -e_a \delta\psi = e_a E_{ind} R \delta t$$

over a small time δt near the time at which a trapped electron bounces. Since P_ζ is an invariant of motion, this variation must be balanced by a radial displacement $\delta\psi$ of the particle such that

$$\delta P_\zeta^{(2)} = -e_a \left.\frac{\delta\psi}{\delta t}\right|_{part} \delta t$$

where $\left.\frac{\delta\psi}{\delta t}\right|_{part} \delta t$ can be seen as a radial velocity of the particle. Momentum conservation requires $\delta P_\zeta^{(1)} + \delta P_\zeta^{(2)} = 0$. Let us remind that $d\psi = B_p R dr$, so that

$$\left.\frac{\delta r}{\delta t}\right|_{part} = -\frac{E_{ind}}{B_p}$$

The corresponding flux is the density of trapped electrons times their radial velocity, hence

$$\Gamma_{N,Ware} = -f_t N_{eq,e} \frac{E_{ind}}{B_p}$$

The scaling of the Ware pinch flux is thus recovered. It is quite remarkable that the collision frequency does not appear in the Ware flux whereas the underlying mechanism is collisional.

5.3.3 Physics of bootstrap current

The processes that lead to a bootstrap current can be understood as follows. Using again the invariance of the canonical toroidal momentum P_ζ, one gets a relationship between the radial displacement of a trapped particle and its parallel velocity

$$\hat{r} \simeq -\frac{m_e v_\parallel}{e B_p}$$

Using $B_p R \simeq r/qB_t$ and the trapping condition for thermal particles $v_\parallel \simeq \epsilon^{1/2} v_{Te}$, with $v_{Te} = \sqrt{T_{eq,e}/m_e}$ the thermal velocity, one recovers the typical radial extent of a trapped particle $\delta_{be} = q\rho_{Te}/\epsilon^{1/2}$ (banana width). However the relation above tells us more. Since it holds at any time, it implies that the displacement is inward (outward) for a co(counter)-current moving electron $v_\parallel/B_p > 0$ (poloidal field has the same sign as plasma current). Let us now consider a specific magnetic surface, on the low field side where trapped particles are located. Some trapped electrons come from the interior of the magnetic surface, with $\delta r > 0$: these electrons move against the current. Other trapped electrons arrive from the exterior and are thus co-current electrons. Because of collisions, some trapped electrons become passing at this location. For a peaked density profile $\partial_r N_{eq,e} < 0$, detrapped co-current electrons are less numerous than counter-current electrons. This means that a negative electromotive force with respect to the current direction is generated. This force must be compensated by the collision friction force between electrons and ions, thus producing a current - see Fig. 20.

Let us put this process in equations. The detrapping collision frequency is ν_{ei}/ϵ, assuming that electron-ion collisions dominate. The force density is the time variation of the electron momentum $m_e v_\parallel \simeq \epsilon^{1/2} m_e v_{Te}$ per unit of volume. The number of relevant electrons is the density difference between trapped electrons that come from inside vs

outside within a banana width, i.e. $f_t \partial_r N_{eq,e} \delta_{be}$. Hence an estimate of the electromotive force density is

$$F_{em} \simeq \frac{\nu_{ei}}{\epsilon} f_t \frac{\partial N_{eq,e}}{\partial r} \delta_{be} \epsilon^{1/2} m_e v_{Te} = f_t \nu_{ei} \frac{\partial N_{eq,e}}{\partial r} \frac{m_e T_{eq,e}}{eB_p}$$

The force balance equation for passing electrons read

$$F_{em} - N_{eq,e} m_e \nu_{ei} \left(V_{\|eq,e} - V_{\|eq,i} \right) = 0$$

It expresses the balance between the electromotive force due to collisional detrapping and the collisional friction between passing electrons and ions. This equation provides the increment of velocity and therefore the bootstrap current $J_{\|boot} = -N_{eq,e} e \left(V_{\|eq,e} - V_{\|eq,i} \right)$

$$J_{\|boot} = -f_t \frac{T_{eq,e}}{B_p} \frac{\partial N_{eq,e}}{\partial r} \tag{60}$$

This expression is in qualitative agreement with detailed calculations given above. It explains why the bootstrap current does not depend explicitly on the collision frequency while the underlying processes are collisional. This curious feature comes from a compensation between the collisional detrapping rate and the collisional drag between electrons and ions.

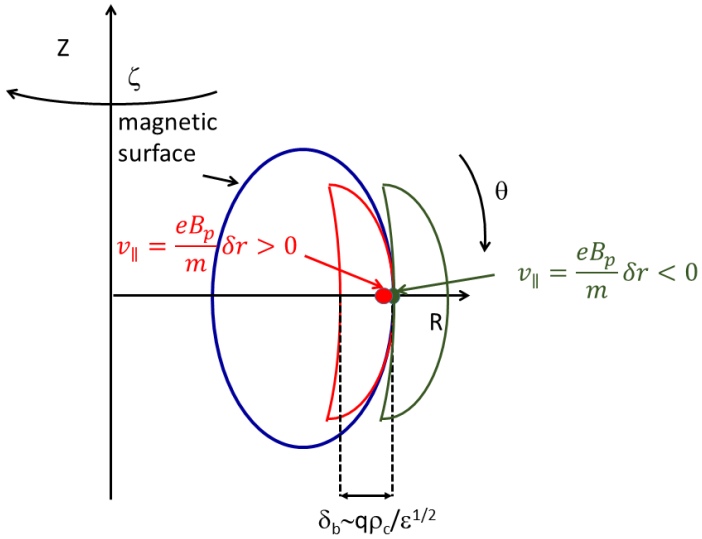

Figure 20: Schematic of the bootstrap current mechanism. The parallel velocity is oriented on each side of an electron banana branch. When the particle comes from the right, $v_\| < 0$, while its sign is opposite when it comes from the left. Because of collisions, trapped electrons become passing on a given magnetic surface. Since the density is not constant, more electrons come from the left than from the right. This process hence procudes an electromotive force along the field line. Its balance with collisional drag produces the bootstrap current.

6 Neoclassical transport with ripple*

A common task encountered in fusion devices is the computation of collisional transport in presence of 2 or more perturbations. The number of perturbations refer here to a reference configuration that is a screw pinch. In tokamaks, a first perturbation corresponds to the $1/R$ decay of the magnetic field. As seen above, it can be treated as a perturbed Hamiltonian $\widetilde{H} = -\mu B_0 \epsilon(r) \cos\theta$, in the limit of small inverse aspect ratio. A second perturbation

must be added when the effect of magnetic ripple is to be accounted for. Magnetic ripple is the corrugation of the toroidal field due to the finite number of coils used to produced the toroidal field, thus leading to a second perturbation $\widetilde{H} = \mu B_0 \delta(r,\theta) \cos(N_b \zeta)$, where N_b is the number of coils, and $\delta(r,\theta)$ the ripple amplitude. Another example is provided by non resonant helical perturbations produced with external coils. For a single helicity, the additional perturbation is $\widetilde{H} = \mu B_0 \delta(r) \cos(N_b \zeta + M_b \theta)$. In this case, the aim is to control edge localised modes (ELMs). Stellarators provide another important class of configurations where several magnetic perturbations coexist. These configurations have all in common that all perturbations resonate at vanishing parallel velocity $v_\parallel = 0$. An additional difficulty comes from the stochastic character of particle trajectories in some specific limits. The kinetic treatment of multiple perturbations that resonant nearby or at the same position in the phase is challenging. It is addressed with some generality in the note "Mean field kinetic theory", in the section "Nearly degenerate Hamiltonian perturbations". The present section essentially applies the expressions derived in this note to the case of magnetic ripple in tokamaks. An overview of neoclassical transport in presence of ripple can be found in [6]. The present section aims at summarising all regimes in a compact form thanks to a principle of minimum entropy production rate.

6.1 Local trapping and stochastic losses

6.1.1 Local trapping

A general expression of the entropy production rate for a non turbulent tokamak plasma, starting from the general expression derived in the note "Mean field kinetic theory", and in presence of ripple can be found in reference [11] - it has been extended to helical perturbations in reference [19]. The calculation is restricted to the case of ripple in a simple circular concentric equilibrium. Moreover a single ion species is considered. The equilibrium Hamiltonian is

$$H_{eq} = \frac{1}{2} m_i v_\parallel^2 + \mu B_0 + e_i \Phi_{eq}(r)$$

where m_i is the mass, $v_\parallel$ the parallel velocity, μ the magnetic moment, B_0 the magnetic field on the magnetic axis, and $\Phi_{eq}(r)$ the mean electric potential. The perturbed Hamiltonian now reads

$$\widetilde{H} = -\mu B_0 \epsilon(r) \cos\theta + \mu B_0 \delta(r,\theta) \cos(N_b \zeta)$$

where $\epsilon(r) = \frac{r}{R_0}$ and $\delta(r,\theta)$ is the amplitude of the ripple perturbation, and N_b the number of coils. It is convenient to decompose the latter in a poloidal modulation $\tilde{\delta}(r,\theta)$ and a poloidal average $\bar{\delta}(r)$, i.e. $\delta(r,\theta) = \bar{\delta}(r)\tilde{\delta}(r,\theta)$, where

$$\bar{\delta}(r) = \left[\int_0^{2\pi} \frac{d\theta}{2\pi} \delta(r,\theta) \right]^{1/2}$$

and

$$\tilde{\delta}(r,\theta) = \frac{\delta(r,\theta)}{\bar{\delta}(r)}$$

Particles are trapped in the helical perturbation when the magnetic fields exhibit local extrema along the field lines. If $N_b q(r) \gg 1$, local trapping occurs when

$$Y(r,\theta) = \alpha(r,\theta) |\sin\theta| < 1$$

where

$$\alpha(r,\theta) = \frac{\epsilon(r)}{N_b q(r) \delta(r,\theta)}$$

This condition defines for each minor radius r a domain in θ where some particles are locally trapped - see example Fig.21. One can define an effective ripple amplitude, which is the depth of the magnetic well along the field lines between successive minima and maxima [6], namely

$$2\delta_{eff} = \frac{B_{max}}{B_{min}} - 1 = 2\delta\left(\sqrt{1-Y^2} - Y\arccos Y\right) \tag{61}$$

The ripple amplitude used throughout this note is then

$$\delta(r,\theta) = \begin{cases} \delta(r,\theta) \text{ if } Y \geq 1 \\ \delta_{eff}(r,\theta) \text{ if } Y < 1 \end{cases} \tag{62}$$

It can be split in a poloidal average and modulation as well. Hence two kinds of trapped particles exist: toroidally trapped, and ripple trapped particles. It should be noted however that above a critical energy that depends on the ripple amplitude, the motion of particles is no longer regular, and becomes stochastic instead. This feature obviously modifies the transport properties, and is treated in the next section.

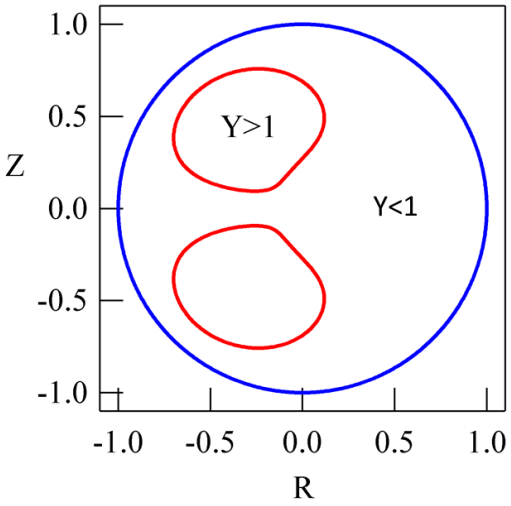

Figure 21: Example of regions where local trapping occur $Y > 1$ or not $Y < 1$, from [11].

6.1.2 Stochastic losses

The calculation of neoclassical transport is done in the adiabatic limit where $N_b\Omega_d \ll \Omega_b$, where Ω_d is the precession frequency of trapped particles, and Ω_b their bounce frequency. In the opposite limit $N_b\Omega_d \gg \Omega_b$, stochasticity develops above a threshold that involves the particle energy and ripple amplitude [20]. We admit here that the neoclassical calculation is valid until stochasticity emerges. This occurs when the Chirikov island overlap parameter is above a critical value S_c of order 1. The Chirikov overlap parameter is found to be [21]

$$S_I = 4\left(\frac{F_c}{\Theta}\right)^{1/2}(N_b q)^{3/4}\frac{\bar{\delta}^{1/2}}{\epsilon^2}\frac{q\rho_T}{R_0}u^{1/2}$$

where $F_c \sim s$ ($s = \frac{d\log q}{d\log r}$ is the magnetic shear), $\Theta = \sqrt{\frac{\pi\theta_b}{2}}$, θ_b is the bounce angle, $\rho_{Ti} = \frac{m_i v_{Ti}}{e_i B_0}$ is the thermal Larmor radius, and $u = \mu B_0/T_{eq} = x^2$ a normalised energy. Hence stochasticity sets on for energetic particles such that $u \geq u_c$, where u_c is defined as

$$u_c = \left(\frac{\Theta}{F_c}\right)\left(\frac{S_{c1}}{4}\right)^2\frac{1}{(N_b q)^{3/2}}\frac{\epsilon^4}{\bar{\delta}}\left(\frac{R_0}{q\rho_{Ti}}\right)^2$$

A difficulty is that this critical energy depends on the bounce angle θ_b, which makes integrals in the phase space somewhat tricky. An approximation consists in setting $\theta_b = \frac{\pi}{2}$, and $S_c = \frac{2}{\pi}$ (a proxy for 2/3 - let us note that Goldston et al. seems to use $S_c = 1/\pi$ [20]), which imposes

$$u_c = \frac{1}{8\pi} \frac{1}{(N_b q)^{3/2}} \frac{\epsilon^4}{\bar{\delta}} \frac{1}{s} \left(\frac{R_0}{q \rho_{Ti}} \right)^2$$

Hence the energy integral in the neoclassical entropy production rate, and calculated for the effect of ripple on banana tips, should be limited to $u \leq u_c$. For $u \geq u_c$, stochastic losses prevail. In this limit, the diffusion coefficient is given by the quasilinear theory

$$D_{QL} = \frac{1}{2} \frac{u^{3/2}}{\theta_b} D_p \frac{\delta^2}{\epsilon^{5/2}}$$

where D_p is the "plateau" diffusion coefficient

$$D_p = \frac{q R_0 v_D^2}{v_{Ti}}$$

Hence the value is about the same as the ripple-plateau diffusion. To simplify the expressions, the quasilinear value is adjusted to match exactly the ripple-plateau entropy production. Above a second critical value of energy, the quasilinear theory does not apply any more. This regime corresponds to the so-called strong perturbation regime. It is described in the work by Goldston et al. [20]. This regime occurs for a redefined Chirikov parameter S_{II} above a critical value S_c. This second Chirikov parameter reads

$$S_{II} = \left(\frac{2 F_K}{\Theta} \right)^{1/2} (N_b q)^{3/2} \frac{\bar{\delta}}{\epsilon^{5/2}} \frac{q \rho_{Ti}}{R_0} u^{1/2}$$

where $F_K = s\theta_b + \frac{1}{\theta_b} \simeq s\theta_b$ as low values of θ_b do not contribute much to the entropy production. The diffusion coefficient reads

$$D = D_{QL} \frac{S_{st}}{S_{II}}$$

where $S_{st} = 2$ in Grua et al. [21]. In the following expressions, the integrals over the bounce angle θ_b have been done analytically, and a fit performed in a second stage.

6.2 Total entropy production rate

The total resonant entropy production reads

$$\dot{S}_{res} = \dot{S}_{rip,I} + \dot{S}_{tor,II} + \dot{S}_{tor,I} + \dot{S}_{rip,II} + \dot{S}_{st}$$

Here the label I means "primary", and II "secondary", while "tor" means toroidal trapping (usual banana particles) and "rip" means local trapping in ripple wells. For instance $\dot{S}_{rip,I}$ means "local trapping is the primary effect". The component $\dot{S}_{st}$ accounts for stochastic losses. Some lengthy but straightforward algebra yields the following expression of the various contributions to the entropy production rate

$$\begin{aligned}
\dot{S}_{rip,I} &= \sqrt{\frac{\pi}{2}} \int dV N_{eq} D_p (N_b q) \left(\frac{\bar{\delta}}{\epsilon} \right)^2 \int_0^{+\infty} du e^{-u} u^2 K_{rip,I}(r,u) \left[\frac{e_i B_p}{T_{eq}} V_t \right]^2 \\
\dot{S}_{tor,I} &= \sqrt{\frac{\pi}{2}} \int dV N_{eq} D_p \int_0^{+\infty} du e^{-u} u^2 K_{tor,I}(r,u) \\
&\quad \left[\frac{1}{\mathcal{N}_{eq}} \frac{d\mathcal{N}_{eq}}{dr} + \left(u - \frac{3}{2} \right) \frac{1}{T_{eq}} \frac{dT_{eq}}{dr} + \frac{e_i B_p}{T_{eq}} V_t \right]^2
\end{aligned}$$

The entropy production rate $\dot{S}_{tor,II}$ is associated with the effect of magnetic drift on ripple trapped particles. It reads

$$\begin{aligned}\dot{S}_{tor,II} &= \frac{16}{9}\left(\frac{2}{\pi}\right)^{3/2}\int dV N_{eq} D_p \left(\frac{\bar{\delta}}{\epsilon}\right)^{3/2}\frac{G_1}{\nu_*} \\ &\int_0^{+\infty} du e^{-u} u^{5/2}\frac{1}{\bar{\nu}(u)}\left[\frac{1}{\mathcal{N}_{eq}}\frac{d\mathcal{N}_{eq}}{dr}+\left(u-\frac{3}{2}\right)\frac{1}{T_{eq}}\frac{dT_{eq}}{dr}\right]^2\end{aligned}$$

The production rate $\dot{S}_{rip,II}$ is due to effect of the ripple perturbation on bananas. If $\nu_* \ll 1/\epsilon^{3/2}$, the expression of $\dot{S}_{rip,II}$ depends on the effective collision frequency ν_{*eff}. It reads

$$\begin{aligned}\dot{S}_{rip,II} &= \left(\frac{2}{\pi}\right)^{3/2}\int dV N_{eq} D_p \frac{1}{N_b q}\left(\frac{\bar{\delta}}{\epsilon}\right)^2\frac{1}{\nu_*} \\ &\int_0^{u_c} du e^{-u} u^{5/2}\frac{1}{\bar{\nu}(u)} K_{rip,II}(r,u)\left[\frac{1}{\mathcal{N}_{eq}}\frac{d\mathcal{N}_{eq}}{dr}+\left(u-\frac{3}{2}\right)\frac{1}{T_{eq}}\frac{dT_{eq}}{dr}\right]^2\end{aligned}$$

The production rate $\dot{S}_{rip,II}$ is small when $\nu_* \gg 1/\epsilon^{3/2}$ (Pfirsch-Schlüter regime), which may need to introduce an additional cut-off.These expressions cover most regimes described in section 2, in particular super-banana transport.

The stochastic component reads

$$\begin{aligned}\dot{S}_{st} &= \sqrt{\frac{\pi}{2}}\int dV N_{eq} D_p N_b q \left(\frac{\bar{\delta}}{\epsilon}\right)^2 \\ &\int_{u_c}^{+\infty} du e^{-u} u^2 K_{st}(r,u)\left[\frac{1}{\mathcal{N}_{eq}}\frac{d\mathcal{N}_{eq}}{dr}+\left(u-\frac{3}{2}\right)\frac{1}{T_{eq}}\frac{dT_{eq}}{dr}\right]^2\end{aligned}$$

In these formula $dV = 4\pi^2 R_0 r dr$ is the volume element, $\bar{\nu}(u) = \bar{\nu}(\sqrt{u})$, $v_D = \frac{T_{eq}}{eB_0R_0}$ is the thermal magnetic drift velocity.

The functions K provide smooth transitions between various collision regimes, and also the transition between the weak and strong stochastic regimes

$$K_{rip,I}(r,u) = G_0 + \min\left(G_0', G_0''\frac{4}{\pi}\mathcal{I}\frac{\nu_*}{N_b q}\left(\frac{\epsilon}{\bar{\delta}}\right)^{3/2}\frac{\bar{\nu}(u)}{u^{1/2}}\right)$$

$$K_{tor,I}(r,u) = \min\left(1, \frac{4}{\pi}\mathcal{I}\nu_*\frac{\bar{\nu}(u)}{u^{1/2}}\right)$$

$$K_{rip,II}(r,u) = \max\left(1, \frac{\pi^2}{8}\nu_*(N_b q)^2\frac{\bar{\nu}(u)}{u^{1/2}}\right)$$

where $\mathcal{I} = 1.38$. The function that ensures a continuous transition from weak to strong perturbation regime reads

$$K_{st}(r,u) = \frac{1}{1+\frac{2}{\sqrt{\pi}}\frac{1}{S_{st}}\left(N_b q\right)^{3/2}\frac{\delta}{\epsilon^{5/2}}\frac{q\rho_{Ti}}{R_0}s u^{1/2}}$$

where S_{st} is related to the transition to stochasticity in the strong perturbation regime. We choose here $S_{st} = 2$.

The function $\min(x,y)$ and $\max(x,y)$ have discontinuous derivatives along the line $y = x$. Reasonable fits are

$$\frac{1}{\min(x,y)} = \frac{1}{x} + \frac{1}{y}$$

and

$$\max(x, y) = x + y$$

When $\alpha \gg 1$, the form factors G_0, G_0', G_0'', G_1 are given by the relations

$$G_0(r) = \int_{Y>1} \frac{d\theta}{2\pi} \tilde{\delta}^2(r,\theta) \qquad G_0'(r) = \int_{Y<1} \frac{d\theta}{2\pi} \tilde{\delta}^2(r,\theta) \qquad G_0''(r) = \int_{Y<1} \frac{d\theta}{2\pi} \tilde{\delta}^{\frac{1}{2}}(r,\theta)$$

and

$$G_1(r) = \int_{Y<1} \frac{d\theta}{\pi} \tilde{\delta}^{\frac{3}{2}}(r,\theta) \sin^2\theta$$

6.3 Expressions of fluxes

6.3.1 How to proceed?

The strategy to determine a neoclassical equilibrium with ripple is rather straightforward. First the extremum of the entropy production rate with respect to density variations yields the particle flux. The ambipolarity constraint reduces to a condition of vanishing ion flux, $\Gamma_N = 0$. This constraint gives a relation between the radial electric field, toroidal velocity (or angular frequency) and gradients of density and temperature (the poloidal velocity can be eliminated using the force balance equation). Second the extremum with respect to the toroidal velocity provides the damping rate in the toroidal direction and therefore another constraint. Finally, the extremum with respect to the temperature gradient yields the thermal diffusivity.

6.3.2 Transport matrix

The procedure explained above can be conveniently recast as a transport matrix relationship, which reads

$$\mathbf{\Gamma} = \mathfrak{M}\mathbf{A} \tag{63}$$

where $\mathbf{\Gamma}$ is the " thermodynamical flux" vector

$$\mathbf{\Gamma} = \begin{pmatrix} \Gamma_N \\ \Gamma_V \\ \Gamma_T \end{pmatrix} = \begin{pmatrix} \frac{\Gamma}{N} \\ \frac{\mathcal{M}}{N e_i B_p} \\ \frac{Q}{NT} \end{pmatrix}$$

and $\mathbf{A}$ is the "thermodynamical force" vector

$$\mathbf{A} = \begin{pmatrix} A_E \\ A_V \\ A_T \end{pmatrix} = \begin{pmatrix} \frac{1}{\mathcal{N}_{eq}} \frac{d\mathcal{N}_{eq}}{dr} \\ \frac{e_i B_p}{T} V_t \\ \frac{1}{T_{eq}} \frac{dT_{eq}}{dr} \end{pmatrix}$$

and $\mathfrak{M}$ is the transport matrix

$$\mathfrak{M} = -D_p \begin{pmatrix} d_{NN} & d_{NV} & d_{NT} \\ d_{VN} & d_{VV} & d_{VT} \\ d_{TN} & d_{TV} & d_{TT} \end{pmatrix}$$

The matrix elements are given in Appendix F. The transport matrix can be reshaped in the following form

$$\mathfrak{M} = -D_p \begin{pmatrix} d_0 + \tilde{d}_0 & d_0 & d_1 + \tilde{d}_1 \\ d_0 & d_0 + \hat{d}_0 & d_1 \\ d_1 + \tilde{d}_1 & d_1 & d_2 + \tilde{d}_2 \end{pmatrix} \tag{64}$$

The elements are detailed in Appendix F. This structure gives some insight in the physics due to ripple, as seen in the next section.

6.3.3 Electric field and toroidal velocity

In principle, the inversion of the relation $\mathbf{\Gamma} = \mathfrak{M}\mathbf{A}$ yields the values of the forces $\mathbf{A}$ given the fluxes $\mathbf{\Gamma}$. However, this is only true in steady-state, which is not the case of most simulations, unless one waits for a very long computation time. In practice, one can expect the ambipolarity condition $\Gamma_N = 0$ to be respected on a short time scale, since any departure from ambipolarity produces an electric field that re-establishes ambipolarity in a short time scale. On the other hand, the temperature takes basically a confinement time before it relaxes to its asymptotic value. So it is reasonable to consider A_T fixed, i.e. to be a given for a simulation time that is short. Momentum should be somewhere in between. We then focus on the two first lines of the transport matrix Eq.(64), which yield the electric field A_E and toroidal velocity A_V given the particle flux Γ_N, which is assumed finite for the time being, and the torque Γ_V. One expects A_E, A_V to be proportional to A_T, i.e. $A_E = -k_E A_T$ (beware the sign), $A_V = k_V A_T$, or equivalently

$$\frac{e_i E_r}{T_{eq}} - \frac{1}{N_{eq}}\frac{dN_{eq}}{dr} = k_E \frac{1}{T_{eq}}\frac{dT_{eq}}{dr}$$

and

$$\frac{e_i B_p}{T_{eq}} V_t = k_T \frac{1}{T_{eq}}\frac{dT_{eq}}{dr}$$

The force balance equation, which is always verified on a very short time scale in GYSELA, can be formulated as

$$\frac{e_i B_0}{T_{eq}} V_p = \frac{1}{\mathcal{N}}\frac{d\mathcal{N}}{dr} + \frac{e_i B_p}{T_{eq}} V_t + \frac{1}{T_{eq}}\frac{dT_{eq}}{dr}$$

which can be rephrased as

$$A_{Vp} = \frac{e_i B_0}{T_{eq}} V_p = A_E + A_V + A_T \tag{65}$$

Hence it yields the poloidal velocity once A_E and A_V are known. Hence one expects $\frac{e_i B_0}{T_{eq}} V_p = k_P A_T$ with

$$k_p = -k_E + k_V + 1$$

In absence of ripple, it is clear that the two first lines the matrix $\mathfrak{M}$, Eq.(64), are the same. This means, as expected, that the system is degenerate. Therefore A_E, A_V cannot be determined separately, only the combination $A_E + A_V$

$$A_E + A_V = -\frac{d_1}{d_0} A_T$$

which happens to yield directly the poloidal velocity

$$\frac{e_i B}{T} V_p = \left(1 - \frac{d_1}{d_0}\right) A_T$$

This is a standard result of neoclassical theory.

With ripple the situation changes dramatically. Subtracting the second line from the first line of the relation $\mathbf{\Gamma} = \mathfrak{M}\mathbf{A}$, one finds the exact relationship

$$\Gamma_V - \Gamma_N = -D_P \left(\hat{d}_0 A_V - \tilde{d}_0 A_E - \tilde{d}_1 A_T\right) \tag{66}$$

If the particle flux is zero, this relation yields the torque Γ_V due to magnetic drag versus the gradients A_E and A_V. All coefficients depend on the ripple amplitude, which makes it particularly attractive. Two limit cases appear:

- friction due to local trapping dominates $\hat{d}_0 \gg \tilde{d}_n$, then $\Gamma_V = -D_P \hat{d}_0 A_V$: the velocity should relax toward 0. Hence $k_T = 0$.

- situation where $\hat{d}_0 \ll \tilde{d}_n$, typically $1/\nu$ regime, or absence of local trapping. In this limit $\Gamma_V = D_P \left(\tilde{d}_0 A_E + \tilde{d}_1 A_T \right)$, which yields directly the radial electric field vs temperature gradient. This is typically the structure found by Connor et al. [22]. As a result, $k_E = -\tilde{d}_1/\tilde{d}_0$.

Let us pursue the analysis of the case with vanishing particle flux $\Gamma_N = 0$. One can then extract an additional constraint

$$A_E = -\frac{d_0}{d_0 + \tilde{d}_0} A_V - \frac{d_1 + \tilde{d}_1}{d_0 + \tilde{d}_0} A_T$$

which is readily implemented in Eq.(66)

$$\Gamma_V = -D_P \left[\left(\hat{d}_0 + \frac{d_0 \tilde{d}_0}{d_0 + \tilde{d}_0} \right) A_V - \left(\frac{\tilde{d}_1 d_0 - \tilde{d}_0 d_1}{d_0 + \tilde{d}_0} \right) A_T \right]$$

This expression bears the exact form that is requested, i.e.

$$\Gamma_V = -\hat{\nu}_\zeta \left[A_V - k_T A_T \right] \tag{67}$$

with

$$k_T = \frac{d_0 \tilde{d}_1 - d_1 \tilde{d}_0}{(d_0 + \tilde{d}_0)(d_0 + \hat{d}_0) - d_0^2} = \frac{d_{VN} d_{NT} - d_{NN} d_{VT}}{d_{NN} d_{VV} - d_{NV}^2}$$

and

$$\hat{\nu}_\zeta = \hat{d}_0 + \frac{d_0 \tilde{d}_0}{d_0 + \tilde{d}_0} = d_{VV} - \frac{d_{NV}^2}{d_{NN}} \tag{68}$$

Note that again all coefficients go to 0 when ripple vanishes, as they should. This means that the case $\Gamma_N = 0$ does behave correctly.

The torque Γ_V Eq.(67) is responsible for a relaxation of the angular toroidal velocity RV_t towards a constant value proportional to the temperature gradient. This process is called magnetic breaking and is illustrated in Fig.22.

6.3.4 Heat flux

The heat flux is given by the following relation

$$\Gamma_T = -D_P \left\{ \left(d_1 + \tilde{d}_1 \right) A_E + d_1 A_V + \left(d_2 + \tilde{d}_2 \right) A_T \right\}$$

At vanishing particle flux $\Gamma_N = 0$, the electric field A_E can be expressed as function of A_V and A_T using Eq.(67). This gives the following result

$$\Gamma_T = -D_P \left\{ \frac{d_1 \tilde{d}_0 - d_0 \tilde{d}_1}{d_0 + \tilde{d}_0} A_V + \left(d_2 + \tilde{d}_2 - \frac{\left(d_1 + \tilde{d}_1 \right)^2}{d_0 + \tilde{d}_0} \right) A_T \right\}$$

Finally, plugging $A_V = k_T A_T$ in the expression above yields the heat diffusivity. However this last step may not be legitimate since the relation $A_V = k_T A_T$ only applies when a steady-state has been reached for the toroidal momentum. This is usually not the case.

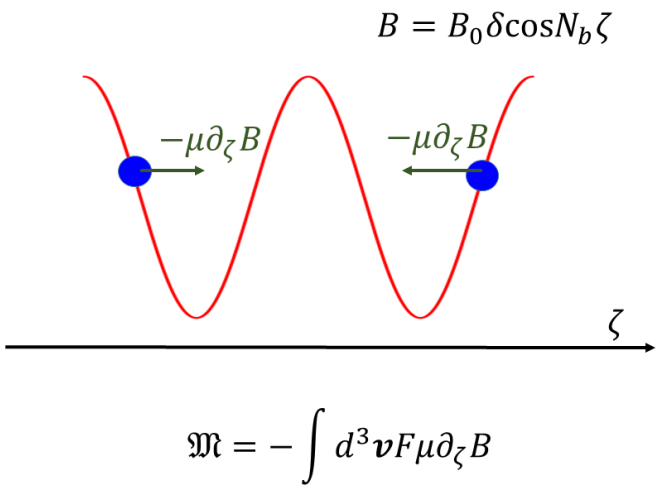

Figure 22: Principle of magnetic breaking. The mirror force exerted on a guiding-centre in a inhomogeneous magnetic field is $-\mu \nabla B$. When the field is oscillating, the mirror force can speed up or slow down a particle. This process is responsible for particle trapping. The mirror force induces a response of the distribution function that oscillates with the same spatial periodicity as the magnetic field corrugation. The resulting average torque is responsible for magnetic breaking.

7 Conclusion

In summary, most result of neoclassical theory can be recovered thanks to a variational principle based on minimum entropy production rate. Its effectiveness is illustrated here with the enhancement of collisional transport by resonant processes, which is at the heart of neoclassical theory of transport. Hence it does not cover the collisional Pfirsch-Schlüter regime. The latter can be added quite easily with a similar approach. When analysed in depth, the key element of neoclassical transport lies in a boundary layer that develops at the interface between trapped and passing domains in the phase space. Loosely speaking, the distribution function is shifted in the parallel velocity direction, whereas trapped particles cannot develop an organised motion, up to their diamagnetic velocity. This leads to a fast variation of the distribution function at the trapped/passing boundary that is regularised by collisions, hence the notion of collisional boundary layer. An extremum of entropy production rate expresses in fact a balance between the increase of entropy production within the boundary layer, and the increase of entropy due to collisions between passing particles, i.e. far away from the boundary layer in the phase space.

Neoclassical theory leads to several essential results. First the poloidal velocity of the main ion species relaxes towards a value proportional to the ion temperature gradient. This is the result of a collisional drag between trapped and passing ions. If the effect of electrons is ignored, the main prediction of neoclassical theory is an ion heat diffusivity that is higher than the classical prediction. When electrons are accounted for, the expressions of fluxes become more complex. Basically the particle flux exhibits non diagonal contributions, called pinch terms. Pinch fluxes are proportional to the density, and not its gradient. One contribution to the pinch velocity is due to thermodiffusion, i.e. is proportional to the electron temperature gradient. A second component of the pinch velocity is proportional to the inductive field, and is called Ware pinch. The electron heat flux bears a similar structure, with thermodiffusion replaced by a heat pinch velocity proportional to the electron density gradient. Finally the Ohm's law appears to be significantly modified. First the conductivity decreases since only passing electrons carry current. Moreover a new term appears in the current density, which is proportional to density and temperature

gradients and is called bootstrap current. The latter plays an important role in tokamaks, as it reduces the amount of current to be driven by induction.

Finally one additional advantage of using a variational approach is its ability to incorporate more complex processes related to the breaking of axisymmetry. The example that is given here is magnetic ripple, which is a corrugation of the magnetic field due to the finite number of coils in a tokamak. It can be extended to helical perturbations. The main effect of such 3D perturbations (3D in the sense of non-axisymmetric) is to enhance dramatically transport at low collisionality. In a nutshell, neoclassical diffusion coefficients that are proportional to the collision frequency are now inversely proportional to it, hence diverge when plasmas get hotter. Fortunately, motion across the magnetic field, in particular due to the $E \times B$ drift, regularises this behaviour, to produce something again proportional to collisional frequency at very low collisionality. Another important consequence of 3D effects is magnetic breaking, i.e. a relaxation of the toroidal velocity, similar to the one observed in the poloidal direction in conventional neoclassical theory.

As a final note, the reader may question the very idea of computing collisional transport since it is known that perpendicular transport is often dominated by turbulent processes. One first obvious answer is that physics along the field lines remain controlled by collisions. Hence resistivity and bootstrap current matter. This is also true for the poloidal velocity, which remains quite often determined by neoclassical relaxation - and same for toroidal velocity in presence of strong ripple. This is of course decisive since flows are known to regulate turbulent transport. In addition, there exists cases where neoclassical terms contribute significantly to perpendicular transport of particles, momentum and heat. One well known example is heavy impurity transport. Another one is Ware pinch, which can overcome its turbulent counterpart in regimes where the inductive field is strong, typically transients. Last but not the least, neoclassical and turbulent processes can interact in a synergistic way. All these reasons imply that collisional processes should never be neglected lightly.

APPENDICES

A Radial displacement due to ripple in a tokamak

Since we are interested in the motion of a banana tip, it is sufficient to analyse the bounce motion of a particle. The motion of the toroidal angle of the banana tip $\bar{\zeta}$ and the canonical toroidal momentum P_ζ is Hamiltonian, i.e.

$$\begin{aligned} \frac{d\bar{\zeta}}{dt} &= \frac{\partial \langle H \rangle_b}{\partial P_\zeta} \\ \frac{dP_\zeta}{dt} &= -\frac{\partial \langle H \rangle_b}{\partial \bar{\zeta}} \end{aligned}$$

where the bracket indicates a bounce average, i.e. an average over the bounce angle. The canonical toroidal momentum is just $P_\zeta = -e_a\bar{\psi}$, where e_a is the algebraic charge and $\bar{\psi}$ the time average of the poloidal flux. The Hamiltonian H is the sum of an "equilibrium" Hamiltonian, that depends on the invariants of motion only, and a perturbed Hamiltonian $\widetilde{H}$. We choose a simple representation if this perturbed Hamiltonian in the case of ripple, which reads $\widetilde{H} = -\mu B_0 \delta \cos(N_c\zeta)$, where μ is the magnetic moment, B_0 is a reference toroidal field, δ the amplitude of the magnetic field ripple assumed constant for simplicity, and N_c the number of toroidal coils in the considered tokamak. Let us remember that the particle toroidal angle reads $\zeta = q\hat{\theta} + \bar{\zeta}$, where $\hat{\theta}$ is the poloidal angle of the banana particle, and $q(\bar{\psi})$ the safety factor. For deeply trapped particles, $\hat{\theta}$ can be approximated by $\theta_b \sin(\alpha_b)$, where θ_b is the bounce poloidal angle, and α_b the bounce angle, i.e. $\alpha_b = \Omega_b t + \alpha_{b0}$, where Ω_b is the bounce frequency, and α_{b0} some initial condition. The bounce average perturbed Hamiltonian then reads

$$\left\langle \widetilde{H} \right\rangle_b = \mu B_0 \delta J_0(N_c q \theta_b) \cos(N_c \bar{\zeta})$$

where J_0 is the Bessel function of index 0. The Hamiltonian $\left\langle \widetilde{H} \right\rangle_b$ depends on $\bar{\psi}$ only via the safety factor. For a small ripple amplitude and low magnetic shear $dq/d\bar{\psi}$, it appears that the motion of the banana tip toroidal angle $\bar{\zeta}$ is essentially ruled by the equilibrium Hamiltonian H_{eq} and is therefore close to the unperturbed precession motion. The new feature is the time variation of $P_\zeta = -e_a\bar{\psi}$, which is no longer an invariant of motion. Since the bounce period is much smaller than a precession period, the variation of $\Delta\bar{\psi}$ after a bounce half-period π/Ω_b is

$$e_a \Delta\bar{\psi} = \frac{\pi}{\Omega_b} \mu B_0 \delta J_0(N_c q \theta_b) N_c \sin(N_c \bar{\zeta})$$

Moreover, for circular concentric magnetic surfaces in the large aspect ratio limit, $\Delta\bar{\psi} = r/qB_0\Delta r_\delta$, where Δr_δ is the radial displacement of the banana tip that is looked for. One then use the following estimate for trapped particles

$$\Omega_b \simeq \frac{1}{qR_0}\sqrt{\frac{\mu B_0 \epsilon}{m_a}}$$

Using $\mu B_0 = m_a v^2/2$, where m_a is the particle mass, one finds

$$\Delta r_\delta = \frac{\pi}{\sqrt{2}} \frac{q^2\delta}{\epsilon^{3/2}} J_0(N_c q \theta_b) N_c \sin(N_c \bar{\zeta}) \rho_c$$

B A model for a multi-species collision operator

The full Boltzmann collision operator is a quadratic non linear operator that acts on distribution functions. It is difficult to handle as such, and is thus often replaced by a simpler operator. The first step consists in linearising the operator around a known bulk distribution function, usually a Maxwellian. Though this step greatly simplify the overall structure operator, it is still difficult to use in practice as in involves integrals over the distribution function that is looked for. In other words it is at this stage an integro-differential operator. A step further consists in replacing the integral part by approximations. A systematic procedure can be devised to achieve this goal, with some flexibility in its implementation. The present appendix gives an example of such a model operator, keeping in mind that many others exist in the literature.

B.1 Requirements on a collisional operator

A multi-species collision operator must satisfy several constraints:

- particle, momentum and energy conservation
- H theorem, i.e. positive entropy production rate
- relaxation towards a Maxwellian, which can be considered as part of the H theorem, since the minimum of entropy production rate should be reached when the distribution function is a Maxwellian.

The Boltzmann collision operator satisfies properties of momentum and energy conservation for every couple of species. This detailed force and energy balance can be expressed as follows. The non linear collision operator for a species "a" is written in the form

$$\mathcal{C}_{tot,a} = \sum_b \mathcal{C}_{tot,ab}\left(F_a, F_b\right) \tag{69}$$

The collisional momentum transfer rate, or equivalently the friction force between species "a" and "b", is defined as

$$\mathbf{R}_{ab} = \int d^3\mathbf{v}\mathcal{C}_{tot,ab}\left(F_a, F_b\right) m_a\mathbf{v}$$

while the collisional energy exchange rate is

$$Q_{ab} = \int d^3\mathbf{v}\mathcal{C}_{tot,ab}\left(F_a, F_b\right) \frac{1}{2} m_a \left(\mathbf{v} - \mathbf{V}_a\right)^2$$

The detailed balance conservation law takes the form

$$\mathbf{R}_{ab} = -\mathbf{R}_{ba} \tag{70}$$

$$Q_{ab} + \mathbf{R}_{ab}\cdot\mathbf{V}_a = -Q_{ba} - \mathbf{R}_{ba}\cdot\mathbf{V}_b \tag{71}$$

If all distribution functions are Maxwellian, exact expressions for collisional momentum $\mathbf{R}_{ab}^M$ and energy exchange rates Q_{ab}^M are [5, 14]

$$\mathbf{R}_{ab}^M = -N_a m_a \nu_{ab}(\mathbf{V}_a - \mathbf{V}_b)$$

and

$$Q_{ab}^M + \mathbf{R}_{ab}^M\cdot\mathbf{V}_a = -3N_a\frac{m_a}{m_a+m_b}\nu_{ab}(T_a - T_b)$$

where N_a, $\mathbf{V}_a$ and T_a are the density, velocity and temperature of the species "a", and ν_{ab} is the momentum transfer rate

$$\nu_{ab} = \frac{4\sqrt{2\pi}}{3}\frac{N_b}{m_a}\left(\frac{1}{m_a}+\frac{1}{m_b}\right)\frac{e_a^2 e_b^2 \ln\Lambda}{\left(4\pi\varepsilon_0\right)^2}\frac{1}{\left(v_{Ta}^2 + v_{Tb}^2\right)^{3/2}}$$

Obviously the properties Eqs.(70,71) are satisfied by Eq.(72,72). It must be kept in mind that the solution of the advection/diffusion problem is not a Maxwellian in presence of a temperature gradient. As a consequence, extra terms appear in the force $\mathbf{R}_{ab}$, in particular a thermal force.

B.2 General structure of a collision operator

We adopt here an operator that is a variant of the Hirshman-Sigmar class of operators. This operator relaxes towards a Maxwellian, satisfies an H-theorem, and verifies the main conservation laws. In addition, the exact inter-species momentum and energy transfer rate are recovered when the distribution functions are Maxwellian [23]. The operator is linearised around unshifted Maxwellian distribution functions F_{M0a} for all species. The collision operator at lowest order is not zero. We take it of the form

$$\mathcal{C}_{tot,ab}\left(F_{M0a}, F_{M0b}\right) = \frac{2}{3}\frac{Q_{ab}^{M}}{N_a T_a}\left(\frac{m_a v^2}{2T_a} - \frac{3}{2}\right) F_{M0a}$$

This operator ensures that the temperatures of the Maxwellian distribution functions are equal at thermodynamical equilibrium. We now turn to the linearised operator, which is decomposed in a similar form as Eq.(69), i.e.

$$C_a\left(F_a\right) = \sum_b \mathcal{C}_{ab}\left(F_a\right)$$

This operator is parametrized by weighted moments of F_{M0a}, F_{M0b} and $\delta F_b = F_b - F_{M0b}$. The argument of this operator is noted F_a rather than δF_a since F_{M0a} belongs to the kernel of this operator, as will be shown below. Each term $\mathcal{C}_{ab}$ can be split in 2 parts

$$\mathcal{C}_{ab} = \mathcal{C}_{ab}^{(t)} + \mathcal{C}_{ab}^{(f)}$$

The first contribution $\mathcal{C}_{ab}^{(t)} = \mathcal{C}_{tot,ab}\left(\delta F_a, F_{M0b}\right)$ is usually called "test particle collision operator", and corresponds to collisions experienced by a particle on a Maxwellian distribution of particles "b". The second $\mathcal{C}_{ab}^{(f)} = \mathcal{C}_{tot,ab}\left(F_{M0a}, \delta F_b\right)$ is sometimes named "field particle collision operator", and rather corresponds to a modification of Rosenbluth potentials due to the perturbed distribution function δF_b.

B.3 Test particle collision operator

The test particle collision operator is most conveniently written in spherical coordinates (v, ξ), where v is the velocity modulus, and $\xi = \frac{v_\parallel}{v}$ a pitch-angle variable. The third variable is the gyro-angle γ. The test particle operator is separable in this set of coordinates and reduces to

$$\mathcal{C}_{ab}^{(t)}\left(F_a\right) = \frac{1}{v^2}\frac{\partial}{\partial v}\left[v^2 D_{v,ab}\left(\frac{\partial F_a}{\partial v} + \frac{m_a v}{T_b}F_a\right)\right] + \nu_{d,ab} L\left(F_a\right)$$

where the operator

$$L\left(F_a\right) = \frac{1}{2}\frac{\partial}{\partial \xi}\left[\left(1-\xi^2\right)\frac{\partial F_a}{\partial \xi}\right] + \frac{1}{2}\frac{1}{1-\xi^2}\frac{\partial^2 F_a}{\partial \gamma^2} \tag{72}$$

accounts for pitch-angle and gyro-angle scattering. The diffusion coefficient in the velocity radial direction is noted $D_{v,ab} = \frac{1}{2}\nu_{v,ab}v^2$. The corresponding diffusion rate $\nu_{v,ab}$ is usually called "parallel" collision rate and noted $\nu_{\parallel,ab}$. We will rather name it "radial velocity collision rate", and avoid the notation $\nu_{\parallel,ab}$ since it brings some confusion. Indeed the parallel direction designates here the direction along the magnetic field. The collision frequency $\nu_{d,ab}$ is the usual collisional deflection rate. The diffusion coefficients in the

velocity space $D_{v,ab}$, and $D_{d,ab}$ are then related to the velocity and deflection collision frequencies $\nu_{v,ab}$ and $\nu_{d,ab}$ via the relations

$$\begin{aligned} D_{v,ab}(v) &= \frac{1}{2}\nu_{v,ab}(v)v^2 = v_{Ta}^2 x_a^2 \nu_{v,ab}(x_a) \\ D_{d,ab}(v) &= \frac{1}{2}\nu_{d,ab}(v)v^2 = v_{Ta}^2 x_a^2 \nu_{d,ab}(x_a) \end{aligned}$$

where v is the velocity modulus (i.e. $E = \frac{1}{2}m_a v^2$) and x_a is a normalized velocity modulus

$$x_a = \sqrt{\frac{E}{T_a}} = \frac{v}{\sqrt{2}v_{Ta}}$$

We introduce a normalizing self-collision frequency ν_{aa} for the species 'a'

$$\nu_{aa} = \frac{4\sqrt{\pi}}{3}\frac{\ln\Lambda}{(4\pi\varepsilon_0)^2}\frac{N_a Z_a^4 e^4}{m_a^2 v_{Ta}^3}$$

With these notations, the velocity, deflection and slowing-down collision frequencies are

$$\nu_{v,ab}(x_a) = \nu_{aa}^{HS}\frac{v_{Ta}}{v_{Tb}}\frac{\Theta(x_b)}{x_a^2}$$

$$\nu_{d,ab}(x_a) = \nu_{aa}^{HS}\frac{v_{Ta}}{v_{Tb}}\frac{\Psi(x_b)}{x_a^2}$$

$$\nu_{s,ab}(v) = \nu_{aa}^{HS}\frac{T_a}{T_b}\left(1+\frac{m_b}{m_a}\right)\frac{v_{Ta}}{v_{Tb}}\Theta(x_b)$$

where

$$\nu_{aa}^{HS} = \sqrt{2}\frac{N_b Z_b^2}{N_a Z_a^2}\nu_{aa}$$

Here x_b is a function of x_a, i.e.

$$\begin{aligned} x_a &= \frac{v}{\sqrt{2}v_{Ta}} \\ x_b &= x_{ba}x_a = \frac{v}{\sqrt{2}v_{Tb}} \\ x_{ba} &= \frac{v_{Ta}}{v_{Tb}} \end{aligned}$$

The functions Ψ, G, Φ depend on the velocity modulus only and are defined as

$$\begin{aligned} \Psi(x) &= \frac{3\sqrt{\pi}}{4}\frac{1}{x}\left[\Phi(x) - G(x)\right] \\ \Theta(x) &= \frac{3\sqrt{\pi}}{2}\frac{G(x)}{x} \\ G(x) &= \frac{1}{2x^2}\left(\Phi(x) - x\Phi'(x)\right) \\ \Phi(x) &= \frac{2}{\sqrt{\pi}}\int_0^x dy \exp\left(-y^2\right) \end{aligned}$$

The function $\Phi(x)$ is the error function, and the function $G(x)$ is the Chandrasekhar function, in accordance with Hirshman-Sigmar [23, 24] and Hinton-Hazeltine [14, 25] papers. These definitions have been chosen such that the deflection and slowing-down frequencies $\nu_{d,ab}$ and $\nu_{s,ab}$ coincide with the definitions given by Hirshman and Sigmar [23]. The notation ν_{aa}^{HS} refers to the interspecies collision rate $1/\tau_{ab}$ defined in [26]. Hence ν_{aa}^{HS} is different from the inter-species momentum transfer rate ν_{ab}. In particular ν_{aa}^{HS} differs from ν_{aa} by a factor $\sqrt{2}$, i.e. $\nu_{aa}^{HS} = \sqrt{2}\nu_{aa}$. Useful asymptotic limits are

$$\begin{aligned} &\text{slow particle } (x \to 0): \quad \Psi(x) \to 1; \quad \Theta(x) \to 1 \\ &\text{fast particle } (x \to \infty): \quad \Psi(x) \to \tfrac{3\sqrt{\pi}}{4}\tfrac{1}{x}; \quad \Theta(x) \to \tfrac{3\sqrt{\pi}}{4}\tfrac{1}{x^3} \end{aligned}$$

B.4 Field particle collision operator

The field particle operator is more intricate. Hirshman and Sigmar proposed a general method based on an expansion on spherical functions and Laguerre polynomials [23]. We adopt here a simpler version, which fits the forces and heat fluxes. It bears some similarity with the operators proposed by Abel et al. [27] and Sugama et al. [28]. This operator is of the form

$$\begin{aligned} \mathcal{C}_{ab}\left(F_a\right) &= \frac{\partial}{\partial \mathbf{v}} \cdot \left(F_{M0a} \mathbf{D}_{ab} \cdot \frac{\partial g_a}{\partial \mathbf{v}} \right) \\ &- \nu_{s,ab} \frac{m_a \mathbf{v}}{T_a} \cdot \left(\mathbf{U}_{d,a} - \mathbf{U}_{ba} \right) F_{M0a} \end{aligned}$$

where

$$g_a = h_a - \frac{m_a v^2}{2T_a} q_{ba}$$

$$h_a = f_a - \frac{m_a \mathbf{v} \cdot \mathbf{U}_{d,a}(v)}{T_a}$$

and $f_a = \frac{F_a}{F_{M0a}}$. The distribution F_{M0a} is the unshifted Maxwellian built with the density N_a and the temperature T_a,

$$F_{M0a}\left(\mathbf{x}, \mathbf{v}, t\right) = N_a\left(\mathbf{x}, t\right) \left(\frac{m_a}{2\pi T_a\left(\mathbf{x}, t\right)} \right)^{3/2} \exp\left(-\frac{E}{T_a\left(\mathbf{x}, t\right)} \right) \tag{73}$$

where

$$\begin{aligned} N_a &= \int d^3\mathbf{v} F_a \\ \frac{3}{2} N_a T_a &= \frac{1}{2} m_a \int d^3\mathbf{v} v^2 F_a \end{aligned}$$

The diffusion tensor $\mathbf{D}_{ab}$ is of the form

$$\mathbf{D}_{ab} = \frac{1}{2} \nu_{v,ab} \mathbf{v}\mathbf{v} + \frac{1}{2} \nu_{d,ab} (v^2 \mathbf{I} - \mathbf{v}\mathbf{v})$$

The velocity $\mathbf{U}_{d,a}$ guarantees that the diffusive part of the collision operator conserves momentum. Each of its components is a function of the velocity modulus v only, i.e.

$$\frac{m_a v^2}{T_a} \mathbf{U}_{d,a}(v) = \frac{3}{4\pi} \int d\Omega \mathbf{v} f_a(v, \xi, \gamma)$$

where $d\Omega = d\gamma d\xi$ is the element of solid angle in the velocity space. Conservation results from the following properties

$$\int d^3\mathbf{v} G(v) \mathbf{v} = 0$$

and

$$\int d^3\mathbf{v} G(v) \mathbf{v} h_a\left(\mathbf{v}\right) = 0$$

for any function G that depends on the velocity modulus only. The latter relation comes from the property

$$\int d\Omega v^i v^j = \frac{4\pi}{3} v^2 \delta^{ij}$$

B.4.1 Momentum conservation

The velocities U_{ab} are "restoring" coefficients adjusted to ensure the *total* momentum conservation of the collision operator, i.e. the momentum transferred from species "a" to species "b" must be the opposite of the momentum transferred from "b" to "a". This leads to the following expression [23]

$$\mathbf{U}_{ab} = \frac{N_a m_a \left\langle \nu_{s,ab} \frac{m_a v^2}{T_a} \mathbf{U}_{d,a} \right\rangle_a}{N_b m_b \left\langle \nu_{s,ba} \frac{m_b v^2}{T_b} \right\rangle_b} = \frac{\left\langle \nu_{s,ab} v^2 \mathbf{U}_{d,a} \right\rangle_a}{\left\langle \nu_{s,ab} v^2 \right\rangle_a}$$

where

$$\langle ... \rangle_a = \frac{2}{\sqrt{\pi}} \int_0^\infty dx_a x_a^2 e^{-x_a^2} \int_{-1}^{+1} d\xi \int_0^{2\pi} \frac{d\gamma}{2\pi} ...$$

The following properties have been used

$$\Lambda_{ab} = N_a m_a \nu_{ab} = N_b m_b \nu_{ba} = \Lambda_{ba} \tag{74}$$

$$\Lambda_{ab} = \frac{1}{3} N_a m_a \left\langle \nu_{s,ab} \frac{m_a v^2}{T_a} \right\rangle_a = \frac{1}{3} N_b m_b \left\langle \nu_{s,ba} \frac{m_b v^2}{T_b} \right\rangle_b$$

Eq.(74) underlies the action/reaction principle Eq.(70).

B.4.2 Energy conservation

The parameters Q_{ab} are adjusted to ensure the conservation of total energy, i.e. the energy transfer rate from species "a" to species "b" must be the opposite to the energy exchange from "b" to "a",

$$Q_{ab} = T_b \frac{N_a \left\langle \nu_{E,ab} \frac{m_a v^2}{2} f_a \right\rangle_a}{N_b \left\langle \nu_{E,ba} \left(\frac{m_b v^2}{2} \right)^2 \right\rangle_b} = T_b \frac{\left\langle \nu_{E,ab} \frac{m_a v^2}{2} f_a \right\rangle_a}{\left\langle \nu_{E,ab} \left(\frac{m_a v^2}{2} \right)^2 \right\rangle_a}$$

where $\nu_{E,ab}$ is the energy loss rate

$$\nu_{E,ab} = -v \nu_{v,ab} \frac{\partial}{\partial v} \ln \left(\nu_{v,ab} F_{M0a} v^5 \right)$$

This definition agrees with the conventional energy loss rate

$$\nu_{E,ab} = 2\nu_{s,ab} - 2\nu_{d,ab} - \nu_{v,ab}$$

for equal temperatures $T_a = T_b$ only. The reason is that the test-particle part of the model operator Eq.(73) differs from the exact one Eq.(72) by a ratio T_b/T_a in the drag term. In other words the diffusion/convection part of the collision operator $\mathcal{C}_{ab}(F_a)$ relaxes towards a Maxwellian F_{M0a} with mass m_a and temperature T_b. Therefore Eq.(75) coincides with Eq.(75) for this particular definition of F_{M0a}. For obvious practical reasons only one reference Maxwellian distribution function should be handled, namely Eq.(73). Hence the definition Eq.(75) of $\nu_{E,ab}$ will be kept. The following property has been used

$$N_a \left\langle \nu_{E,ab} \left(\frac{m_a v^2}{2} \right)^2 \right\rangle_a = \frac{3 T_a T_b}{m_a + m_b} \Lambda_{ab} = N_b \left\langle \nu_{E,ba} \left(\frac{m_b v^2}{2} \right)^2 \right\rangle_b$$

This relationship is related to the equipartition principle Eq.(71). The collisional friction force is readily calculated

$$\mathbf{R}_{ab} = -N_a m_a \nu_{ab} \left(\mathbf{U}_{ab} - \mathbf{U}_{ba} \right)$$

It can be verified that $\mathbf{U}_{d,a} = \mathbf{U}_{ab} = \mathbf{V}_a$ for Maxwellian distribution functions (in the low Mach number limit)

$$f_{Ma} = 1 + \frac{m_a}{T_a}\mathbf{v}\cdot\mathbf{V}_a$$

The exact form of the collisional momentum exchange Eq.(72) for a Maxwellian is then recovered, i.e. $\mathbf{R}_{ab} = \mathbf{R}_{ab}^M$. The collisional energy exchange rate can also be calculated

$$Q_{ab} + \mathbf{R}_{ab}\cdot\mathbf{V}_a = -3\frac{1}{m_a+m_b}N_a m_a \nu_{ab}\left[\left(1+q_{ab}\right)T_a - \left(1+q_{ba}\right)T_b\right]$$

For Maxwellian distribution functions Eq.(75), $Q_{ab} = Q_{ba} = 0$ because $\left\langle \nu_{E,ab} v^2 \right\rangle_a$ is null. Hence the equipartition term Q_{ab}^M Eq.(72) is identical to the expected value Eq.(75), i.e. $Q_{ab} = Q_{ab}^M$. The collision operator Eq.(73) is self-adjoint and satisfies an H-theorem when temperatures are equal. Also the known limit forms of the collision operator are recovered.

B.5 Parallel friction force

Keeping only the first two Sonine polynomials, the normalized distribution function reduces to

$$F_a \simeq 1 + \frac{v_\parallel}{v_{Ta}^2}\left[V_{\parallel a} - \frac{2}{5}\frac{q_{\parallel a}}{N_a T_a}\left(\frac{5}{2} - x_a^2\right)\right] \tag{75}$$

Let us call $C_{\parallel,ab}$ the term that deals with momentum exchange between different species. The rate of parallel momentum exchange is given by

$$R_{\parallel ab} = -N_a m_a \nu_{ab}\left(U_{\parallel ab} - U_{\parallel ba}\right)$$

The two quantities $U_{\parallel d,a}(v)$ and $U_{\parallel ab}$ are computed by using the approximate distribution function Eq.(75)

$$U_{\parallel d,a} = V_{\parallel a} - \frac{2}{5}\frac{q_{\parallel a}}{N_a T_a}\left(\frac{5}{2} - x_a^2\right)$$

$$U_{\parallel ba} = V_{\parallel b} - \frac{3}{5}\frac{q_{\parallel b}}{N_b T_b}\left(\frac{1}{1+x_{ba}^2}\right)$$

leading to

$$\begin{aligned} C_{\parallel,ab} &= \nu_{s,ab}\frac{m_a}{T_a}v_\parallel F_{M0a} \\ &\quad \left[V_{\parallel b} - V_{\parallel a} + \frac{2}{5}\frac{q_{\parallel a}}{N_a T_a}\left(\frac{5}{2} - x_a^2\right) - \frac{3}{5}\frac{q_{\parallel b}}{N_b T_b}\left(\frac{1}{1+x_{ba}^2}\right)\right] \end{aligned}$$

The collisional drag force becomes

$$\begin{aligned} R_{\parallel ab} &= -N_a m_a \nu_{ab} \\ &\quad \left[V_{\parallel a} - V_{\parallel b} - \frac{3}{5}\frac{q_{\parallel a}}{N_a T_a}\left(\frac{1}{1+x_{ab}^2}\right) + \frac{3}{5}\frac{q_{\parallel b}}{N_b T_b}\left(\frac{1}{1+x_{ba}^2}\right)\right] \end{aligned}$$

For a Maxwellian, the result is exact and reduces to the friction force :

$$R_{\parallel M,ab} = -N_a m_a \nu_{ab}\left[V_{\parallel a} - V_{\parallel b}\right]$$

Note that particles b are more massive than particles a, i.e. $m_b \gg m_a$, then $x_{ab} = v_{Tb}/v_{Ta} \ll 1$ and $x_{ba} = v_{Ta}/v_{Tb} \gg 1$ so that

$$R_{\parallel ab} \simeq -N_a m_a \nu_{ab}\left[V_{\parallel a} - V_{\parallel b} - \frac{3}{5}\frac{q_{\parallel a}}{N_a T_a}\right]$$

C Constraints on the solution of the Fokker-Planck equation

Let us now address the case with collisions ruled by the equation Eq.(9). As said, the solution of $\{H, F\} = 0$ is a function of invariants of motion $(H, \mu, \psi_*, \epsilon_\parallel)$, or equivalently of the 3 action variables $\mathbf{J}$, while the solution of $C(F) = 0$ is a local Maxwellian

$$F_M(v_\parallel, \mu, \psi, \theta) = N_{eq} \left(\frac{m_a}{2\pi T_{eq}}\right)^{3/2} \exp\left\{-\frac{1}{T_{eq}}\left[\frac{1}{2}m_a\left(v_\parallel - V_{\parallel eq}\right)^2 + \mu B_{eq}\right]\right\} \tag{76}$$

where $N_{eq}, T_{eq}, V_{\parallel eq}$ are the density, temperature and parallel velocity, and depend in general on (ψ, θ), but on ζ because of axisymmetry. In general, a Maxwellian distribution function is not a function of the invariants of motion for two reasons:

- all fields depend on (ψ, θ), and not ψ_*
- the local Maxwellian Eq.(76) does not depend explicitly on the Hamiltonian $H = \frac{1}{2}m_a v_\parallel^2 + \mu B_{eq}(\psi, \theta) + e_a \Phi_{eq}(\psi, \theta)$, because the variables $(v_\parallel, \mu)$ appear separately, but also because of a mix-up with the mean parallel velocity $V_{\parallel eq}$, and also the absence of the electric potential.

This can be partly cured by introducing the following approximations:

- all fields depend on ψ only[20]. One then introduces the effective density

$$\mathcal{N}_{eq}(\psi) = N_{eq}(\psi) \exp\left(\frac{e_a \Phi_{eq}(\psi)}{T_{eq}(\psi)}\right)$$

- the Mach number $\frac{V_\parallel}{\sqrt{T_{eq}/m_a}}$ is supposed to be small, or order ρ_*.

The distribution function can then be reformulated as

$$F_M(H, \psi) = F_{M0}(H, \psi)\left[1 + \frac{m_a}{T_{eq}(\psi)} v_\parallel V_{\parallel eq}(\psi)\right]$$

where

$$F_{M0}(E, \psi) = N_{eq}(\psi)\left(\frac{m_a}{2\pi T_{eq}(\psi)}\right)^{3/2} \exp\left\{-\frac{E}{T_{eq}(\psi)}\right\}$$

or equivalently

$$F_{M0}(H, \psi) = \mathcal{N}_{eq}(\psi)\left(\frac{m_a}{2\pi T_{eq}(\psi)}\right)^{3/2} \exp\left\{-\frac{H}{T_{eq}(\psi)}\right\}$$

is called "unshifted" Maxwellian distribution function. We get closer - however $\{H, F_M\} \neq 0$ so that this reformulated local Maxwellian F_M *is still not solution* of the drift-kinetic equation. There are two reasons for this

- $v_\parallel$ is not an invariant of motion. Let us note however that passing particles are not far from satisfying this property. Indeed whenever $H \gg \mu B_{eq}$, then $dv_\parallel/dt \simeq 0$.

[20] In other words, poloidal asymmetries of the density, temperature, potential and velocity are ignored. They are small for density, potential and temperature in normal conditions - this is no longer true, in particular when the plasma rotates or is heated with radio-frequency heating. For the parallel velocity, this is a very poor approximation since poloidal asymmetries are of the order of ϵ, so no small except for vanishingly small inverse aspect ratios

- ψ differs from ψ_* by $-\frac{m_a v_\parallel}{e_a}\frac{I}{B_{eq}}$. Hence

$$F_M(H,\psi_*) = F_M(H,\psi) - \frac{m_a v_\parallel}{e_a}\frac{I}{B_{eq}}\frac{\partial F_M}{\partial \psi}(H,\psi)$$

  The second term in the r.h.s. does not satisfy $C[F]=0$ because of a term $v_\parallel\left(\frac{E}{T_{eq}}-\frac{3}{2}\right)$, and also again non invariance of $v_\parallel$.

It then appears that a local Maxwellian cannot be solution of the drift-kinetic equation because it is not a function of the invariants of motion. The departure from a dependence on **J** only is thus due to collisions, and is responsible for a transport dubbed neoclassical.

In principal the distribution function should be expanded over a set or polynomials (Legendre and Sonine) to build a full solution. In other words, any function F of energy E and pitch angle $\xi = v_\parallel/v$, where $v=\sqrt{2E/m}$ is the velocity modulus can be expanded as

$$F(E,\xi) = \left\{\sum_{\ell=0}^{+\infty}\sum_{n=0}^{+\infty} F_{n\ell}\mathcal{P}_\ell(\xi)S_n\left(\frac{E}{T_{eq}}\right)\right\}\exp\left(-\frac{E}{T_{eq}}\right)$$

where $\mathcal{P}_\ell$ and S_k are respectively Legendre and Sonine polynomials. Legendre are orthogonal polynomials with respect to the natural scalar product for a pitch-angle that spans the interval $[-1,1]$, i.e.

$$\frac{1}{2}\int_{-1}^{1} d\xi \mathcal{P}_\ell(\xi)\mathcal{P}_{\ell'}(\xi) = \frac{1}{2\ell+1}\delta_{\ell\ell'}$$

They are eigenfunctions of the pitch-angle scattering operator defined in Appendix B (first term in the r.h.s. of Eq.(72)), with eigenvalues $\ell(\ell+1)/2$. Sonine polynomials are technically speaking Laguerre polynomials of index 3/2, and therefore orthogonal with respect to a suitable scalar product in energy

$$\int_0^{+\infty} d\mathcal{E}\mathcal{E}^{3/2}e^{-\mathcal{E}}S_n(\mathcal{E})S_{n'}(\mathcal{E}) = \frac{\Gamma\left(n+\frac{5}{2}\right)}{\Gamma(n+1)}\delta_{nn'}$$

Sonine polynomials are not in general eigenvectors of a collision operator[21] - but their choice will appear natural in view of the discussion below. In principle all components $F_{n\ell}$ should be computed, and indeed polynomial expansion is the basis for many codes that solve for collisional transport. From the analytical standpoint, this is a formidable task. However it turns out that most results of neoclassical theory can be derived by just keeping the first two Legendre polynomials $\mathcal{P}_0=1$ and $\mathcal{P}_1=\xi$, and also the two first Sonine polynomials $S_0=1$ and $S_1=\frac{5}{2}-\mathcal{E}$. So we go on with a more intuitive (and less ambitious) programme by expressing the distribution function as

$$F_0(\mathbf{J}) = F_{M0}(\mathbf{J})\left\{1+\frac{m_a}{T_{eq}}\bar{v}_\parallel(\mathbf{J})W_\parallel(\mathbf{J})\right\} \tag{77}$$

where $\bar{v}_\parallel(\mathbf{J})$ has the same parity as the parallel velocity (i.e. proportional to $\mathcal{P}_1$), but is a function of the invariants of motion. This function can be calculated exactly in standard neoclassical theory, at least for some model operators - we will build it up in a different way. The notation **J** stands for $(H,\mu,\psi_*,\epsilon_\parallel)$.

[21] The function $f_n = e^{-\mathcal{E}}S_n$ is solution of the differential equation $\partial_\mathcal{E}\left(\mathcal{E}^{5/2}\partial_\mathcal{E} f_n\right) = -n\mathcal{E}^{3/2}f_n$, or equivalently $v^{-2}\partial_v\left(D_v v^2\partial_v f_n\right) = -2nD_v f_n$ with $D_v = v^2$. Comparing with Eq.(72) in Appendix B, this is equivalent to a Fokker-Planck operator with a constant collision frequency, whereas the latter is velocity dependent for Coulombian collisions, typically $\nu_v \sim 1/v^3$.

D Moments of the distribution function

We are now in position to compute from Eq.(16) the mean parallel velocity

$$V_\parallel(\psi,\theta) = \frac{1}{N_{eq}} \int d^3\mathbf{p} v_\parallel F_0$$

and the parallel heat flux

$$q_\parallel(\psi,\theta) = \frac{P_{eq}}{N_{eq}} \int d^3\mathbf{p} \left(\frac{E}{T_{eq}} - \frac{5}{2}\right) v_\parallel F_0$$

Let us first mention the following identity

$$\begin{aligned}\int d^3\mathbf{p} F_{M0} m_a v_\parallel^2 U\left(\psi,\theta,E,v_\parallel\right) &= N_{eq}T_{eq}\frac{2}{\sqrt{\pi}}\int_0^{+\infty}\frac{dE}{T_{eq}}\exp\left(-\frac{E}{T_{eq}}\right)\left(\frac{E}{T_{eq}}\right)^{3/2} \\ &\quad \int_{-1}^{1} d\xi \xi^2 U\left(\psi,\theta,E,\xi\right)\end{aligned}$$

for any function U. This justifies a posteriori the choice of scalar products and therefore of Legendre and Sonine polynomials for the projection of the distribution function[22]. This property allows a straightforward derivation of the identities

$$\int d^3\mathbf{p} F_{M0} m_a v_\parallel^2 = N_{eq}(\psi) T_{eq}(\psi)$$

$$\int d^3\mathbf{p} F_{M0} m_a v_\parallel^2 \left(\frac{E}{T_{eq}} - \frac{5}{2}\right) = \frac{5}{2} N_{eq}(\psi) T_{eq}(\psi)$$

This identities in turn provide an easy calculation of moments of the piece of distribution function related to $V_{*\zeta}$. The part related to $W_\parallel$ requires a bit more care, because $\bar{v}_\parallel$ differs from $v_\parallel$. Its form Eq.(17) strongly suggests to use the weighted volume integral Eq.(12). The integrals of interest reads

$$\int d^3\mathbf{p} F_{M0} m_a v_\parallel \bar{v}_\parallel S_n = N_{eq}(\psi) T_{eq}(\psi) f_c(\psi) b(\psi,\theta) \delta_{n0}$$

and

$$\int d^3\mathbf{p} F_{M0} m_a v_\parallel \bar{v}_\parallel \left(\frac{E}{T_{eq}} - \frac{5}{2}\right) S_n = \frac{5}{2} N_{eq}(\psi) T_{eq}(\psi) f_c(\psi) b(\psi,\theta) \delta_{n1}$$

where $f_c(\psi) = \frac{3}{4}\int_0^{\lambda_{max}} d\lambda v_\lambda(\psi,\theta)$ depends weakly on θ and is close to a fraction of passing particles.

E Pedestrian derivation of neoclassical fluxes

In order to illustrate the spirit of neoclassical calculations, without making use of a variational formulation, the drift kinetic equation is solved in a simple geometry of circular concentric magnetic surfaces.

[22] In the special case where U does not depend on ξ, this identity reads $\frac{1}{N_{eq}T_{eq}}\int d^3\mathbf{p} F_{M0} m_a v_\parallel^2 U(\psi,\theta,E) = \frac{4}{3\sqrt{\pi}}\int_0^{+\infty} d\mathcal{E} e^{-\mathcal{E}} \mathcal{E}^{3/2} U(\psi,\theta,\mathcal{E})$, where $\mathcal{E} = E/T_{eq}$. It is noted $\{U\}$ in the literature.

E.1 Fluxes and kinetic equation

E.1.1 Fluxes

One key objective of neoclassical theory is to calculate particle and heat fluxes. Let us consider one species, with charge e_a and mass m_a. The guiding-centre velocity is of the form $\mathbf{v} = v_\parallel \mathbf{b} + \mathbf{v}_E + \mathbf{v}_D$, where $v_\parallel$ is the parallel velocity, $\mathbf{v}_E$ the $E \times B$ drift velocity, and $\mathbf{v}_D$ is magnetic drift velocity ($\mathbf{b}$ is the unit vector along the magnetic field)[23]. In absence of turbulence, and assuming that the electric potential is a magnetic flux function [24], the radial component of the velocity is the projection $\mathbf{v}_D^r = \mathbf{v}_D \cdot \nabla r$ of the magnetic drift velocity. Hence the neoclassical particle flux reads

$$\Gamma_N = \int d^3\mathbf{v} \int \frac{d\theta}{2\pi} F v_D^r$$

where F is the distribution function, and

$$v_D^r = -v_D \sin\theta \frac{1}{T_{eq}} \left(m_a v_\parallel^2 + \mu B_{eq} \right)$$

where $v_D = \frac{T_{eq}}{e_a B_0 R_0}$, and $\mu = \frac{1}{2} m_a v_\perp^2 / B(\mathbf{X})$, where B_0 and R_0 are reference magnetic field and major radius, $\mathbf{X}$ the guiding-centre position, m_a the particle mass, and e_a its algebraic charge. Since $v_\parallel^2 / v_\perp^2$ scales as ϵ in the domain of interest, the parallel velocity can be ignored against the perpendicular velocity. A normalized perpendicular energy $u = \mu B_0 / T_{eq}$ is also introduced, so that

$$v_D^r = -v_D u \sin\theta$$

At this level of approximation, the normalised perpendicular energy u is the same as the normalised energy $\frac{E}{T_{eq}} = x^2$, where $E = 1/2 m_a v_\parallel^2 + \mu B_{eq}(r, \theta)$ is the kinetic energy, so that $u = x^2$. The heat flux expression is similar to the particle flux, with an extra energy in the integrand. The final expression of fluxes is therefore

$$\Gamma_N = -v_D \int d^3\mathbf{v} u \int \frac{d\theta}{2\pi} F \sin\theta \tag{78}$$

$$\Gamma_T = -v_D T_{eq} \int d^3\mathbf{v} u^2 \int \frac{d\theta}{2\pi} F \sin\theta \tag{79}$$

E.1.2 Perturbative approach

The distribution function F is expressed as a function of the total energy $H = 1/2 m_a v_\parallel^2 + \mu B_{eq}(r, \theta) + e_a \Phi_{eq}$, μ, r and θ, where $\Phi_{eq}(r)$ is the electric potential. Note H and μ are invariants of motion, but not the radial position r of the guiding-centre. The third invariant of motion is the canonical toroidal momentum

$$P_\zeta = -e_a \psi + m_a \frac{I(r)}{B(r, \theta)} v_\parallel$$

where ψ is the opposite of the poloidal flux normalised to 2π. For circular concentric magnetic surfaces, the flux function $\psi(r)$ is such that $d\psi = B_0 \frac{r}{q} dr$ - in the following we

[23] To simplify the notations, species label "a" is omitted except in charge and mass. It must be kept in mind though that all macroscopic fields like density, velocity and temperature may be different for each species. Same for the magnetic drift velocity

[24] Poloidal asymmetries of the electric potential matter for momentum of heavy impurity transport, which are thus not discussed here.

will make an indistinct use of ψ or r as a radial variable that labels magnetic flux surfaces. The kinetic equation then reads

$$v_\parallel \nabla_\parallel F + \mathbf{v}_D \cdot \nabla F + \frac{e_a E_{ind}}{m_a} \frac{\partial F}{\partial v_\parallel} = \mathcal{C}\left[F\right]$$

where $\mathcal{C}\left[F\right]$ is a collision operator, and $\nabla_\parallel F = \frac{1}{qR_0}\partial_\theta$, where $q(r)$ is the safety factor. Note that the derivatives in the drift kinetic equation must be performed *at constant H and* μ. The term related to the magnetic drift velocity $\mathbf{v}_D$ is responsible for neoclassical transport, as already seen from the structure of the fluxes. Moreover v_D/v_T scales as ρ_*. Hence an expansion is appropriate, i.e. $F = F_0 + F_1 + ...$, where

$$v_\parallel \nabla_\parallel F_0 - \mathcal{C}\left[F_0\right] = 0 \tag{80}$$

$$v_\parallel \nabla_\parallel F_1 - \mathcal{C}\left[F_1\right] = -\mathbf{v}_D \cdot \nabla F_0 - \frac{e_a E_{ind}}{m_a} \frac{\partial F_0}{\partial v_\parallel} \tag{81}$$

The solution of Eq.(80) is a function of r and energy that we choose as an unshifted Maxwellian

$$F_0 = F_{M0} = \frac{\mathcal{N}_{eq}}{(2\pi)^{3/2}} \left(\frac{m_a}{T_{eq}}\right)^{3/2} \exp\left(-\frac{H}{T_{eq}}\right)$$

where $\mathcal{N}_{eq}(r) = N_{eq} \exp\left(\frac{e_a \Phi_{eq}}{T_{eq}}\right)$, and $N_{eq}(r)$, $T_{eq}(r)$ are the equilibrium density and temperature. Let us introduce the "Spitzer" distribution function F_{sp} defined as

$$\mathcal{C}\left[F_{sp}\right] = -\frac{e_a E_{ind}}{T_{eq}} F_{M0} v_\parallel$$

Considerations on parity leads to the following formulation of the "Spitzer" distribution function

$$F_{sp} = F_{M0} \frac{m_a v_\parallel U_{sp\parallel}}{T_{eq}}$$

where $U_{sp\parallel}(H, r)$ is called "Spitzer" parallel velocity. It is useful to introduce the auxiliary function τ_{sp} defined as follows

$$C\left[F_{M0} v_\parallel \tau_{sp}\right] = F_{M0} v_\parallel$$

The function τ_{sp} can be interpreted as a collision time (inverse of a collision frequency). Once τ_{sp} is calculated, the velocity $U_{sp\parallel}$ and distribution function F_{sp} are readily found

$$U_{sp\parallel} = -\frac{e_a E_{ind}}{m_a} \tau_{sp} \tag{82}$$

$$F_{sp} = -\frac{e_a E_{ind}}{T_{eq}} \tau_{sp} v_\parallel F_{M0} \tag{83}$$

To solve Eq.(81), it is useful to make use of the invariance of P_ζ, at order one in ρ_*, namely

$$\mathbf{v}_D \cdot \nabla \Psi = I v_\parallel \nabla_\parallel \left(\frac{m_a v_\parallel}{e_a B_{eq}}\right)$$

Hence Eq.(81) can be rewritten as

$$v_\parallel \nabla_\parallel \left(F_1 + I \frac{m_a v_\parallel}{e_a B} \frac{\partial F_{M0}}{\partial \psi}\right) = \mathcal{C}\left[F_1 - F_{sp}\right] \tag{84}$$

Far from the trapped domain $v_\parallel \gg \sqrt{\epsilon} v_T$, the unperturbed distribution is a *local* shifted Maxwellian

$$F_M = F_{M0}\left(1 + \frac{m_a v_\parallel V_{\parallel eq}}{T_{eq}}\right) \tag{85}$$

where $V_{\|eq}(r)$ the fluid parallel velocity, assumed to be much smaller than the thermal velocity, say ρ_*. At this stage, the parallel velocity $V_{\|eq}(r)$ is the same for all species. It makes then sense to introduce an auxiliary distribution function

$$G_1 = F_1 - F_{M0}\frac{m_a v_\| V_{\|eq}}{T_{eq}} - F_{sp}$$

Noting that $\mathcal{C}\left[F_{M0}\frac{mv_\|V_{\|eq}}{T_{eq}}\right] = 0$, it then appears that the Fokker-Planck equation Eq.(84) can be rephrased as

$$v_\|\nabla_\|\left(G_1 + F_{M0}\frac{m_a v_\|}{T_{eq}}\left(V_{\|eq} + U_{sp\|} + V_{*\zeta}\right) + \right) = \mathcal{C}\left[G_1\right] \tag{86}$$

where

$$V_{*\zeta} = I\frac{T_{eq}}{e_a B_{eq}}\frac{\partial \ln F_{M0}}{\partial\psi}\bigg|_{\psi,H}$$

is a kinetic diamagnetic velocity.

E.1.3 Thermodynamic forces

A delicate step is the calculation of $\partial_\psi F_{M0}$, which must be performed at constant total Hamiltonian H, which differs from kinetic energy E since $H = E + e_a\Phi_{eq}(r)$. The gradient of F_0 is related to thermodynamic forces, responsible for fluxes. Using Eq.(85), one finds the following expression

$$\frac{\partial \ln F_{M0}}{\partial\psi}\bigg|_{\psi,H} = \frac{\partial}{\partial\psi}\ln N_{eq} + \frac{e_a}{T_{eq}}\frac{\partial\Phi_{eq}}{\partial\psi} + \left(\frac{E}{T_{eq}} - \frac{3}{2}\right)\frac{\partial}{\partial\psi}\ln T_{eq}$$

The latter can be restricted to its perpendicular contribution since the parallel part is ϵ times smaller. Finally Eq.(86) can be recast as

$$v_\|\nabla_\|\left(G_1 + F_{M0}\frac{m_a v_\|}{T_{eq}}U_{\|tot}\right) = \mathcal{C}\left[G_1\right]$$

where

$$U_{\|tot} = V_{\|eq} + U_{sp\|} + V_{*\zeta}$$

or equivalently

$$\frac{\epsilon}{q}U_{\|tot} = \frac{T_{eq}}{e_a B_0}\frac{\partial\Xi}{\partial r}$$

with

$$\frac{\partial\Xi}{\partial r} = \frac{\partial}{\partial r}\ln N_{eq} + \frac{e_a}{T_{eq}}\frac{\partial\Phi_{eq}}{\partial r} + e_a\frac{B_p}{T_{eq}}\left(V_{\|eq} + U_{sp\|}\right) + \left(x^2 - \frac{3}{2}\right)\frac{\partial}{\partial r}\ln T_{eq}$$

where $B_p = \frac{\epsilon}{q}B_0$ is the poloidal field. A useful alternative expression for $U_{\|tot}$ is obtained by using the force balance equation (or more precisely its radial projection)

$$\frac{\partial}{\partial r}\ln N_{eq} + \frac{e_a}{T_{eq}}\left(\frac{\partial\Phi_{eq}}{\partial r} + B_p V_t\right) - \frac{e_a}{T_{eq}}B_t V_p + \frac{\partial}{\partial r}\ln T_{eq} = 0 \tag{87}$$

where the parallel velocity $V_{\|eq}$ has been replaced by the toroidal velocity V_t, since these are the same at the requested order in ϵ. Combining these equations, a compact expression of $U_{\|tot}$ is found.

$$\frac{\epsilon}{q}U_{\|tot} = \frac{T}{e_a B_0}\frac{\partial\Xi}{\partial r} = V_p + \frac{1}{e_a B_t}\left(x^2 - \frac{5}{2}\right)\frac{\partial T_{eq}}{\partial r} + \frac{\epsilon}{q}U_{sp\|} \tag{88}$$

The combination $\partial_r \Phi_{eq} + B_p V_t$ in Eq.(87) indicates that the radial electric field cannot be calculated separately from the parallel (in fact toroidal) velocity. This is generic for any axisymmetric system. Toroidal symmetry has to be broken (at this order of the calculation) to compute the radial electric field and toroidal velocity separately. This appears clearly in the expression Eq.(88), which does not depend on the radial electric field nor on the toroidal velocity. Another way of understanding this degeneracy is that neoclassical transport is "automatically" ambipolar, i.e. the ambipolarity condition does not bring a new information that would allow calculating the electric field. Eq.(88) allows understanding the logical steps of a neoclassical calculation:

- the particle fluxes are calculated as functions of V_p and $\partial_r \ln T_{eq}$ for each species. The ambipolarity condition provides the poloidal velocity of the species whose contribution to the radial current is the largest, usually the main ion.
- The poloidal velocity for each species can be calculated by combining the force balance equations. Fluxes for species other than the main ion can then be calculated versus density and temperature gradients.
- The thermal fluxes are calculated using the previous information.

E.1.4 Normalised Fokker-Planck equation

It is reminded here that the Hamiltonian

$$H_{eq} = \frac{1}{2} m_a v_\parallel^2 + \mu B_0 \left(1 - \epsilon \cos\theta\right) + e_a \Phi_{eq}$$

is an invariant of motion. This property is sufficient to describe properly the physics of trapping. The problem at hand belongs to the category of boundary layers. It is useful to introduce the dimensionless pitch-angle variable

$$p = \frac{m_a^{1/2} v_\parallel}{(\mu B_0 \varepsilon)^{1/2}} = \frac{v_\parallel}{x v_T \epsilon^{1/2}}$$

where x is a normalised energy defined above. Let us define a normalized Hamiltonian as

$$k = \frac{1}{2} p^2 - \cos\theta$$

up to a constant on a given magnetic surface. It appears that p and θ are conjugated variables with respect to the Hamiltonian k. Moreover

$$v_\parallel \nabla_\parallel F = x \frac{v_T}{q R_0} \epsilon^{1/2} p \frac{\partial F}{\partial \theta}$$

where F is a function of k, x and[25] θ. As explained in the introduction, the contribution to fluxes come from a boundary layer in the phase space near the trapped/passing boundary $k = 1$ (deeply trapped particles correspond to $k \simeq -1$). The distribution function tends to develop a singularity in the velocity space along the direction of the momentum-like variable p. Therefore the dominant term in the collision operator has to be a diffusion along the p direction, namely

$$\mathcal{C}(G_1) = \frac{1}{2} \frac{\left\langle \Delta v_\parallel^2 \right\rangle}{x^2 v_T^2 \epsilon} \frac{\partial^2 G_1}{\partial p^2}$$

where $< \Delta v_\parallel^2 >$ is a collisional scattering diffusion coefficient and generalised to electrons. It is homogeneous to a velocity diffusion coefficient and is of the form $< \Delta v_\parallel^2 >=$

[25] Note that $p \partial_\theta F = -\{k, F\}$ where $\{f, g\} = \partial_\theta f \partial_p g - \partial_p f \partial_\theta g$ is a Poisson bracket. This relationship allows to bridge this derivation with the one done in the note on mean field statistics

$2\nu v_T^2 x^2 \bar{\nu}(x)$. It is convenient to introduce the normalized distribution functions f and g defined as

$$G_1 = \epsilon^{1/2} \frac{U_{\|tot}}{v_T} F_{M0} x g$$
$$f = g + p$$

Also, the velocity integration in the vicinity of the trapped/passing boundary reads

$$\int d^3\mathbf{v} F_{M0} ... = N_{eq}\sqrt{\epsilon} \int_0^{+\infty} 2x dx \exp\left(-x^2\right) \int_{-\infty}^{\infty} \frac{dp}{\sqrt{2\pi}} ...$$

Hence the overall problem can be summarized as follows

$$\begin{pmatrix} \Gamma_N \\ \Gamma_T/T_{eq} \end{pmatrix} = -\frac{1}{\sqrt{2\pi}} N_{eq} \frac{qR_0}{v_T} v_D^2 \int_0^{+\infty} 2x dx \exp\left(-x^2\right) x^4 \begin{pmatrix} 1 \\ x^2 \end{pmatrix} \Lambda \frac{\partial \Xi}{\partial r} \tag{89}$$

where

$$\Lambda = \int_{-\infty}^{\infty} dp \int \frac{d\theta}{2\pi} g \sin\theta$$

and $g(k,\theta)$ is solution of

$$p\frac{\partial g}{\partial_\theta} - \eta \frac{\partial^2 g}{\partial p^2} = \sin\theta \tag{90}$$

where $\eta = \nu_* \bar{\nu}/x$. Eq.(90) can also be written $p\partial_\theta f = -\{k, f\} = \eta \partial_{pp} f$. It is reminded that $k = \frac{1}{2}p^2 - \cos\theta$. Since $f = g + p$, g can be safely replaced by f in the collision operator, consistently with a previous remark on the innocuous effect of collisions on a shifted Maxwellian. In the "f-description", the g function is replaced by $f - p$ in the definition of Λ. Though the difference between f and g is an odd function of p, which at first sight does not contribute to Λ, this shift is necessary to ensure the convergence of integrals in p. In other words, g, not f, is a localized function of p in the boundary layer.

E.2 Explicit solution for a single species

We restrict the calculation to a single ion species (no Spitzer function). It can be easily extended to electrons by using appropriate collision frequencies, and including the Spitzer function.

E.2.1 Plateau regime

It is reminded that in the kinetic equation Eq.(90), p is a function of (k,θ), i.e.

$$p = \mathrm{sgn}(p)\sqrt{2(k + \cos\theta)} \tag{91}$$

In plateau regime, $\nu_* \geq 1$, the variation of g with k is smooth, i.e. details of the distribution function in the domain $|k| < 1$ do not matter. Therefore trapping can be neglected, i.e. $p \simeq sg(\xi)\sqrt{2k}$ so that p and θ can be treated as independent variables. Thus Eq.(90) is a linear differential equation that can be solved exactly. Using Fourier transforms, the following solution is found[26]

$$g = -\frac{1}{2} \int_0^{+\infty} d\rho \exp\left\{-\frac{2}{3}\eta\rho^3\right\} \sin\left(\theta - \rho p\right)$$

A straightforward integration provides $\Lambda = \frac{\pi}{2}$. The collision operator is often replaced in the literature by a proxy called Krook operator $-\eta g$, so that the solution is

$$g = -\frac{p}{p^2 + \eta^2} \cos\theta + \frac{\eta}{p^2 + \eta^2} \sin\theta$$

[26]This solution was already derived in the lecture note on mean field kinetic theory, which is of course not a coincidence. The reader is referred to this note for details.

However it turns out that $\Lambda = \frac{\pi}{2}$ *is the same*! This apparent coincidence results from the smoothness of g in the velocity space, which does not depend on the details of the dissipation (the final result does not depend on ν_*). It will be seen that this trick cannot be used in the banana regime. The particle flux in plateau regime is given by the expression

$$\Gamma_N = -\sqrt{\frac{\pi}{2}} N_{eq} \frac{qR_0}{v_T} v_D^2 \left(\frac{\partial}{\partial r} \ln N_{eq} + \frac{e_a}{T_{eq}} \frac{\partial \Phi_{eq}}{\partial r} + \frac{e_a}{T_{eq}} B_p V_t + \frac{3}{2} \frac{\partial}{\partial r} \ln T_{eq} \right) \tag{92}$$

The ambipolarity condition imposes that the sum of fluxes over all species must vanish. For small impurity concentrations, the main ion flux dominates over the electron flux by a factor $\sqrt{m_i/m_e}$. Hence the ambipolarity constraint implies that the parenthesis in Eq.(92) vanishes for ions. Using the force balance equation Eq.(87), one finds the value of the main ion poloidal velocity $V_p = -\frac{1}{2} \frac{\partial_r T_{eq}}{e_a B_0}$. For each species other than the main ion, the flux is calculated by using the main ion poloidal velocity and combining the force balance equations to find the poloidal velocity of the considered species. Also the heat flux for the main ion species can be calculated and reads

$$\Gamma_T = -3\sqrt{\frac{\pi}{2}} N_{eq} \frac{qR_0}{v_T} v_D^2 \frac{\partial T_{eq}}{\partial r}$$

E.2.2 Banana regime

When $\nu_* \ll 1$, it appears easier to solve in f, i.e. to solve $-\{k, f\} = \eta \partial_{pp} f$. Moreover, multiplying Eq.(90) and integrating over the (p, θ) variables leads to an alternative expression of Λ

$$\Lambda = \eta \int_{-\infty}^{\infty} dp \int \frac{d\theta}{2\pi} \left(\frac{\partial f}{\partial p} - 1 \right)^2$$

The solution is of the form $f(k, \theta) = f_0(k) + \eta f_1(k, \theta) + ...$, where f_1 is given by

$$p \partial_\theta f_1 = \eta \frac{\partial^2 f_0}{\partial p^2} \tag{93}$$

Hence the bulk f_0 of the distribution function is aligned with the constant energy contour lines $k = cte$, which form an island in the $(\theta, v_\parallel)$ space. A boundary layer appears near the separatrix, described by the function f_1. The width of the boundary layer depends on ν_*. A typical solution is illustrated on Fig.23.

The solubility constraint, obtained by dividing the Fokker-Planck equation Eq.(93) by p and integrating over θ, provides $\partial_k f_0$

$$\frac{\partial f_0}{\partial k} = \frac{C}{Q(k)}$$

where

$$Q(k) = \oint \frac{d\theta}{2\pi} \xi(k, \theta)$$

The constant C is determined from boundary conditions and regularity constraints. Inside the island, $-1 \leq k \leq 1$, one has $C = 0$, otherwise the solution would be singular. Outside the island, $C = 1$ to ensure a smooth match with $\partial_p f_0 \to 1$ when $|p| \to \infty$. After a bit of algebra, one finds

$$\Lambda = 2\mathcal{I}\nu_*$$

where

$$\mathcal{I} = \lim_{L \to \infty} \left(\sqrt{2L} - \int_1^L \frac{dk}{Q(k)} \right) \simeq 1.38$$

Plugging this expression into Eq.(89), one finds the expression of the particle flux

$$\Gamma_N = -C_\Gamma N \frac{qR_0}{v_T} v_D^2 \left(\partial_r \ln N_{eq} + \frac{e_a}{T_{eq}} \frac{\partial}{\partial r} \Phi_{eq} + \frac{e_a}{T_{eq}} B_p V_t + (1 - k_{neo}) \frac{\partial}{\partial r} \ln T_{eq} \right)$$

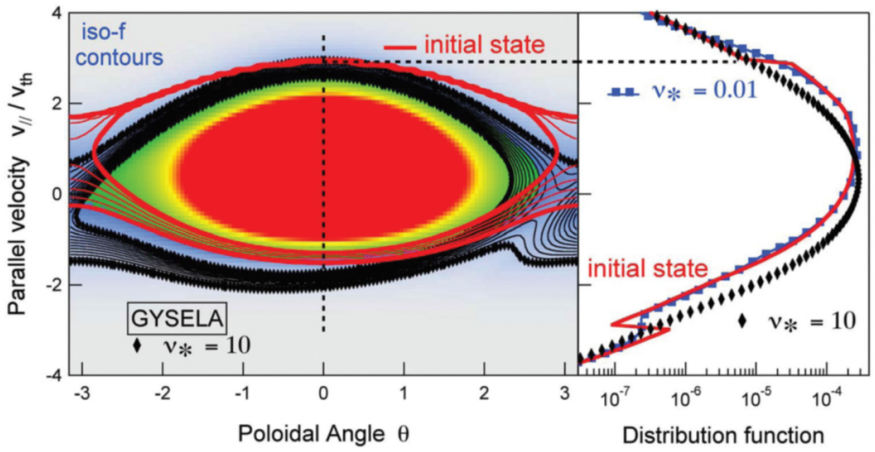

Figure 23: Contour lines of the distribution function in the $(\theta, v_{\|})$ space for two values of ν_*, calculated with GYSELA (Dif-Pradalier et al.).

where $C_\Gamma = 1.1\nu_*$ and

$$k_{neo} = \frac{\int_0^{+\infty} 2dx \exp\left(-x^2\right) x^4 \bar{\nu} \left(\frac{5}{2} - x^2\right)}{\int_0^{+\infty} 2dx \exp\left(-x^2\right) x^4 \bar{\nu}} \simeq 1.17$$

The ambipolarity condition provides the main ion poloidal velocity $V_\theta = k_{neo} \frac{\partial_r T}{e_a B}$, from which all fluxes can be calculated. The heat flux is then

$$\Gamma_T = -1.35 n \frac{qR_0}{v_T} v_D^2 \nu_* \frac{\partial T_{eq}}{\partial r}$$

F Transport matrix with ripple

This appendix provides the details of the elements of the transport matrix with ripple.

F.1 Elements of the transport matrix

The transport matrix $\mathfrak{M}$ is symmetrical. Its 6 independent elements are given by the following expressions. Diagonal elements:

$$\begin{aligned}
d_{NN} &= \sqrt{\frac{\pi}{2}} \int_0^{+\infty} du e^{-u} u^2 K_{tor,I}(r,u) \\
&+ \frac{32}{9} \left(\frac{2}{\pi}\right)^{3/2} \left(\frac{\bar{\delta}}{\epsilon}\right)^{3/2} \frac{G_1}{\nu_*} \int_0^{+\infty} du e^{-u} u^{5/2} \frac{1}{\bar{\nu}(u)} \\
&+ 2 \left(\frac{2}{\pi}\right)^{3/2} \frac{1}{N_b q} \left(\frac{\bar{\delta}}{\epsilon}\right)^2 \frac{1}{\nu_*} \int_0^{u_c} du e^{-u} u^{5/2} \frac{1}{\bar{\nu}(u)} K_{rip,II}(r,u) \\
&+ \sqrt{\frac{\pi}{2}} N_b q \left(\frac{\bar{\delta}}{\epsilon}\right)^2 \int_{u_c}^{+\infty} du e^{-u} u^2 K_{st}(r,u)
\end{aligned}$$

$$\begin{aligned}
d_{VV} &= \sqrt{\frac{\pi}{2}} (N_b q) \left(\frac{\bar{\delta}}{\epsilon}\right)^2 \int_0^{+\infty} du e^{-u} u^2 K_{rip,I}(r,u) \\
&+ \sqrt{\frac{\pi}{2}} \int_0^{+\infty} du e^{-u} u^2 K_{tor,I}(r,u)
\end{aligned}$$

$$
\begin{aligned}
d_{TT} &= \sqrt{\frac{\pi}{2}} \int_0^{+\infty} du e^{-u} u^2 K_{tor,I}(r,u) \left(u - \frac{3}{2}\right)^2 \\
&+ \frac{32}{9} \left(\frac{2}{\pi}\right)^{3/2} \left(\frac{\bar{\delta}}{\epsilon}\right)^{3/2} \frac{G_1}{\nu_*} \int_0^{+\infty} du e^{-u} u^{5/2} \frac{1}{\bar{\nu}(u)} \left(u - \frac{3}{2}\right)^2 \\
&+ 2 \left(\frac{2}{\pi}\right)^{3/2} \frac{1}{N_b q} \left(\frac{\bar{\delta}}{\epsilon}\right)^2 \frac{1}{\nu_*} \int_0^{u_c} du e^{-u} u^{5/2} \frac{1}{\bar{\nu}(u)} K_{rip,II}(r,u) \left(u - \frac{3}{2}\right)^2 \\
&+ \sqrt{\frac{\pi}{2}} N_b q \left(\frac{\bar{\delta}}{\epsilon}\right)^2 \int_{u_c}^{+\infty} du e^{-u} u^2 K_{st}(r,u) \left(u - \frac{3}{2}\right)^2
\end{aligned}
$$

Non diagonal elements

$$
d_{NV} = \sqrt{\frac{\pi}{2}} \int_0^{+\infty} du e^{-u} u^2 K_{tor,I}(r,u)
$$

$$
\begin{aligned}
d_{NT} &= \sqrt{\frac{\pi}{2}} \int_0^{+\infty} du e^{-u} u^2 K_{tor,I}(r,u) \left(u - \frac{3}{2}\right) \\
&+ \frac{32}{9} \left(\frac{2}{\pi}\right)^{3/2} \left(\frac{\bar{\delta}}{\epsilon}\right)^{3/2} \frac{G_1}{\nu_*} \int_0^{+\infty} du e^{-u} u^{5/2} \frac{1}{\bar{\nu}(u)} \left(u - \frac{3}{2}\right) \\
&+ 2 \left(\frac{2}{\pi}\right)^{3/2} \frac{1}{N_b q} \left(\frac{\bar{\delta}}{\epsilon}\right)^2 \frac{1}{\nu_*} \int_0^{u_c} du e^{-u} u^{5/2} \frac{1}{\bar{\nu}(u)} K_{rip,II}(r,u) \left(u - \frac{3}{2}\right) \\
&+ \sqrt{\frac{\pi}{2}} N_b q \left(\frac{\bar{\delta}}{\epsilon}\right)^2 \int_{u_c}^{+\infty} du e^{-u} u^2 K_{st}(r,u) \left(u - \frac{3}{2}\right)
\end{aligned}
$$

$$
d_{VT} = \sqrt{\frac{\pi}{2}} \int_0^{+\infty} du e^{-u} u^2 K_{tor,I}(r,u) \left(u - \frac{3}{2}\right)
$$

F.2 Reformulation

Regarding the underlying physics, it is interesting to split the coefficients into those which depend on the ripple amplitude, and those which do not. let us define the u-dependent integrand

$$
\mathcal{K}(u) = \sqrt{\frac{\pi}{2}} e^{-u} u^2 K_{tor,I}(r,u)
$$

$$
\begin{aligned}
\tilde{\mathcal{K}}(u) &= \frac{32}{9} \left(\frac{2}{\pi}\right)^{3/2} \left(\frac{\bar{\delta}}{\epsilon}\right)^{3/2} \frac{G_1}{\nu_*} e^{-u} u^{5/2} \frac{1}{\bar{\nu}(u)} \\
&+ 2 \left(\frac{2}{\pi}\right)^{3/2} \frac{1}{N_b q} \left(\frac{\bar{\delta}}{\epsilon}\right)^2 \frac{1}{\nu_*} \left[1 - Y\left(u - u_c\right)\right] e^{-u} u^{5/2} \frac{1}{\bar{\nu}(u)} K_{rip,II}(r,u) \\
&+ \sqrt{\frac{\pi}{2}} N_b q \left(\frac{\bar{\delta}}{\epsilon}\right)^2 Y\left(u - u_c\right) e^{-u} u^2 K_{st}(r,u)
\end{aligned}
$$

$$
\hat{\mathcal{K}}(u) = \sqrt{\frac{\pi}{2}} \left(N_b q\right) \left(\frac{\bar{\delta}}{\epsilon}\right)^2 e^{-u} u^2 K_{rip,I}(r,u)
$$

where Y is the Heaviside function. The following sub-coefficients are then defined

$$
d_n = \int_0^{+\infty} du \left(u - \frac{3}{2}\right)^n \mathcal{K}(u)
$$

$$\tilde{d}_n = \int_0^{+\infty} du \left(u - \frac{3}{2}\right)^n \tilde{\mathcal{K}}(u)$$
$$\hat{d}_n = \int_0^{+\infty} du \left(u - \frac{3}{2}\right)^n \hat{\mathcal{K}}(u)$$

Let us stress some important properties

- The coefficients d_n do not depend on the ripple amplitude. Therefore the underlying physics is the standard neoclassical theory.

- The coefficients $\tilde{d}_n$ and $\hat{d}_n$ both depend on the ripple amplitude. However they do not cover the same physics. Coefficients $\hat{d}_n$ are finite only when local trapping occur. On the contrary $\tilde{d}_n$ essentially cover the physics of ripple on banana tips, magnetic drift on locally trapped particles, and stochastic losses.

With these definitions, the transport matrix bear a "simple" form

$$\mathfrak{M} = -D_p \begin{pmatrix} d_0 + \tilde{d}_0 & d_0 & d_1 + \tilde{d}_1 \\ d_0 & d_0 + \hat{d}_0 & d_1 \\ d_1 + \tilde{d}_1 & d_1 & d_2 + \tilde{d}_2 \end{pmatrix} \tag{94}$$

This structure turns to give some insight in the physics due to ripple.

References

[1] R.D. Hazeltine and J.D. Meiss. *Plasma Confinement*. Dover, 1992.

[2] R.J Goldston and P.H Rutherford. *Introduction to Plasma Physics*. CRC Press, 1995.

[3] Per Helander and D.J. Sigmar. *Collisional Transport in Magnetized Plasmas*. Cambridge University Press, 2002.

[4] H. E. Mynick. Transport optimization in stellarators. *Physics of Plasmas*, 13(5):058102, 2006.

[5] Per Helander. Theory of plasma confinement in non-axisymmetric magnetic fields. *Reports on Progress in Physics*, 77(8):087001, jul 2014.

[6] P.N. Yushmanov. *Diffusive transport processes caused by ripple in tokamaks*, volume 16 of *Review of Plasma Physics*. Consultants Bureau, New York, 1990.

[7] A. A. Galeev, R. Z. Sagdeev, H. P. Furth, and M. N. Rosenbluth. Plasma diffusion in a toroidal stellarator. *Phys. Rev. Lett.*, 22:511–514, Mar 1969.

[8] K.C. Shaing, S.A. Sabbagh, and M.S. Chu. An approximate analytic expression for neoclassical toroidal plasma viscosity in tokamaks. *Nuclear Fusion*, 50(2):025022, feb 2010.

[9] A. Samain and F. Nguyen. Onsager relaxation of toroidal plasmas. *Plasma Physics and Controlled Fusion*, 39(8):1197–1243, aug 1997.

[10] X. Garbet, G. Dif-Pradalier, C. Nguyen, Y. Sarazin, V. Grandgirard, and Ph. Ghendrih. Neoclassical equilibrium in gyrokinetic simulations. *Physics of Plasmas*, 16(6):062503, 2009.

[11] X. Garbet, J. Abiteboul, E. Trier, Ö. Gürcan, Y. Sarazin, A. Smolyakov, S. Allfrey, C. Bourdelle, C. Fenzi, V. Grandgirard, P. Ghendrih, and P. Hennequin. Entropy production rate in tokamaks with nonaxisymmetric magnetic fields. *Physics of Plasmas*, 17(7):072505, 2010.

[12] M. N. Rosenbluth, R. D. Hazeltine, and F. L. Hinton. Plasma transport in toroidal confinement systems. *The Physics of Fluids*, 15(1):116–140, 1972.

[13] F. L. Hinton and Marshall N. Rosenbluth. Transport properties of a toroidal plasma at low to intermediate collision frequencies. *The Physics of Fluids*, 16(6):836–854, 1973.

[14] F. L. Hinton and R. D. Hazeltine. Theory of plasma transport in toroidal confinement systems. *Rev. Mod. Phys.*, 48:239–308, Apr 1976.

[15] S. P. Hirshman, D. J. Sigmar, and J. F. Clarke. Neoclassical transport theory of a multispecies plasma in the low collision frequency regime. *The Physics of Fluids*, 19(5):656–666, 1976.

[16] C. S. Chang and F. L. Hinton. Effect of finite aspect ratio on the neoclassical ion thermal conductivity in the banana regime. *The Physics of Fluids*, 25(9):1493–1494, 1982.

[17] M. Taguchi. Improved method for calculating neoclassical transport coefficients in the banana regime. *Physics of Plasmas*, 21(5):052504, 2014.

[18] J. Wesson. *Tokamaks*. Oxford University Press, 1997.

[19] X Garbet, J Abiteboul, Y Sarazin, A Smolyakov, S Allfrey, V Grandgirard, P Ghendrih, G Latu, and A Strugarek. Entropy production rate in tokamak plasmas with helical magnetic perturbations. *Journal of Physics: Conference Series*, 260(1):012010, nov 2010.

[20] R. J. Goldston, R. B. White, and A. H. Boozer. Confinement of high-energy trapped particles in tokamaks. *Phys. Rev. Lett.*, 47:647–649, Aug 1981.

[21] P. Grua and J.-P. Roubin. Collisionless diffusion regimes of trapped particles in a tokamak induced by magnetic field ripples. *Nuclear Fusion*, 30(8):1499–1509, aug 1990.

[22] J.W. Connor and R.J. Hastie. Neoclassical diffusion arising from magnetic-field ripples in tokamaks. *Nuclear Fusion*, 13(2):221, mar 1973.

[23] S. P. Hirshman and D. J. Sigmar. Approximate fokker planck collision operator for transport theory applications. *The Physics of Fluids*, 19(10):1532–1540, 1976.

[24] S. P. Hirshman and D. J. Sigmar. Neoclassical transport of a multispecies toroidal plasma in various collisionality regimes. *The Physics of Fluids*, 20(3):418–426, 1977.

[25] F.L. Hinton. *Collisional transport in plasma*, volume I of *Basic Plasma Physics, Handbook of Plasma Physics*. North Holland Publishing Company, Amsterdam, 1983.

[26] S.P. Hirshman and D.J. Sigmar. Neoclassical transport of impurities in tokamak plasmas. *Nuclear Fusion*, 21(9):1079–1201, sep 1981.

[27] I. G. Abel, M. Barnes, S. C. Cowley, W. Dorland, and A. A. Schekochihin. Linearized model fokker planck collision operators for gyrokinetic simulations. i. theory. *Physics of Plasmas*, 15(12):122509, 2008.

[28] H. Sugama, T.-H. Watanabe, and M. Nunami. Linearized model collision operators for multiple ion species plasmas and gyrokinetic entropy balance equations. *Physics of Plasmas*, 16(11):112503, 2009.